Balance Manifolds in Lotka–Volterra Systems

by

Atheeta Ching

A thesis submitted in conformity with the requirements

for the degree of Doctor of Philosophy

Department of Mathematics

Faculty of Mathematical & Physical Sciences

University College London

2019

Disclaimer

I, Atheeta Ching, confirm that the work presented in this thesis is my own. Where information has been derived from other sources, I confirm that this has been indicated in the thesis.

Signature _____

Date _____

Abstract

The Lotka-Volterra equations are a dynamical system in the form of an autonomous ODE. The aim of this thesis is to explore the carrying simplex for non-competitive Lotka-Volterra systems for the case of 2- and 3-species, where it is referred to as a balance simplex. Carrying simplices were developed by M.W. Hirsch in a series of papers. They are hypersurfaces which asymptotically attract all non-zero solutions in the phase portrait. This essentially means that all the non-trivial dynamics occur on the carrying simplex, which is one dimension less than the system itself. Many of its properties have been studied by various authors, for example: E.C. Zeeman, M.L. Zeeman, S. Baigent, J. Mierczyński.

The first few chapters of this thesis explores the 2-species scaled Lotka-Volterra system, where all intrinsic growth rates and intraspecific interaction rates are set to the value 1. This simplification of the model allows for an explicit, analytic form of the balance simplex to be found. This is done by transforming the system to polar co-ordinates and explicitly integrating the new system. The balance simplex for this 2-species model is precisely composed of the heteroclinic orbits connecting non-zero steady states, along with these states themselves.

The later chapters of this thesis focuses on the 3-species case. The existence of the balance simplex in particular parameter cases is proven and it is shown to be

piecewise analytic (when the interaction matrix containing the parameters is strictly copositive). These chapters also work towards plotting the balance simplex so it can be visualised for the 3-species system.

In another chapter, more general planar Kolmogorov models are considered. Conditions sufficient for the balance simplex to exist are given, and it is again composed of heteroclinic orbits between non-zero steady states.

This thesis was completed under the supervision of ***Stephen Baigent****.*

Impact Statement

Our research and results will primarily be useful for those studying the areas of population ecology and continuous autonomous dynamical systems. The carrying simplex has been an area of mathematical interest as it implies all the non-trivial dynamics of the system occurs on a hypersurface, which is one dimension less than the system itself. Our work extends the existence of the carrying simplex beyond competitive systems where we call it a balance simplex or manifold. Currently we have published two papers on this research, with more to come. These will be useful particularly for other mathematicians and ecologists, who may build on this research in the future.

In Chapter 6, we discuss general planar Kolmogorov models and provide sufficient conditions for the existence of the balance manifold when the system has at most one interior steady state. These types of models cover many different ecological models thus our work may be useful outside of academia too, in the area of species preservation or population ecology. For example, the results are applicable to models with facultative mutualism, or where a prey species has a Holling type-II functional response. Researchers who study these planar Kolmogorov systems will be able to test whether the system has a balance manifold using our conditions. Note that not all of our conditions are necessary for the balance manifold to exist, so researchers may also be able to determine other sufficient conditions by comparing our conditions with their model.

Our work on 2-species scaled Lotka–Volterra systems provides explicit and analy-

tic expressions for the balance simplex. We believe these results will be beneficial for future research as the balance simplex in the 3-species system matches these expressions on the planar boundaries. The curvature of the balance simplex can also be explicitly studied. The curvature of the carrying simplex for Lotka–Volterra models has been studied by a number of researchers (e.g. E.C. Zeeman, M.L. Zeeman, S. Baigent) as it has implications for the stability of the unique interior steady state when it exists.

In Chapter 5, we explore a method to plot the balance simplex in the 3-species system which works in non-competitive cases. M.L. Zeeman and M. LaMar developed *CSimplex* for the program *Geomview* which plots the carrying simplex for competitive 3-species systems. Our method, based on Darboux polynomials, is not just a numerical result, but gives an insight as to why the method works and the solution is in the form of a zero set to a series which satisfies the dynamics of the system. We believe these methods may be useful for those studying invariant manifolds in 3-dimensional systems (thus to pure mathematicians as well).

Acknowledgments

I would like to thank my parents and sister for their eternal love and support which has been my North Star in this journey and life. I would also like to thank all my aunties and uncles who have always kept me in their prayers.

Thanks to my friends for always being there and allowing me to enjoy life, both in and out of the office. Thanks to everyone in the mathematics department of UCL, particularly the others in my office (past and present). I would also like to acknowledge the EPSRC for funding my research.

Of course, I would like to thank my supervisor, Steve, whose insight and advice has made this work possible.

Atheeta Ching, *University College London*, 2019

To my late aunt, Mamee.

Contents

List of Tables

List of Figures

List of Symbols

$\mathbb{N}$	set of natural numbers $\{1, 2, 3, \ldots\}$
$\mathbb{R}^n_{\geq 0}$	non-negative orthant $[0, \infty)^n$
$\mathbb{R}^n_{>0}$	positive orthant $(0, \infty)^n$
x	population density vector $x = (x_1, \ldots, x_n) \in \mathbb{R}^n_{\geq 0}$
$x < y$	$x_i < y_i$ for all $i = 1, \ldots, n$
$x \leq y$	$x_i \leq y_i$ for all $i = 1, \ldots, n$
Σ	carrying simplex, balance simplex/manifold
α_{ij}	effect species j has on species i
A	interaction matrix with entries α_{ij}
$\mathcal{R}(0)$	basin of repulsion of the origin
$\partial\mathcal{R}(0)$	boundary of $\mathcal{R}(0)$ relative to $\mathbb{R}^n_{\geq 0}$
$\mathcal{J}(s)$	Jacobian matrix at the steady state s
∇	gradient operator
div	divergence operator
N	total population density $N = x_1 + \ldots + x_n$
u	species proportion vector with entries $u_i = \frac{x_i}{N}$

Chapter 1

An Introduction to Lotka–Volterra Systems and Carrying Simplices

1.1 The Lotka–Volterra equations

The Lotka–Volterra equations, in their predator-prey form, were first used in the early 20$^{\text{th}}$ century. Lotka used them to model chemical reactions [55], and later applied them to organic systems of herbivores and plants [56]. The same equations were also published by Volterra who was asked to investigate the population of fish in the Adriatic Sea after World War I [91].

Whilst the original model was not realistic in its assumptions (e.g. the environment and food supply for the prey does not change over time), the model in its general form has been an area of mathematical interest [97].

Definition 1.1.1 For an n-species system, the general Lotka–Volterra equations for $i = 1, \ldots, n$ are:

$$\begin{aligned} \frac{dx_i}{dt} &= x_i \left(r_i - \sum_{j=1}^{n} \alpha_{ij} x_j \right) \\ &=: x_i f_i \\ &=: F_i \end{aligned} \tag{1.1}$$

where x_i is the density of species i, thus $x = (x_1, \ldots, x_n) \in \mathbb{R}^n_{\geq 0} = [0, \infty)^n$, the non-negative orthant. The per capita growth rate of species i is given by f_i which is a polynomial of degree 1. This model assumes that individuals from the same species are identical in terms of their interactions and fitness. The intrinsic growth rate of species i is given by r_i and represents the growth rate of an individual of species i when there is no interaction with any other individuals.

Definition 1.1.2 If $i = j$, α_{ii} is called an intraspecific interaction coefficient, the effect species i has on itself. If $i \neq j$, α_{ij} is called an interspecific interaction coefficient, the effect species j has on species i (a different species).

Note that for the system (1.1), we have used a minus sign in front of these interaction coefficients, so if $\alpha_{ij} > 0$, then species j has a negative effect on species i. If additionally $\alpha_{ji} > 0$, we say that species i and j compete with one another. If these coefficients are both negative, we say that the species are co-operating, and if the coefficients are different signs, we say one species predates on the other. The latter case may not represent the classic predator-prey model, depending on the sign of the intrinsic growth rates.

Definition 1.1.3 We say (1.1) is a competitive Lotka–Volterra system if $r_i > 0$ and $\alpha_{ij} > 0$ for all $i, j \in 1, \ldots, n$.

We will only consider systems where r_i and α_{ij} are constant for all i, j. Systems where this is not true have also been studied [49]. For example, if r_i and α_{ij} depend on time with a delay period, it can be used to model seasonal shifts in the environment and changes in animal behaviour [65], making the model more realistic but harder to work with analytically in higher dimensions. Putting a time delay on the variable x_i can be used to represent a gestation period for the species; eating another species is not instantly beneficial to the predator's population size [26, 96]. This delay can also be used to model species migration in and out of the system [16]. Alternatively, species migration can be modelled with multiple habitats (known as patches), each with their own Lotka–Volterra system, with a term for species movement between patches [32,60]. Another example of making the Lotka–Volterra model more realistic is having the intraspecific interaction coefficients α_{ii} depend on x_i, this dependency is usually written as a separate term from the constant intraspecific effect [105]. This can be used to model the Allee effect which describes how small populations benefit from increasing the number of individuals (e.g. it will be easier to find a mate or gather resources together) but large populations do not due to the increase in intraspecific competition [21, 82].

Lotka–Volterra models have been extended to study different areas. For example,

the effect infectious diseases has on a Lotka–Volterra system [89], or finding travelling wave solutions to Lotka–Volterra systems with a diffusion term [25]. Outside of population dynamics, the Lotka–Volterra system can also be used in finance and manufacturing [20, 39, 52]. Modis considered company stocks as species competing for investors as the resource [64]. Chiang used the competitive model to forecast the markets for two different types of semiconductors in Taiwan, based on past data [17]. In physics, the Lotka–Volterra models have been used in the study of lasers, where the variables can represent the electromagnetic field intensity and the population inversion [45, 73]. The equations have also been used in cosmology, for example, Perez et al. [68] showed that Friedmann–Lemaître cosmological dynamics can be viewed as a Lotka–Volterra system where the species are barotropic fluids, leading them to find a Lyapunov function to describe the asymptotic behaviour.

An important property of the n-species Lotka–Volterra model is that there exists a homeomorphism which maps it to the $(n+1)$-strategy replicator equations [37,67], essentially meaning the behaviour of models can be made equivalent. The replicator equations are key to the study of game theory which can be used to model behaviour and exploring which strategies will prevail in certain contexts [37]. For example, game theory can be used to explain ritualistic fighting behaviour in animals and why individuals of the same species typically do not fight each other to the death, but rather until an individual surrenders [80].

The dynamics of the Lotka–Volterra system can be analysed through the phase portrait and steady state analysis [37]. The phase portrait shows how solutions to the system change over time through the use of orbits. It is easy to see that $\mathbb{R}^n_{\geq 0}$ is invariant for the system. In fact, the interior of the orthant, $\mathbb{R}^n_{>0} = (0, \infty)^n$, is also invariant for the system but of course as time goes to infinity, species can become extinct thus the limit point of an initial population may not belong in $\mathbb{R}^n_{>0}$. We now list some basic theory typical from analysing dynamical systems [69].

Definition 1.1.4 We define the flow of (1.1) as the unique solution to the system, denoted by $\varphi_t : \mathbb{R}^n_{\geq 0} \to \mathbb{R}^n_{\geq 0}$ where $t \in \mathbb{R}$. We call φ_t a semiflow if we only consider $t \geq 0$. When the point $x_0 \in \mathbb{R}^n_{\geq 0}$ is fixed, the trajectory through x_0 is denoted $\varphi_t(x_0)$ and is the same as the map: $x_0 \mapsto x(t, x_0)$. The image of $\mathbb{R}$ under this map gives the orbit of x_0.

Definition 1.1.5 We denote by $O^+(x) = \{\varphi_t(x) : t \geq 0\}$ the forward orbit through x and $O^-(x) = \{\varphi_t(x) : t \leq 0\}$ the backward orbit through x. The orbit through x is denoted by $O(x) = O^+(x) \cup O^-(x)$.

Definition 1.1.6 A steady state of (1.1) is a point $s \in \mathbb{R}^n_{\geq 0}$ which satisfies $F(s) = (F_1(s), \ldots, F_n(s)) = 0$. Equivalently, $\phi_t(s) = s$ for all $t \in \mathbb{R}$. In literature s is also referred to as a fixed point, critical point or an equilibrium point.
An interior steady state $s^* \in \mathbb{R}^n_{>0}$ of (1.1) is a point such that $f(s^*)$
$= (f_1(s^*), \ldots, f_n(s^*)) = 0$. For (1.1), s^* is typically unique when it exists, otherwise there are infinitely many points satisfying $f(s^*) = 0$. In the unique case we say the interior steady state does not exist if $s^* \notin \mathbb{R}^n_{>0}$.

Definition 1.1.7 The *ω-limit* of a point x, denoted by $\omega(x)$, is the set of all points y for which there exists some sequence $t_n \to \infty$ such that $\lim_{n\to\infty} \varphi_{t_n}(x) = y$. Similarly, the *$\alpha$-limit* of x, denoted $\alpha(x)$ is the set of all points z for which there exists some sequence $t_n \to \infty$ such that $\lim_{n\to\infty} \varphi_{-t_n}(x) = z$.

Theorem 1.1.1 ([69]) *For any system where the vector field is C^1 (continuously differentiable), e.g. (1.1), if an orbit through x is contained in a compact subset of $\mathbb{R}^n_{\geq 0}$, then $\alpha(x)$ and $\omega(x)$ are non-empty, compact, connected subsets of $\mathbb{R}^n_{\geq 0}$ (by a connected set, say C, we mean a set which cannot be divided into two disjoint non-empty subsets which are open in C).*

Definition 1.1.8 A homoclinic orbit is an orbit which has its α-limit and ω-limit

equal to the same steady state. A heteroclinic orbit has its α-limit and ω-limit equal to different steady states.

Definition 1.1.9 Let s be a steady state of (1.1), we call any orbit which has its α-limit equal to p an unstable orbit of p. Similarly, any orbit which has its ω-limit equal to p is called a stable orbit of p.

Theorem 1.1.2 (Poincaré-Bendixson [84]) *Let $\frac{dx}{dt} = F(x)$ be an ODE system defined on an open set of $\mathbb{R}^2$. Let $\omega(x)$ be a compact, non-empty ω-set which contains a finite number of steady states. Then one of the following holds:*

1. *$\omega(x)$ is precisely one steady state.*
2. *$\omega(x)$ is a periodic orbit.*
3. *$\omega(x)$ is a connected set containing steady states with homoclinic and heteroclinic orbits connecting these states.*

Definition 1.1.10 ([69]) Let N be a neighbourhood of $s \in \mathbb{R}^n_{\geq 0}$. The local stable manifold of s relative to N is $W^s_{loc}(s) = \{x \in N : O^+(x) \subset N \text{ and } \varphi_t(x) \to s \text{ as } t \to \infty\}$. The global stable manifold is $W^s(s) = \bigcup_{t \leq 0} \varphi_t(W^s_{loc}(s))$.
The local unstable manifold of p relative to N is $W^u_{loc}(s) = \{x \in N : O^-(x) \subset N \text{ and } \varphi_t(x) \to s \text{ as } t \to -\infty\}$. The global unstable manifold is $W^u(s) = \bigcup_{t \geq 0} \varphi_t(W^u_{loc}(s))$.

Definition 1.1.11 The basin of repulsion of a steady state s, $\mathcal{R}(s)$, is the set of all points x such that $\lim_{t\to\infty} \varphi_{-t}(x) = s$, i.e. $\mathcal{R}(s) = W^u(s)$. The basin of attraction of s, $\mathcal{B}(s)$, is the set of all points y such that $\lim_{t\to\infty} \varphi_t(y) = s$, i.e. $\mathcal{B}(s) = W^s(s)$. Note that these sets are open [83].

Definition 1.1.12 The Jacobian matrix of (1.1) is the $n \times n$ matrix $\mathcal{J} = \left[\frac{\partial F_i}{\partial x_j}\right]$. When $i \neq j$, $\frac{\partial F_i}{\partial x_j} = x_i \frac{\partial f_i}{\partial x_j}$ and when $i = j$, $\frac{\partial F_i}{\partial x_i} = x_i \frac{\partial f_i}{\partial x_i} + f_i$.

Definition 1.1.13 A steady state s is called hyperbolic if $\mathcal{J}(s)$ has no eigenvalues with their real part equal to zero.

We will typically only consider the cases where all steady states are hyperbolic since the local dynamics are completely known due to the following theorem:

Theorem 1.1.3 (The Hartman–Grobman Theorem [69]) *Let E be an open subset of $\mathbb{R}^n$ containing the origin and let φ_t be the flow of a nonlinear system, e.g. (1.1), where the vector field F is C^1. Suppose that $F(0) = 0$, and that $A := \mathcal{J}(0)$ has no eigenvalue with zero real part. Then there exists a homeomorphism H of an open set U containing the origin onto an open set V containing the origin such that for each $x_0 \in U$, there is an open interval $I_0 \subset \mathbb{R}$ containing zero such that*

$$H \circ \varphi_t(x_0) = e^{At} H(x_0), \text{ for all } t \in I_0, \tag{1.2}$$

i.e. H maps orbits of the nonlinear system near the origin onto orbits of the linearised system $\left(\frac{dx}{dt} = Ax\right)$ near the origin and preserves the parametrisation by time. This result can be applied to steady states which are not on the origin by a linear change of co-ordinates.

This theorem means that Jacobian analysis is an effective way to determine the local dynamics around hyperbolic steady states. The signs of the eigenvalues of a steady state determine its stability type.

Theorem 1.1.4 (The Stable Manifold Theorem [69]) *Let E be an open subset of $\mathbb{R}^n$ containing the origin and let φ_t be the flow of a nonlinear system, e.g. (1.1), where the vector field F is C^1. Suppose that the origin is a hyperbolic steady state: $F(0) = 0$ and $\mathcal{J}(0)$ has k eigenvalues with negative real part and $n - k$ eigenvalues with positive real part. Then there exists a k-dimensional differentiable manifold S tangent to the stable subspace (spanned by the corresponding eigenvectors) of the*

linearised system of (1.1) at 0 *such that for all* $t \geq 0$, $\varphi_t(S) \subset S$ *and for all* $x_0 \in S$, $\lim_{t\to\infty} \varphi_t(x_0) = 0$.

Similarly, there exists an $n-k$ *dimensional differentiable manifold* U *tangent to the unstable subspace of the linearised system of (1.1) at* 0 *such that for all* $t \leq 0$, $\varphi_t(U) \subset U$ *and for all* $x_0 \in U$, $\lim_{t\to-\infty} \varphi_t(x_0) = 0$.

We call S *the stable manifold of* 0 *and* U *the unstable manifold of* 0. *This result can be applied to steady states which are not on the origin by a linear change of co-ordinates.*

Definition 1.1.14 ([43, 69]) M is an n-dimensional analytic manifold if there exists an open covering $\{\mathcal{O}_\alpha\}$ where each cover is homeomorphic to $\mathbb{R}^n$ by $\phi_\alpha : \mathcal{O}_\alpha \to \mathbb{R}^n$ such that when $\mathcal{O}_\alpha \cap \mathcal{O}_\beta$ is nonempty then the composition map

$$\phi_\alpha \circ \phi_\beta^{-1} : \ \phi_\beta(\mathcal{O}_\alpha \cap \mathcal{O}_\beta) \to \phi_\alpha(\mathcal{O}_\alpha \cap \mathcal{O}_\beta) \tag{1.3}$$

is analytic meaning it can be represented by a convergent power series in a neighbourhood of any point in $\phi_\beta(\mathcal{O}_\alpha \cap \mathcal{O}_\beta)$.

1.2 The scaled Lotka–Volterra system

In this thesis, we will consider some simplifications to the standard Lotka–Volterra system so that we can find some analytical results. Namely, we set all intrinsic growth rates r_i and intraspecific interaction coefficients α_{ii} to the value 1, we called this the scaled Lotka–Volterra system. A classic example of this system is the May-Leonard model for three competing species [59].

Definition 1.2.1 The scaled Lotka–Volterra system for $i = 1, \ldots, n$ is given by:

$$\begin{aligned} \frac{dx_i}{dt} &= x_i \left(1 - x_i - \sum_{\substack{j \neq i \\ j=1}}^{n} \alpha_{ij} x_j \right) \\ &=: x_i f_i \\ &=: F_i. \end{aligned} \tag{1.4}$$

Compared to the general model (1.1), we have set $2n$ out of the $n^2 + n$ parameters to have the value 1. Whilst this may seem quite restricted, particularly in the 2-species case where four out of six parameters will be fixed, any general Lotka–Volterra system with equal, positive intrinsic growth rates $r_i = r > 0$ and non-zero intraspecific interaction coefficients α_{ii} can be written as a scaled Lotka-Volterra system with the change of variables $\widetilde{x}_i(t) = \frac{\alpha_{ii}}{r} x_i \left(\frac{t}{r}\right)$. This follows from the remark before equation (1.1) in Tineo [85] (after correcting the expression in their argument of x_i).

By setting $\alpha_{ii} = 1$, the system (1.4) has steady states on each axis given by the standard unit basis vectors – a column vector of 0s with 1 in the i^{th} entry. We will refer to these as the *axial steady states*. Having positive intrinsic growth rates r_i means the origin is an unstable node, it is easy to verify that the Jacobian matrix at the origin is a diagonal matrix with entries r_i, see Definition 1.1.12. In (1.4), the Jacobian matrix at the origin is the identity matrix which has the eigenvalue 1 with multiplicity n.

Since the origin is an unstable node and $\alpha_{ii} = 1 > 0$ for all $i \in \{1, \ldots, n\}$, it is clear then that every axial steady state is stable on the axis it lies on. Indeed, the dynamics on the x_i axis is given by:

$$\frac{dx_i}{dt} = x_i(1 - x_i). \tag{1.5}$$

If $x_i < 1$ then $\frac{dx_i}{dt} > 0$, if $x_i > 1$ then $\frac{dx_i}{dt} < 0$. This also means the dynamics on each axis remains bounded for all time.

We are interested in studying a particular $(n-1)$-dimensional surface for the scaled Lotka–Volterra system (1.4) which does not exist as a connected surface if the dynamics in $\mathbb{R}^n_{\geq 0}$ are unbounded. In the 2-species system, the case we need to exclude is when the two species are strongly co-operative, i.e. $\alpha_{12}\alpha_{21} > 1$ and both $\alpha_{12}, \alpha_{21} < 0$. Physically, this means the two species benefit from each other so much that it outweighs any intraspecific competition. In our model, both species populations would tend to infinity – this unrealistic outcome can occur due to positive feedback; each species benefits proportionally to the other's population size, which in turn increases their growth rate and their own population size.

1.3 The carrying simplex

Hirsch studied the properties of convergence for co-operative and competitive systems of continuous differential equations in a series of papers [33–35].

Definition 1.3.1 Consider a C^1 system of differential equations in $\mathbb{R}^n$,

$$\frac{dx_i}{dt} = F_i(x_1, \ldots, x_n) = F_i(x), \qquad i = 1, \ldots, n. \tag{1.6}$$

This system is called co-operative if $\frac{\partial F_i}{\partial x_j} \geq 0$ for $i \neq j$, and competitive if $\frac{\partial F_i}{\partial x_j} \leq 0$ for $i \neq j$.

Note that a competitive system is co-operative when time is reversed, i.e. $t < 0$. A feature of co-operative systems is that the flow is monotone [34, 44]. We use the standard notation for vector ordering, e.g. $x \leq y$ if $x_i \leq y_i$ for all i, and other inequalities having the analogous meaning. A flow φ_t of a system is monotone if $\varphi_t(x) \leq \varphi_t(y)$ for all $x \leq y$ and $t > 0$, meaning it is order preserving. Hirsch used

this property to prove theorems such as there are no attracting non-constant periodic solutions in co-operative systems [34]. Another related property is that if all forward orbits in a co-operative system are bounded, then the forward orbit of almost every initial state converges to an equilibrium [79].

Hirsch's purpose for the series of papers [33–35] was to explore when the long-term behaviour of dynamical systems are known. When modelling systems that exist in the real world, we typically encounter models in which almost all orbits to converge to a steady state or asymptotically approach a periodic orbit. Systems which lack this property and cannot be approximated by other systems which do have this property can be said to be chaotic or possess strange attractors [33].

Hirsch found that research into the long-term behaviour of different types systems is divided into two approaches. The first considers exploring the consequences of certain assumptions about the large scale structure of the system, e.g. the structural stability [75, 76] – whether properties and dynamics of the system remain similar under a small perturbation of the parameters or variables. The techniques used tend to be topological as examples come from geometry and physics. A benefit of this approach is that it gives a wider, conceptual understanding of such systems, but may not help in understanding a specific system.

The second approach focuses on specific classes of systems that arise in areas such as biology, chemistry and economics where it may be hard to determine whether these systems have a given structural property. Hirsch's aim was to blend both of these approaches by using the structural ideas to analyse classes of systems typically used to model real systems such as those in biology.

In his third paper of this series [35], Hirsch focused on the long-term dynamics of competitive Kolmogorov-type systems:

Definition 1.3.2 Consider a Kolmogorov-type system in $\mathbb{R}^n_{\geq 0}$,

$$\frac{dx_i}{dt} = F_i(x) = x_i f_i(x), \qquad i = 1, \ldots, n, \tag{1.7}$$

where the per capita growth rates $f_i(x)$ are C^1. It is called competitive if $\frac{\partial f_i}{\partial x_j} \leq 0$ for $i \neq j$. If $\frac{\partial f_i}{\partial x_j} < 0$ for all i, j, we call this system totally competitive.

Remark 1.3.1 *Hirsch [35] only considered competitive systems with the following properties:*

1. *Dissipation: There is a compact invariant set (called the fundamental attractor) which uniformly attracts each compact set of initial points. This also implies that infinity is repelling.*

2. *Irreducibility: The community matrix* $\left[\frac{\partial f_i}{\partial x_j}\right]$ *is irreducible in* $\mathbb{R}^n_{\geq 0}$*; for any* $x \in \mathbb{R}^n_{\geq 0}$ *and* $i \neq j$*, there exists a finite sequence* $i = s_1, \ldots, s_m = j$ *such that*

$$\frac{\partial f_{s_k}}{\partial x_{s_{k+1}}}(x) \neq 0 \text{ for } k = 1, \ldots, m-1.$$

   This essentially means that each species (directly or indirectly) influences every other species.

Both of these conditions are satisfied for totally competitive Kolmogorov systems.

An example of a Kolmogorov-type system is the general Lotka–Volterra equations. If we consider a competitive Lotka–Volterra system in which $r_i > 0$ and $\alpha_{ij} > 0$ for all i, j, then it is totally competitive.

Hirsch's key result is the existence of the carrying simplex, which he defines more succinctly in a later paper [36]:

Definition 1.3.3 A **carrying simplex** of the competitive system (1.7) is a set $\Sigma \subset \mathbb{R}^n_{\geq 0} \setminus 0$ with the following properties:

1. Σ is compact and invariant to the flow of (1.7), φ_t.

2. The solution orbit of every non-zero point $x \in \mathbb{R}^n_{\geq 0}$ is asymptotic with some point $y \in \Sigma$, i.e. $\lim_{t\to\infty}|\varphi_t(x) - \varphi_t(y)|= 0$. We will say that systems with this property are asymptotically complete.

3. Σ is *unordered*, i.e. if $x, y \in \Sigma$ and $x \geq y$, then $x = y$.

The final property means that any line from the origin intersects Σ only once. This can then be used to prove that Σ is homeomorphic to the $(n-1)$-simplex, $\Delta^{n-1} = \{x \in \mathbb{R}^n_{\geq 0} | \sum_i x_i = 1\}$, by radial projection: $x \mapsto \frac{x}{\sum_i x_i}$ [36]. Carrying simplices are Lipschitz continuous manifolds, thus they are continuous but not necessarily C^1-continuous. Conditions for the interior of Σ to be C^1-continuous were given by Brunovský [12] and Miercyński [61,63]. Examples of systems where the boundary of Σ is not C^1-continuous can be found in [62].

We briefly define what it means for a manifold to be Lipschitz.

Definition 1.3.4 ([70]) Given two metric spaces (X, d) and (X', d'), a function $f : X \to X'$ is called Lipschitz if there exists a constant L such that

$$d'(f(x), f(y)) \leq L\, d(x, y) \tag{1.8}$$

for all $x, y \in X$.

If every $x \in X$ has a neighbourhood U such that $f|_U$ is Lipschitz, then f is called locally Lipschitz.

A function $f : X \to X'$ is called a lipeomorphism (or bi-Lipschitz) if it is a bijection such that f and f^{-1} are locally Lipschitz [57].

Definition 1.3.5 ([57]) A Lipschitz n-manifold is a separable metric space M such that every point $x \in M$ has a closed neighbourhood U which is lipeomorphic to $[-1, 1]^n$ (recall that a space is called separable if it has a countable, dense subset).

Carrying simplices as a concept were first introduced by Smale [77] who showed that an arbitrary smooth flow in Δ^{n-1} can be embedded as an attractor in a competitive system in the form of (1.7) with the additional conditions that the origin is an unstable node, and $\frac{\partial f_i}{\partial x_j} < 0$ for all i, j (these conditions means the assumptions of Remark 1.3.1 are satisfied). Hirsch builds on this, showing that in fact all of the non-trivial dynamics of any such competitive system occur on a manifold which is one dimension less than the system itself.

Theorem 1.3.2 (Carrying simplex [35]) *In the competitive system (1.7) (with assumptions from Remark 1.3.1), assume additionally that the origin is an unstable node, and that at every non-zero steady state, we have* $\frac{\partial f_i}{\partial x_j} < 0$ *for all* i, j. *Then* $\Sigma = \partial\mathcal{R}(\infty)$ *(the boundary relative to* $\mathbb{R}^n_{\geq 0}$ *of the basin of repulsion of infinity* $\mathcal{R}(\infty)$*) satisfies the conditions in Definition 1.3.3 to be a carrying simplex.*

The condition that $\frac{\partial f_i}{\partial x_j} < 0$ for all i, j at every non-zero steady state ensures that these states cannot be unstable nodes [35]. Indeed, take any of these non-zero steady states, say s, and a small positive vector $\varepsilon \in \mathbb{R}^n_{>0}$. At least one $f_i(s) = 0$ for some i, thus by continuity $f_i(s + \varepsilon) < 0$. This means $\frac{dx_i}{dt}(s + \varepsilon) < 0$ implying that s is not an unstable node.

Since all non-zero steady states and other ω-limit sets lie on Σ, it essentially contains all the 'interesting' dynamics of the system [35]. For example, periodic orbits occur only on Σ, when they exist.

In [36], Hirsch states sufficient conditions for a carrying simplex of (1.7) to be unique. This can also be applied to discrete systems where the concept of a carrying simplex also exists and has been well studied [24, 40, 72]. Smith [78] considered discrete periodic Kolmogorov systems with the Poincaré map [84], providing several conditions which were conjectured for the existence of a carrying simplex. This was later proved by Wang and Jiang [92] with an additional condition based an inequality involving the ratio of two points and their orbits. Carrying simplices are

also applicable to a range of more general models, including nonautonomous and random competitive Kolmogorov systems [74].

In [5], Baigent proved that for 3-dimensional totally competitive Kolmogorov systems (1.7), the carrying simplex is unique using a method of surface evolution.

Theorem 1.3.3 ([5]) *Consider a 3-dimensional totally competitive Kolmogorov system (1.7) which generates a semiflow φ_t for which the origin is a repeller. Then there is a unique Lipschitz invariant surface Σ such that if M is a plane with unit normal $N > 0$ for which $M_0 = M \cap \mathbb{R}^3_{\geq 0} \neq \emptyset$ then $M_t = \varphi_t(M_0)$ is a sequence of smooth surfaces (with corners) that converges uniformly to Σ.*

The theory of carrying simplices for both continuous and discrete-time is an active research field, but to the best of our knowledge, all known results for carrying simplices relate to competitive [24, 35, 36, 40, 92] or type-K competitive systems [53, 54]. Type-K competitive systems are Kolmogorov systems where the matrix $\left[-\frac{\partial f_i}{\partial x_j}\right]$ can be written in the following block matrix form:

$$\left[-\frac{\partial f_i}{\partial x_j}\right] = \begin{pmatrix} M_1 & -M_2 \\ -M_3 & M_4 \end{pmatrix}, \tag{1.9}$$

where M_1 is a $k \times k$ matrix, M_2 is a $(n-k) \times k$ matrix, M_3 is a $k \times (n-k)$ matrix and M_4 is a $(n-k) \times (n-k)$ matrix. Both $M_2, M_3 \geq 0$, and M_1 and M_4 have non-negative off-diagonal elements. Note that for Lotka–Volterra systems, this matrix is equal to $A := [\alpha_{ij}]$. For $n = 3$, $k = 2$, an example is if species 1 and 3 are co-operating, species 2 and 3 are also co-operating, but species 1 and 2 are competing. This does not cover predator-prey type relationships.

1.4 The carrying simplex in competitive Lotka–Volterra systems

When we study Lotka–Volterra systems with positive intrinsic growth rates for all species and positive intraspecific interaction coefficients, we will observe that $\partial\mathcal{R}(\infty) = \partial\mathcal{R}(0)$ [101]. For competitive Lotka–Volterra systems, we will define the carrying simplex to be the following uniquely defined set:

Definition 1.4.1 For competitive Lotka–Volterra systems, the carrying simplex Σ will always refer to the set $\partial\mathcal{R}(0)$. It satisfies the properties discussed by Hirsch (e.g. Definition 1.3.3).

Recall that we call a Lotka–Volterra system competitive if $r_i > 0$ and $\alpha_{ij} > 0$ for all i, j. The condition $r_i > 0$ is equivalent to the origin being an unstable node, and $-\alpha_{ij} = \frac{\partial f_i}{\partial x_j} < 0$ means the system is totally competitive and satisfies Theorem 1.3.2. With a change in co-ordinates, it can be shown that the dynamics on $\Sigma \subset \mathbb{R}^n_{\geq 0}$ follow an $(n-1)$-species Lotka–Volterra system but it is not typically competitive [10].

Definition 1.4.2 ([37]) In biology, the carrying capacity (of an environment for a particular species) is the maximum number of individuals from that species which the environment can sustain when there are no interactions with other species. Theoretically, when the population is above the carrying capacity, it will decrease in size, if it below the carrying capacity, it will increase in size.

The reason Σ is called the carrying simplex is because it can be considered as the higher dimensional version of the carrying capacity, separating solutions which are growing from the origin from those which are declining from infinity. Indeed, the 0-dimensional carrying simplex (for a 1-species system) is exactly the carrying capacity. However, in higher dimensions the carrying simplex contains states where some species (but not all) may be extinct.

The carrying simplex is particularly useful for analysing 3-dimensional systems as the dynamics on planar systems are relatively well understood. In fact, in the 3-species competitive Lotka–Volterra system, the convexity of the boundary edges of Σ can determine whether an interior steady state is globally stable or repelling when it exists [101]. In this paper, Zeeman and Zeeman also found a computational condition for when an interior steady state of an n-species competitive system is globally attracting or repelling. This is based on the tangent plane of Σ at the interior steady state, thus the structure of Σ can provide information on the system as a whole.

Theorem 1.4.1 ([101]) *Given the competitive Lotka–Volterra n-species system with an interior steady state x^*, let H be the tangent plane to the carrying simplex Σ at x^*. If $\Sigma \setminus \{x^*\}$ lies above H then x^* is a global attractor in $\mathbb{R}^n_{>0}$, if $\Sigma \setminus \{x^*\}$ lies below H then x^* repels in $\mathbb{R}^n_{>0}$ excluding its 1-dimensional stable manifold.*

This theorem is based around a split-Lyapunov function with respect to H.

Definition 1.4.3 ([101]) The split-Lyapunov function V with respect to H is a function defined on $\mathbb{R}^n_{>0}$ such that:

$$\dot{V} > 0 \text{ in the region below } H,$$
$$\dot{V} = 0 \text{ on } H,$$
$$\dot{V} < 0 \text{ in the region above } H.$$

The split-Lyapunov function can be thought of as a generalisation of some $\frac{dx_i}{dt}$ and its nullcline. Zeeman and Zeeman found a split-Lyapunov function which works for any competitive Lotka–Volterra system, and a more computable version of Theorem 1.4.1 based on conditions for the signs of eigenvalues. Full details are in [101]. In [5], Baigent shows that in a competitive 3-species system, it is the local curvature near x^*

which can determine whether x^* is globally attracting or repelling in $\mathbb{R}^3_{>0}$, assuming Σ near x^* is of differentiability class C^2. In competitive 2-species Lotka–Volterra systems, it is known that the interior of Σ is C^1 [63].

In this thesis, we will explore the carrying simplex in 2- and 3-species scaled Lotka–Volterra systems. When these systems are not competitive, we will refer to Σ as the balance simplex (which is still defined as $\partial\mathcal{R}(0)$). We refer to it by a different name as we expect the aforementioned properties from the carrying simplex will no longer hold in the non-competitive systems.

We know the balance simplex must be invariant to the flow and contain all non-zero steady states. Thus in the 2-species case, we expect it to be composed of heteroclinic orbits connecting these non-zero steady states. Our aim for this case is to find an explicit, analytic solution for the balance simplex. For the 3-species case, our goal will be to find a reliable method of plotting the balance simplex, after proving its existence.

1.5 Thesis outline

The rest of this thesis is written as follows:

Chapters 2 and 3 considers Σ in general 2-species scaled Lotka–Volterra systems. In Chapter 2, we examine the partial derivatives of the transformed system, where we work with the proportion of species 1, and the total population density as variables. We find the parameter space where the partial derivatives of the dynamics remain bounded, meaning we can follow the ideas of Baigent's paper [5] using the Hadamard graph transform method [29]. This will prove the existence of Σ when $\alpha_{12}, \alpha_{21} < 2$, $\alpha_{12}, \alpha_{21} \neq 1$, and the system is not co-operative. This parameter space includes cases where species are weakly competitive, or where there is a predator-prey type relationship between the species and predation is not very strong.

In Chapter 3 we transform the 2-species system into polar co-ordinates. By doing this, we can solve the system using an integrating factor to find the general solution explicitly and identify the balance simplex. In this chapter, we will cover all possible parameter cases, as long as the dynamics are bounded (i.e. we exclude the strongly co-operative case where both $\alpha_{12}, \alpha_{21} < 0$ and $\alpha_{12}\alpha_{21} \geq 1$).

Chapters 4, 5 and 6 considers Σ in general 3-species scaled Lotka–Volterra systems. In Chapter 4, we follow the ideas of the 2-species explicit solution. We will find a parametric series solution in the form $x_1 = G(T_1, T_2), x_2 = T_1 G(T_1, T_2), x_3 = T_2 G(T_1, T_2)$. It matches exactly one of the known solutions on the boundaries, using this we can prove the existence of Σ when the dynamics of the system are bounded and $\alpha_{ij} < 1$ and $\alpha_{ij}\alpha_{ji} < 1$ for all $i \neq j$, $i, j \in \{1, 2, 3\}$. Physically, this excludes the case where species are strongly competitive or strongly co-operative. It also excludes the case where one species is heavily predated on by another. Additionally, this parametric solution gives the explicit form of Σ in the special case where $\alpha_{ij} = \frac{n}{n+1}$, $n \in \mathbb{N}$, for all $i \neq j$ (where G is now a polynomial). In this chapter we also prove that when the balance simplex exists, it is asymptotically complete. This also applies to the 2-species scaled Lotka–Volterra system.

In Chapter 5, we prove the existence of Σ as long as the interaction matrix $A = [\alpha_{ij}]$ is strictly copositive and compare this space to the parameter space discussed in Chapter 4. Physically, this means that the average fitness of the population is always positive.

Chapter 6 focuses on plotting an approximation of Σ in the 3-species system, since in general we do not have an explicit expression. The method resembles finding a Darboux polynomial [22], but we find an infinite series instead.

In Chapter 7 we consider general planar Kolmogorov systems with at most one interior steady state. By analysing the stability and Poincaré index [69] of steady states, we provide sufficient conditions for the balance manifold to exist. In this

chapter, we do not refer to Σ as the balance simplex as it may not project radially 1-to-1 to the unit simplex.

In Chapter 8 we give some concluding remarks on our results and state some possible areas for research in the future.

Chapter 2

The Extension of Parameters for Boundedness

In this chapter, we consider the 2-species scaled Lotka-Volterra system where all intrinsic growth rates and intraspecific interaction coefficients are set to the value 1. We have the following system:

$$\begin{aligned} \frac{dx_1}{dt} &= x_1(1 - x_1 - \alpha x_2) =: F_1, \\ \frac{dx_2}{dt} &= x_2(1 - \beta x_1 - x_2) =: F_2, \end{aligned} \tag{2.1}$$

where we have denoted the interspecific interaction coefficients as $\alpha_{12} =: \alpha$ and $\alpha_{21} =: \beta$. We will denote the interaction matrix by A:

$$A = \begin{pmatrix} 1 & \alpha \\ \beta & 1 \end{pmatrix}. \tag{2.2}$$

To ensure we only consider hyperbolic steady states, we exclude the case where $\alpha = 1$ or $\beta = 1$. Towards the end of the chapter, our calculations will follow the ideas of Baigent's papers [4, 5] who proved the existence and uniqueness of the carrying simplex for the 3-species competitive Lotka–Volterra model using a method based on the graph transform method by Hadamard [29].

The idea is to start with an initial surface close to the origin such that under the semiflow of the system, φ_t ($t \geq 0$), it forms a sequence of increasing surfaces. Another initial surface is taken sufficiently far from the origin such that under the semiflow it forms a sequence of decreasing surfaces. Baigent showed that these two sequences converge to the same unique, invariant Lipschitz surface Σ which asymptotically attracts all non-zero solutions, i.e. the carrying simplex. This was achieved by examining how the unit normal of these surfaces changes in time, and by using the fact that competitive flows are order-preserving in backwards time, i.e. if $\varphi_t(x) \leq \varphi_t(y)$ then $\varphi_s(x) \leq \varphi_s(y)$ for all $s \leq t$. The methods and proofs used also apply to the 2-species competitive case.

The aim of this thesis is to explore the carrying simplex in non-competitive systems, we refer to this as a balance simplex, as not all the properties of a carrying simplex will hold. We know that for the Lotka–Volterra model with positive intrinsic growth rates, the carrying simplex is the boundary (relative to $\mathbb{R}^n_{\geq 0}$) of the basin of repulsion of the origin, which is equal to the boundary (relative to $\mathbb{R}^n_{\geq 0}$) of the basin of repulsion of infinity [101]. Thus in the 2-species model, the carrying simplex is composed of the (unique) heteroclinic orbits connecting non-zero steady states, including these states [4].

Definition 2.0.1 For the n-species Lotka–Volterra equations, the balance simplex Σ will always refer to the set $\partial\mathcal{R}(0)$, the boundary (relative to $\mathbb{R}^n_{\geq 0}$) of the basin of repulsion of the origin $\mathcal{R}(0)$. When the system is competitive, it is precisely the carrying simplex.

Remark 2.0.1 *We will often refer to the balance simplex as a manifold to keep the terminology consistent with the carrying simplex. In the upcoming chapters of this thesis, we will see that Σ may not be smooth everywhere, however it will be composed piecewise of analytic manifolds (namely the unstable manifolds of non-zero steady states).*

For non-competitive systems, we do not generally have the property of order preservation in backwards time. Instead, we consider a transformation of the 2-species system into the total population density and the proportion of species 1. We will find the space where the parameters (α and β) keep the partial derivatives of the dynamics bounded. This enables us to find a sequence of Lipschitz surfaces as in Baigent's paper [5].

2.1 Jacobian analysis

Before we start, it will be useful to classify the stability of the steady states of (2.1). The Jacobian matrices are:

$$\mathcal{J}(0,0) = \begin{pmatrix} 1 & 0 \\ 0 & 1 \end{pmatrix}, \tag{2.3}$$

$$\mathcal{J}(0,1) = \begin{pmatrix} 1-\alpha & 0 \\ -\beta & -1 \end{pmatrix}, \tag{2.4}$$

$$\mathcal{J}(1,0) = \begin{pmatrix} -1 & -\alpha \\ 0 & 1-\beta \end{pmatrix}, \tag{2.5}$$

$$\mathcal{J}(x^*) = \begin{pmatrix} -x_1^* & -\alpha x_1^* \\ -\beta x_2^* & -x_2^* \end{pmatrix}; \quad x_1^*,\ x_2^* > 0. \tag{2.6}$$

We denote the interior steady state by $x^* := \left(\frac{\alpha-1}{\alpha\beta-1}, \frac{\beta-1}{\alpha\beta-1}\right)$ which exists when it lies in $\mathbb{R}^2_{>0}$. By examining the signs of the traces and determinants:

- The origin is always an unstable node.
- If $\alpha < 1$ and $\beta > 1$, then x^* does not exist, $(0,1)$ is a saddle point and $(1,0)$ is a stable node.
- If ($\alpha = 1$ and $\beta > 1$) or ($\alpha < 1$ and $\beta = 1$), then x^* does not exist. One of the Jacobian matrices of the axial steady states will have an eigenvalue of 0 meaning that state is non-hyperbolic. We do not consider these cases but discuss them here for completeness. By plotting the phase plane and considering the nullclines, we again find that $(0,1)$ is a saddle point and $(1,0)$ is a stable node.
- If ($\alpha \geq 1$ and $\beta < 1$) or ($\alpha > 1$ and $\beta \leq 1$), then x^* does not exist and $(0,1)$ is a stable node and $(1,0)$ is a saddle point.

- If both $\alpha, \beta > 1$ then x^* exists as a saddle point and both axial steady states are stable nodes.

- If both $\alpha, \beta < 1$ and $\alpha\beta < 1$, then x^* exists as a stable node and both axial states are saddle points.

- If both $\alpha, \beta < 1$ and $\alpha\beta \geq 1$, then x^* does not exist and both axial steady states are saddle points; the dynamics are unbounded. The concept of a balance simplex is not applicable and both species are strongly co-operative.

- If both $\alpha = \beta = 1$ then all the points on the line $x_2 = 1 - x_1$ (joining both axial steady states) are interior steady states. For this case, this line is the carrying simplex.

Note that when the axial steady states are saddle points, their stable manifold is always the axis they lie on. This can be shown with the eigenvectors, or the fact that the origin and infinity are always repelling in our system. For these axial saddle points, the unstable manifold is tangent to the (unique) unstable eigenvector pointing into $\mathbb{R}^2_{>0}$ and forms the heteroclinic orbit. Note also that in this system one of the ends of all heteroclinic orbits is a saddle point.

Note the following:

Lemma 2.1.1 *The system (2.1) has no interior non-trivial periodic orbits.*

Proof: Follows directly from the statement of the Dulac Theorem [69] with the Dulac function $\sigma(x) = \frac{1}{x_1 x_2}$. Indeed,

$$\operatorname{div}(\sigma(F_1, F_2)) = -\frac{1}{x_1} - \frac{1}{x^2} < 0;\ x = (x_1, x_2) \in \mathbb{R}^2_{>0},$$

and so there can be no non-trivial periodic orbits lying completely in $\mathbb{R}^2_{>0}$. □

2.2 Transformation to (u,N)-co-ordinates

Consider the n-species scaled Lotka–Volterra system. We transform this to the (u, N) co-ordinates where $u = (u_1, \ldots, u_n)^T$ is the vector containing the proportions of each species, and $N = x_1 + \ldots + x_n$ is the total population density. Note that $u_i = \frac{x_i}{N},\ i = 1, \ldots, n$. The dynamics in this new co-ordinate system is given by:

$$\begin{aligned}
\frac{dN}{dt} &= \sum_{i=1}^{n} N u_i (1 - N(Au)_i) \\
&= N - N^2 u^T A u, \\
\frac{du_i}{dt} &= u_i(1 - N(Au)_i) - u_i(1 - N u^T A u) \\
&= u_i N (u^T A u - (Au)_i),
\end{aligned}$$

where $i = 1, \ldots, n-1$ and the proportion of species n is given by $u_n = 1 - u_1 - \ldots - u_{n-1}$. We can rescale time by N without affecting the qualitative behaviour on the phase plane (except that it will no longer show that $N = 0$ is a steady state). The positions and stability of the other steady states remain unaffected. Keeping the same notation for t and the derivative, we have the system:

$$\frac{dN}{dt} = 1 - N u^T A u, \tag{2.7}$$

$$\frac{du_i}{dt} = u_i (u^T A u - (Au)_i), \qquad i = 1, \ldots, n-1. \tag{2.8}$$

Note that the u_i dynamics are now independent of N. This decoupling of the u dynamics has been used by several authors (e.g. [15, 104]) and relies on the fact that all species have the same intrinsic growth rate (in this case, $r_i = 1$).

For now, we focus on the 2-species case, where the proportion of species 1 is denoted by u (and the proportion of species 2 is $1 - u$). An example of the phase portrait in both co-ordinate systems is shown in Figure 2.1. We will denote $B :=$

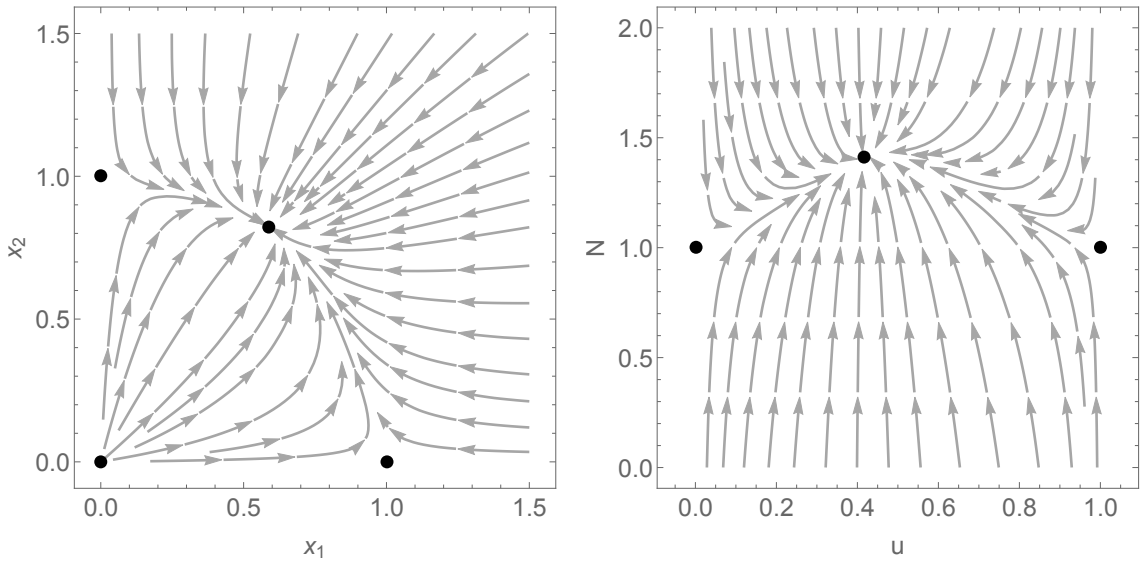

(a) (x_1, x_2)-co-ordinates (b) (u, N)-co-ordinates

Figure 2.1: A competitive 2-species scaled Lotka–Volterra system (2.1) where $\alpha = 0.5$ and $\beta = 0.3$ shown in the two co-ordinates systems we consider. Recall that u is the proportion of species 1, and N is the total population density of both species. The black points are the steady states. The interior steady state is globally attracting on the interior.

$\alpha + \beta - 2$. In (u, N) co-ordinates, the space we consider is $[0, 1] \times [0, \infty)$ and the dynamics are:

$$\begin{aligned} \frac{dN}{dt} &= 1 - (1 + Bu - Bu^2)N \\ &=: 1 - h(u)N, \qquad (2.9) \\ \frac{du}{dt} &= u(1-u)(1 - \alpha + Bu) \\ &=: g(u). \qquad (2.10) \end{aligned}$$

Note that u can be solved for independently of N, and the solution for this system is in the form $N = N(u(t), t)$ which is smooth as the vector field is smooth [8]. Additionally, we assume the system is bounded, from the previous section we know the unbounded case is where both species are strongly co-operative, i.e. $\alpha, \beta < 0$ and $\alpha\beta \geq 1$. The new co-ordinate system maps the origin $(x_1, x_2) = 0$ to the line $N = 0$. The axial steady states $(x_1, x_2) = (0, 1)$ and $(1, 0)$ are mapped to $(u, N) = (0, 1)$ and

$(1,1)$ (respectively). We consider an initial condition $N(u,0) = \epsilon > 0$ (where ϵ is arbitrarily small) for $u \in [0,1]$ and evolve this line with the flow of the system over time. Note that on this initial line, $\frac{\partial N}{\partial u}$ is bounded. We consider:

$$\frac{dN}{dt} = \frac{\partial N}{\partial t} + g(u)\frac{\partial N}{\partial u} = 1 - h(u)N. \tag{2.11}$$

Taking the partial derivative with respect to u and rearranging using the total time derivative:

$$\begin{aligned} & \frac{\partial}{\partial t}\frac{\partial N}{\partial u} + g'(u)\frac{\partial N}{\partial u} + g(u)\frac{\partial^2 N}{\partial u^2} = -h'(u)N - h(u)\frac{\partial N}{\partial u}, \\ \Rightarrow \quad & \frac{d}{dt}\frac{\partial N}{\partial u} = -(h(u) + g'(u))\frac{\partial N}{\partial u} - h'(u)N, \end{aligned} \tag{2.12}$$

where the prime $'$ is used to denote the derivative with respect to u. On $u \in [0,1]$, the polynomials h and h' are bounded and we are assuming N remains bounded. If we additionally have $h(u) + g'(u) > 0$ for $u \in [0,1]$ this would mean that $\frac{\partial N}{\partial u}$ remains bounded for $t > 0$ and thus $\frac{\partial N}{\partial t}$ is also bounded for $t > 0$ by equation (2.11). This means the solution $N(u,t)$ is a Lipschitz function in u and t (see [66] and also Lemma 2.2.1); as we evolve our initial line with the flow, it remains Lipschitz and we know it remains bounded (with respect to the N co-ordinate).

Definition 2.2.1 A function $f : \mathbb{R}^2 \to \mathbb{R}$ is called Lipschitz if it is Lipschitz continuous, i.e. $|f(x) - f(y)| \leq C||x - y||$ for all $x, y \in \mathbb{R}^2$ where C is a constant, independent of x, y. The norm $||\cdot||$ is the Euclidean norm.

Lemma 2.2.1 *If $\frac{\partial N}{\partial u}$ and $\frac{\partial N}{\partial t}$ are bounded for $u \in [0,1]$, $t \geq 0$ then $N(u,t)$ is a Lipschitz function in the variables u and t.*

Proof: Define the finite constants:

$$M_1 = \sup\left\{ \left| \frac{\partial N}{\partial u}(u,t) \right| \mid (u,t) \in [0,1] \times [0,\infty) \right\}, \tag{2.13}$$

$$M_2 = \sup\left\{\left|\frac{\partial N}{\partial t}(u,t)\right| \mid (u,t) \in [0,1]\times[0,\infty)\right\}. \tag{2.14}$$

Let $u_1, u_2 \in [0,1]$, $t_1, t_2 > 0$. By the triangle inequality:

$$|N(u_1,t_1) - N(u_2,t_2)| \leq |N(u_1,t_1) - N(u_1,t_2)| + |N(u_1,t_2) - N(u_2,t_2)|. \tag{2.15}$$

Using the Mean Value Theorem [71], there exists some T between t_1 and t_2 such that

$$\frac{N(u_1,t_1) - N(u_1,t_2)}{t_1 - t_2} = \frac{\partial N}{\partial t}(u_1,T), \tag{2.16}$$

thus $|N(u_1,t_1) - N(u_1,t_2)| \leq M_2|t_1 - t_2|$. Similarly $|N(u_1,t_2) - N(u_2,t_2)| \leq M_1|u_1 - u_2|$. We find that:

$$\begin{aligned} |N(u_1,t_1) - N(u_2,t_2)| &\leq M_2|t_1 - t_2| + M_1|u_1 - u_2| \\ &\leq \sqrt{M_1^2 + M_2^2}\ ||(u_1,t_1) - (u_2,t_2)||, \end{aligned} \tag{2.17}$$

where we have used the Cauchy–Schwarz inequality [71]. Thus $N(u,t)$ is a Lipschitz function in the variables u and t, with the Lipschitz constant $\sqrt{M_1^2 + M_2^2}$. □

Therefore, we can form a sequence of uniformly bounded functions that are Lipschitz, $\{N(u,t)\}_{t\in\mathbb{N}} = \{N_t\}$, of which there exists a convergent subsequence, converging to a function which is also Lipschitz. This follows from a version of the Arzelà–Ascoli theorem [66, 71]:

Theorem 2.2.2 (Arzelà–Ascoli) *If $\{f_n\}_{n\in\mathbb{N}}$ is a uniformly bounded sequence of real valued functions on $[a,b]$ such that each f_n is Lipschitz continuous with the same Lipschitz constant, then there is a subsequence that converges uniformly on $[a,b]$. The limit function is also Lipschitz continuous with the same Lipschitz constant.*

The fact that each function in $\{N_t\}$ has the same Lipschitz constant follows from

the fact that the partial derivatives of N can be bounded by the same bound for any $t > 0$ (see M_1 and M_2 in the proof of Lemma 2.2.1).

2.3 The boundedness of $\frac{\partial N}{\partial u}$

The condition $h(u) + g'(u) > 0$ is equivalent to requiring $\max_{u\in[0,1]}[-h(u) - g'(u)] < 0$ which simplifies to:

$$\max_{u\in[0,1]}[\alpha - 2 + u(2(1-\alpha) - 3B) + 4Bu^2] =: \max_{u\in[0,1]}[M(u)] < 0. \tag{2.18}$$

Recall that $B = \alpha + \beta - 2$. $M(u)$ has a turning point $\widetilde{u} = \frac{-2(1-\alpha)+3B}{8B}$, at which the second derivative is $M''(\widetilde{u}) = 8B$. We now have several distinct cases:

1. $\widetilde{u} \in (0,1)$ and $B > 0$. This implies $\widetilde{u}$ is a minimum so we want the endpoints of $M(u)$ to be negative, i.e. $\max\{\alpha - 2, \beta - 2\} < 0$.

2. $\widetilde{u} \in (0,1)$ and $B < 0$. Here, $\widetilde{u}$ is a maximum, so we want $M(\widetilde{u}) < 0$. This simplifies to $9\alpha^2 - 16\alpha + 14\alpha\beta - 16\beta + 9\beta^2 < 0$ which gives an ellipse contained in $[-1,2]^2$ of the $\alpha\beta$-plane. The condition $\widetilde{u} \in (0,1)$ will remove parts of this ellipse.

3. $\widetilde{u} \notin (0,1)$. For this case, just consider the end points again, i.e. we want $\max\{\alpha - 2, \beta - 2\} < 0$.

4. $B = 0$ (which occurs on the line $\alpha + \beta = 2$). In this case, we would consider (2.18) directly, which gives $\max\{\alpha - 2, -\alpha\} < 0$.

The regions on which one of these cases is satisfied will be denoted by Ω, shown in Figure 2.2. We can conclude that any $(\alpha, \beta) \in \Omega$ implies $\frac{\partial N}{\partial u}$ remains bounded for any $t > 0$ (thus also the boundedness of $\frac{\partial N}{\partial t}$). This then implies our functions

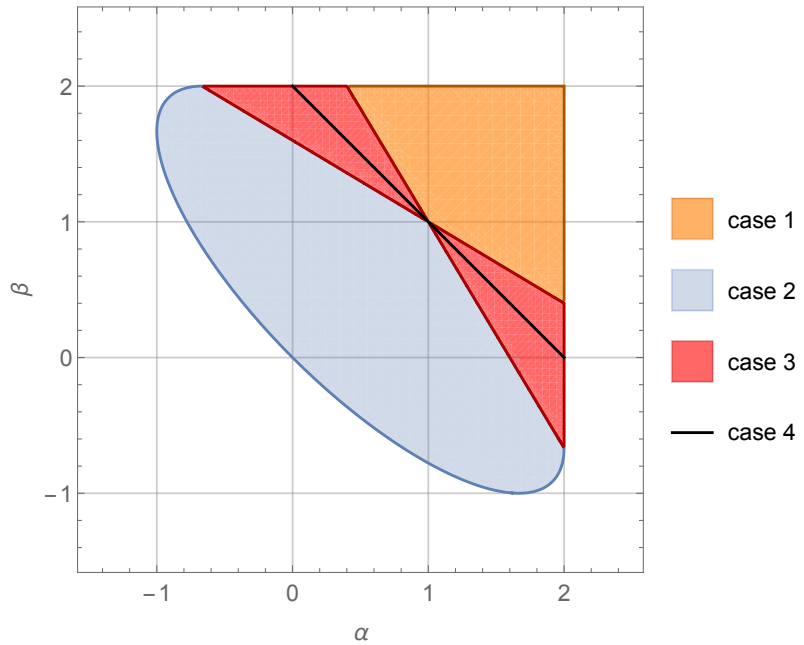

Figure 2.2: The four distinct, open regions on the $\alpha\beta$-plane which imply the boundedness of $\frac{\partial N}{\partial u}$. The union of these regions is denoted by Ω. Note that Ω does not include values where both $\alpha, \beta < 0$ (the co-operative case).

$\{N_t\}$ are Lipschitz and so on as described previously. We will show these functions converge to the balance simplex (Definition 2.0.1).

The most notable result is that we have regions where one of the parameters is positive and the other negative which has not been discussed before in the context of carrying simplices. The disadvantage of changing to (u, N) co-ordinates is that our region does not cover all competitive cases (specifically, the case where the species are very strongly competing), where we know the carrying simplex exists by the work of Hirsch [35]. This parameter space does include cases where species are weakly competitive, or where there is a predator-prey type relationship between the species but the prey is not strongly beneficial to the predator.

2.4 Convergence to a unique balance simplex

With the assumption $(\alpha, \beta) \in \Omega$, we have a sequence of uniformly bounded Lipschitz functions $\{N_t\}$ in the uN-plane. For the solution $N(u,t)$ with fixed t, denote the region underneath it (containing the line $N = 0$) by $N_-(u,t) = \{(u_0, N_0) \mid N_0 < N(u_0,t)\}$ and the (unbounded) region above it by $N_+(u,t) = \{(u_0, N_0) \mid N_0 > N(u_0,t)\}$.

If we start with $N(u,0) = \epsilon > 0$ sufficiently small, then $\frac{dN}{dt} > 0$ thus the set $N_-(u,t_1) \subset N_-(u,t_2)$ for any $0 \leq t_1 < t_2$. This means that $\{N_t\}$ is an increasing (with respect to the N co-ordinate at each u), uniformly bounded sequence of Lipschitz functions which converges to some Σ_1, say. Similarly, if $\epsilon > 0$ was sufficiently large, then $\frac{dN}{dt} < 0$ and $N_-(u,t_2) \subset N_-(u,t_1)$ for any $0 \leq t_1 < t_2$. In this case, $\{N_t\}$ is now a decreasing, uniformly bounded sequence of Lipschitz functions which converges to some Σ_2, say. We have found two limits from above and below and aim to show they are equal. When discussing convergence using the (x_1, x_2)-co-ordinates, we will denote these two limit sets as Σ_1^x and Σ_2^x.

Lemma 2.4.1 *Σ_1 lies in the region under Σ_2, i.e. for any fixed $u_0 \in [0,1]$, $\Sigma_1(u_0) \leq \Sigma_2(u_0)$. The same statement holds in the x_1x_2-plane in the sense that the first intersection of any ray in $\mathbb{R}^2_{\geq 0}$ from the origin must either be with Σ_1^x, or both Σ_1^x and Σ_2^x simultaneously.*

Proof: In the uN-plane, the statement holds due to the construction of Σ_1 and Σ_2. In the x_1x_2-plane, the statement follows when considering the analogous limit sets Σ_1^x and Σ_2^x. □

Lemma 2.4.2 *In the uN-plane, Σ_1 and Σ_2 both intersect the line $u = 0$ at the steady state $(0,1)$, and the line $u = 1$ at the steady state $(1,1)$.*

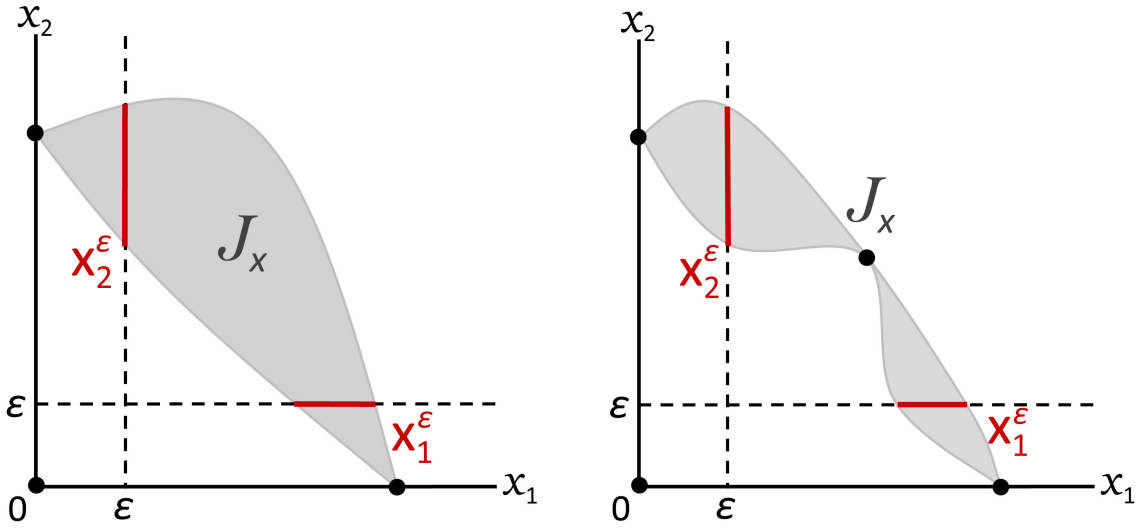

(a) x^* does not exist (b) x^* does exist

Figure 2.3: The region J_x is shaded in grey. The red lines are X_1^ε and X_2^ε which are dependent on the arbitrarily small parameter $\varepsilon > 0$. When the interior steady state x^* does exist, we expect that $x^* \in \partial J_x$ due to its invariance. In this case, J_x is split into two distinct regions.

In the x_1x_2-plane, Σ_1^x and Σ_2^x both intersect the x_1-axis at the axial steady state $(1, 0)$ and the x_2-axis at the axial steady state $(0, 1)$.

Proof: Since Σ_1 and Σ_2 are the limits of a sequence of functions which evolve with the flow of the system (2.9) and (2.10), they are invariant to the flow. Thus they are also invariant on the lines boundary lines $u = 0$ and $u = 1$.

Recall that for the system (2.1) in x-co-ordinates, there is a unique non-zero steady state which attracts all positive points on the x_1-axis, and similarly for the x_2-axis. This also true for the lines $u = 0$ and $u = 1$ when we consider the uN-plane, where the steady states are $(1, 0)$ and $(1, 1)$. It is clear then that $\Sigma_1 \cap \{u = 0\} = \Sigma_2 \cap \{u = 0\} = (0, 1)$ and $\Sigma_1 \cap \{u = 1\} = \Sigma_2 \cap \{u = 1\} = (1, 1)$.

The statement in the x_1x_2-plane follows when considering Σ_1^x and Σ_2^x. □

Claim 1 *Let J_u be the region enclosed by Σ_1 and Σ_2. It is not possible for $\Sigma_1 \neq \Sigma_2$ and J_u to have an area of 0 for the system (2.9), (2.10).*

Proof: Σ_1 and Σ_2 are continuous, Lipschitz curves which are invariant to the flow of (2.9), (2.10). The only possibility for the statement of the claim to be true is if Σ_1

and Σ_2 differs from each other by 'spikes' of zero area. The neighbourhood around these spikes would contradict the Lipschitz property (Definition 2.2.1). □

Lemma 2.4.3 *The two limit functions Σ_1 and Σ_2 are equal.*

Proof: Suppose $\Sigma_1 \neq \Sigma_2$ and that there is a non-empty region enclosed by the two curves called J_u (the case where the inequality holds but this enclosed region is empty was handled in Claim 1). By Lemma 2.4.2, $\partial J_u \cap \{u = 0\} = (0, 1)$ and $\partial J_u \cap \{u = 1\} = (1, 1)$, where ∂J_u denotes the boundary of J_u.

The change in co-ordinates $(x_1, x_2) \mapsto (u, N)$ is a bijection if we exclude the origin in the x_1x_2-plane and the line $N = 0$ in the uN-plane. We know that $N = 0$ is repelling so it does not intersect Σ_1 or Σ_2. Thus we can map Σ_1 and Σ_2 back to the x_1x_2-plane where they are still continuous, bounded curves denoted by Σ_1^x and Σ_2^x respectively. In the x_1x_2-plane, J_u is mapped to a region we will denote by J_x (the shaded region in Figure 2.3). The boundary ∂J_x touches the x_1-axis at $(1, 0)$ and the x_2-axis at $(0, 1)$. Following Baigent's paper [4], we work with these regions in the x_1x_2-plane.

Consider a small $\varepsilon > 0$ and the domain $[\varepsilon, \infty)^2 =: \mathbb{R}^2_{\geq\varepsilon}$. Denote $J_x \cap \mathbb{R}^2_{\geq\varepsilon}$ by J_x^ε. For the boundary ∂J_x^ε, label the horizontal segment $\partial J_x^\varepsilon \cap \{x_2 = \varepsilon\} =: X_1^\varepsilon$ and the vertical segment $\partial J_x^\varepsilon \cap \{x_1 = \varepsilon\} =: X_2^\varepsilon$ (See again Figure 2.3 showing these regions). We know that X_1^ε and X_2^ε each resemble the connected lines shown in Figure 2.3 since ε can be made arbitrarily small and we are only considering hyperbolic steady states (the local dynamics are completely known due to the Hartman–Grobman Theorem [69]). Since the axial steady states are either saddles or stable nodes (recall the classification in Section 2.1), ∂J_x will not intersect the lines $x_1 = \varepsilon$ or $x_2 = \varepsilon$ each more than twice.

Let $\sigma(x) = \frac{1}{x_1x_2}$ for any $x \in \mathbb{R}^2_{\geq\varepsilon}$. Recall that the vector field of the system (2.1)

is denoted by $F_i(x) := x_i f_i(x)$ and $F = (F_1, F_2)$.

$$\operatorname{div}(\sigma F) = -\frac{1}{x_1} - \frac{1}{x_2}, \tag{2.19}$$

note that in $\mathbb{R}^2_{\geq\varepsilon}$, $\operatorname{div}(\sigma F) < 0$.

Now we consider the Divergence Theorem [81] on J_x^ε:

$$\int_{\partial J_x^\varepsilon} \sigma F \cdot n \, dS = \int_{J_x^\varepsilon} \operatorname{div}(\sigma F) \, dV, \tag{2.20}$$

where n denotes the outward pointing unit normal vector of ∂J_x^ε (taken anticlockwise), dS is a line element and dV is a volume element. We know that

$$\int_{J_x^\varepsilon} \operatorname{div}(\sigma F) \, dV < 0, \tag{2.21}$$

and the value of this integral decreases as $\varepsilon > 0$ decreases, since the integrand is negative and J_x^ε would increase in area. We know that on $\partial J_x^\varepsilon \setminus (X_1^\varepsilon \cup X_2^\varepsilon)$, $F.n = 0$ since ∂J_x is composed of the limit sets Σ_1^x and Σ_2^x which are tangent to flow everywhere, except at the finite number of steady states, where $F = 0$.

If x^* exists, it lies on ∂J_x due to invariance. At this point, the unit normal is well defined:

$$n = \frac{\nabla F}{|\nabla F|}, \tag{2.22}$$

$$\nabla F(x^*) = (-x_1^*, -x_2^*)^T \neq 0. \tag{2.23}$$

For the line integral then, we have

$$\begin{aligned} \int_{\partial J_x^\varepsilon} \sigma F \cdot n \, dS &= 0 - \int_{X_1^\varepsilon} \frac{f_2(x_1, \varepsilon)}{x_1} dx_1 - \int_{X_2^\varepsilon} \frac{f_1(\varepsilon, x_2)}{x_2} dx_2 \\ &= -\int_{X_1^\varepsilon} \frac{1 - \beta x_1 - \varepsilon}{x_1} dx_1 - \int_{X_2^\varepsilon} \frac{1 - \varepsilon - \alpha x_2}{x_2} dx_2. \end{aligned} \tag{2.24}$$

Using the triangle inequality:

$$\left|\int_{\partial J_x^\varepsilon} \sigma F \cdot n \, dS\right| \leq |X_1^\varepsilon| \max_{x \in X_1^\varepsilon} \left|\frac{1-\beta x_1 - \varepsilon}{x_1}\right| + |X_2^\varepsilon| \max_{x \in X_2^\varepsilon} \left|\frac{1-\varepsilon-\alpha x_2}{x_2}\right|. \tag{2.25}$$

Recalling Lemma 2.4.2, we note that as $\epsilon \to 0$, X_1^ε and X_2^ε become shorter in length and all points on these lines converge to $(x_1, x_2) = (1, 0)$ and $(0, 1)$ respectively, thus the terms in the maximum functions remain bounded in this limit. This means the line integral (2.24) is tending to 0 as $\varepsilon \to 0$, whereas the area integral (2.21) is becoming larger in magnitude (since it is negative and decreasing as $\varepsilon > 0$ decreases).

We can thus choose an $\varepsilon > 0$ such that (2.20) does not hold, contradicting the Divergence Theorem. We can conclude that J_x has an area of 0 and $\Sigma_1 = \Sigma_2$. □

With the calculations in the proof of Lemma 2.4.3, we also find the following:

Corollary 2.4.4 *The system (2.1) has no interior non-trivial closed orbits.*

Proof: The non-trivial periodic orbits were covered by Lemma 2.1.1. The only remaining case is homoclinic orbits of the interior steady state x^*. We consider the Divergence Theorem for the homoclinic orbit $H(x^*)$, and the function $\sigma = \frac{1}{x_1 x_2}$ in $\mathbb{R}^2_{>0}$. See equation (2.20) but with J_x^ε replaced with $H(x^*)$.

On $H(x^*)$, n is perpendicular to F everywhere except possibly at x^*. From (2.22), $n(x^*)$ is finite thus will not effect the value of the line integral. Since the integrand $\sigma F \cdot n = 0$ everywhere else on $H(x^*)$, the line integral is zero, contradicting the equality with the area integral from the Divergence Theorem. Thus no such homoclinic orbit exists $H(x^*)$. □

2.5 Extension of the previous parameter space

Our previous parameter space Ω was contained in $[-1,2]^2$. We can improve on this result by using a different transformation from the (x_1, x_2) co-ordinates in $\mathbb{R}^2_{\geq 0}$. For $a, b > 0$, let $x_1 = Sva$ and $x_2 = S(1-v)b$; we consider the new co-ordinates (v, S) where

$$S = \frac{1}{a}x_1 + \frac{1}{b}x_2, \tag{2.26}$$

$$v = \frac{x_1}{aS}. \tag{2.27}$$

Note that the boundedness of the system in (x_1, x_2) co-ordinates implies the boundedness of S. When $x_1 = 0$ we have $v = 0$, otherwise $v = (1 + \frac{ax_2}{bx_1})^{-1}$ so $v \in [0,1]$. The dynamics are:

$$\begin{aligned}\frac{dS}{dt} &= S + S^2[b(v-1)(1+v(\alpha-1)) + av(v(\beta-1)-\beta)],\\ \frac{dv}{dt} &= S(1-v)v[b(v-1)(\alpha-1) + av(\beta-1)].\end{aligned} \tag{2.28}$$

By rescaling time by S and simplifying, we have:

$$\begin{aligned}\frac{dS}{dt} &= 1 - S[b + v(b(\alpha-2)+a\beta) + v^2(b(1-\alpha)+a(1-\beta))]\\ &=: 1 - \widetilde{h}(v)S,\\ \frac{dv}{dt} &= v(1-v)[b(v-1)(\alpha-1) + av(\beta-1)]\\ &=: \widetilde{g}(v).\end{aligned} \tag{2.29}$$

Note that

$$\frac{dS}{dt} = \frac{\partial S}{\partial t} + \widetilde{g}(v)\frac{\partial S}{\partial v}. \tag{2.30}$$

We can find our parameter space following the previous method,

$$\frac{d}{dt}\frac{\partial S}{\partial v} = -\left(\widetilde{h}(v) + \widetilde{g}'(v)\right)\frac{\partial S}{\partial v} - \widetilde{h}'(v)S. \tag{2.31}$$

We want $\widetilde{h}(v) + \widetilde{g}'(v) > 0$ on $v \in [0,1]$ which is equivalent to $\max_{v\in[0,1]}[-\widetilde{h}(v) - \widetilde{g}'(v)] < 0$, i.e.

$$\begin{aligned}&\max_{v\in[0,1]} b(\alpha-2) + v[b(6-5\alpha) + a(2-3\beta)] + 4v^2[b(\alpha-1) + a(\beta-1)]\\ &=: \max_{v\in[0,1]} \widetilde{M}(v) < 0.\end{aligned} \tag{2.32}$$

$\widetilde{M}(v)$ has a turning point

$$v_{\widetilde{M}} = \frac{b(5\alpha-6) + a(3\beta-2)}{8[b(\alpha-1) + a(\beta-1)]}, \tag{2.33}$$

at which the second derivative of $\widetilde{M}$ is $d := 8[b(\alpha-1) + a(\beta-1)]$. Now we have several distinct cases:

1. $v_{\widetilde{M}} \in (0,1)$ and $d > 0$. This implies $v_{\widetilde{M}}$ is a minimum so we want the end points of $\widetilde{M}(v)$ to be negative, i.e. $\max\{b(\alpha-2), a(\beta-2)\} < 0$. Since $a, b > 0$ this is equivalent to $\max\{\alpha-2, \beta-2\} < 0$.

2. $v_{\widetilde{M}} \in (0,1)$ and $d < 0$. This implies $v_{\widetilde{M}}$ is a maximum and we want $\widetilde{M}(v_{\widetilde{M}}) < 0$. The simplifies to $b^2(2-3\alpha)^2 + a^2(2-3\beta)^2 - 2ab(4+2\alpha+2\beta-7\alpha\beta) < 0$.

3. $v_{\widetilde{M}} \notin (0,1)$. For this case, we just consider the end points again, i.e. we want $\max\{\alpha-2, \beta-2\} < 0$.

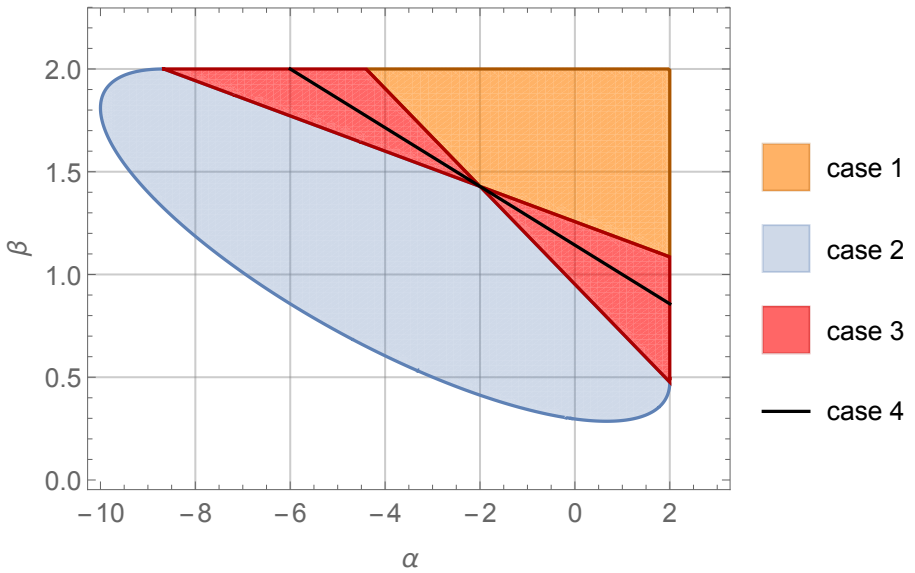

Figure 2.4: The union of cases 1 to 4 is $\widetilde{\Omega}$, where $\frac{\partial S}{\partial v}$ remains bounded. This is the parameter space where we can form a series of Lipschitz functions to show the balance simplex Σ exists. This example uses $a = 7$ and $b = 1$ in the transformation to (v, S) co-ordinates.

4. $d = 0$ which occurs on the line $b(\alpha-1)+a(\beta-1) = 0$. In this case, we consider equation (2.32) directly, i.e. $\max\{b(\alpha-2), 4b(1-\alpha)+a(2-3\beta)\} < 0$. Using $d = 0$ and $a, b > 0$ this simplifies to $\max\{\alpha-2, \beta-2\} < 0$.

Let $\widetilde{\Omega}$ be the space where the parameters (α, β) satisfies one of the cases above, where $\frac{\partial S}{\partial v}$ remains bounded for any $t > 0$. An example of this region is shown in Figure 2.4. If $\widetilde{\Omega}$ is non-empty then the sequence of functions $\{S(v,t)\}_{t\in\mathbb{N}} =: \{S_t\}$ are Lipschitz and we can follow the previous arguments to find a unique Σ. Note that the transformation $(x_1, x_2) \mapsto (v, S)$ is still bijective, excluding the origin $(x_1, x_2) = (0, 0)$ and the line $S = 0$.

Our plots show that the previous parameter space Ω can be extended in one of the negative directions to form $\widetilde{\Omega}$. This transformation still does not include the co-operative case where both $\alpha, \beta < 0$. Since the competitive case has already been studied, we focus on the case where α and β have different signs.

Lemma 2.5.1 *Suppose α and β are not equal to 1, have different signs and $\max\{\alpha, \beta\} < 2$. Then the balance simplex Σ exists.*

Proof: Without loss of generality suppose $0 < \alpha < 2$ and $\beta < 0$. It is always possible to choose $a > 0$ and $b > 0$ such that $d = 8[b(\alpha-1)+a(\beta-1)] > 0$. By doing this, we are in case 1 or 3 of $\widetilde{\Omega}$. However, $\max\{\alpha-2, \beta-2\} < 0$ is automatically satisfied, so regardless of $v_{\widetilde{M}}$, we have $(\alpha, \beta) \in \widetilde{\Omega}$. This means we can find $a, b > 0$ such that $\frac{\partial S}{\partial v}$ remains bounded for any non-negative time and we can repeat the previous arguments in Section 2.4 to find a unique Σ. □

The physical interpretation of $0 < \alpha < 2$ and $\beta < 0$ is that species 1 benefits from species 2, whilst species 2 has a negative effect from species 1. Species 1 can then be described as a predator of species 2. Note that this is not the classic Lotka–Volterra predator-prey system since all of our species have the same intraspecific competition coefficients and positive intrinsic growth rates.

2.6 Conclusions

In this chapter, we have proved the existence of the balance simplex for (2.1) when both interspecific interaction coefficients satisfy $\alpha, \beta < 2$, $\alpha, \beta \neq 1$ and the system is not co-operative. This parameter space includes cases where species are weakly competitive, or where there is a predator-prey type relationship between the species and predation is not very strong. The balance simplex is analogous to the carrying simplex for the Lotka–Volterra 2-species model in that it is an invariant curve which asymptotically attracts all non-zero solutions. It separates $\mathbb{R}^2_{\geq 0}$ into two regions where orbits have their α-limit as either the origin, or infinity.

The method differs slightly from the one used by Baigent [5] as it involves using the uN-plane, where u is the proportion of species 1, and $N = x_1 + x_2$ is the total number of individuals in the system. This enabled us to find conditions on the parameters α and β where the partial derivatives of N remain bounded for all $t > 0$, this is shown in Figure 2.2. With these conditions, we have a sequence of uniformly

bounded, Lipschitz functions (in the variables u and t) starting either near the origin, or far from it. There will be a convergent subsequence and we showed the limits of these two sets of sequences are equal to the (invariant) balance simplex. We were able to extend this parameter space to non-competitive cases, as long as the system was not co-operative and both $\alpha, \beta < 2$ and $\alpha, \beta \neq 1$.

Whilst the existence of $\Sigma = \partial\mathcal{R}(0)$ could have been examined through the use of the Poincaré-Bendixson Theorem [84] (which we will consider in Chapter 7), our method here shows that Σ is still an attracting Lipschitz manifold for some non-competitive systems.

Chapter 3

The Explicit Solution for the Balance Simplex of 2-Species Scaled Lotka–Volterra Systems

In this chapter, we discuss the methods and results of our recent paper [18], where we derive explicit expressions for the balance simplex in 2-species scaled Lotka–Volterra systems with any parameters (as long as the dynamics are bounded). The main method will involve transforming the system to polar co-ordinates where the exact solution can be found using an integrating factor. We discuss the convergence of this solution in different parameter cases and show that it can also be written in the form of a Gaussian hypergeometric function [6].

3.1 Background

For a Lotka–Volterra system with 2-species, the phase portraits are well known [10,37,47]. However, explicit solutions are rare, whether for actual solutions [58,88], or for invariant manifolds [9,98]. Here we obtain an explicit and analytic solution for the heteroclinic orbits that connect non-zero steady states in a scaled Lotka–Volterra system (see (3.1) on the next page). This solution, which we call a *balance simplex* Σ, attracts all non-zero solutions and is invariant under the flow of the system. It also divides the phase plane into two distinct regions. The lower region (containing the origin) has solutions which are repelled by the origin. The unbounded region above Σ has solutions in the phase plane which are declining from infinity.

In the case where both species compete against one another, Σ is precisely the *carrying simplex* introduced by Hirsch [35]. The carrying simplex is a Lipschitz manifold that attracts all non-trivial solutions and has been studied in more general and higher dimensional systems (for continuous time see, for example, [5, 35, 85] and for discrete-time [40, 41]). Our solution Σ provides an explicit example of an analogue of the carrying simplex which also applies to predator-prey type or a co-operative interactions. Figure 3.1 shows schematic views of the carrying simplex and the balance simplex in a planar system.

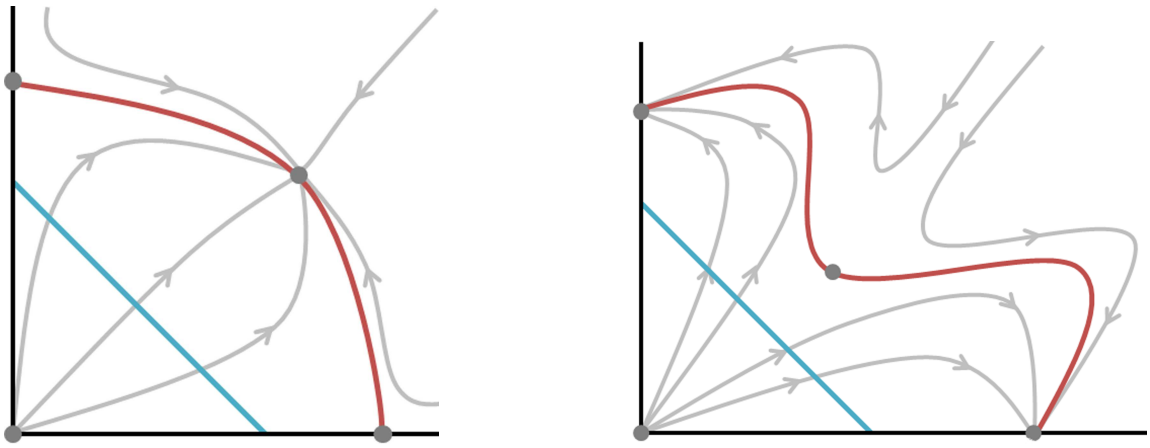

(a) Carrying simplex (b) Balance simplex

Figure 3.1: A general diagram of a carrying simplex and balance simplex in red. The diagonal blue line is the unit simplex and the four grey points in each plot are steady states of the system. The grey curves are solution orbits of the system.

3.2 2-species scaled Lotka–Volterra system

Recall the 2-species scaled Lotka–Volterra system, where all intrinsic growth rates are equal to 1 and the intraspecific interaction coefficients for both species are 1. The former condition means that the origin is always an unstable node, and the latter condition ensures there are no periodic orbits in $(0,\infty)^2$ [37] (see also Corollary 2.4.4 from Chapter 2). Taken together these conditions also mean that each species has a normalised carrying capacity of 1, i.e. we have two axial steady states: $(0,1)$ and $(1,0)$. The resulting system is:

$$\begin{aligned}\frac{dx_1}{dt} &= x_1(1-x_1-\alpha x_2),\\ \frac{dx_2}{dt} &= x_2(1-\beta x_1-x_2).\end{aligned} \tag{3.1}$$

> **Standing assumption:** The interspecific interaction coefficients α and β can be of any sign or zero, but $\alpha,\beta \neq 1$ (these cases will be discussed in Section 3.9).

Note that all solutions are repelled from infinity apart from in the strongly co-

operative case (where both $\alpha, \beta < 0$ and $\alpha\beta \geq 1$) which we do not consider as all positive solutions will be unbounded; the concept of a balance simplex is not applicable.

The system (3.1) has at most one interior steady state, $x^* = \left(\frac{\alpha-1}{\alpha\beta-1}, \frac{\beta-1}{\alpha\beta-1}\right)$, which we say exists when $x^* \in (0,\infty)^2$, i.e. when both $\alpha, \beta > 1$ or both $\alpha, \beta < 1$ and $\alpha\beta < 1$.

Definition 3.2.1 For the bounded system (3.1), we define the balance simplex Σ to be the boundary (taken relative to $\mathbb{R}^2_{\geq 0}$) of the basin of repulsion of the origin, i.e. $\Sigma = \partial\mathcal{R}(0)$.

Following the concept of the carrying simplex, the balance simplex will have the following properties:

i) Σ is compact and invariant under the flow of the system.

ii) Σ globally attracts all non-zero points in $[0,\infty)^2$. Note that this is not the same as asymptotic completeness from carrying simplices (see Chapter 1 Definition 1.3.3), which will be proven in Chapter 4 Theorem 4.5.2.

Thus Σ is compact, connected and contains all non-zero steady states, and Σ separates solutions which are repelled by the origin from those which decline from infinity. For the vast majority of parameter cases, we expect Σ to project radially 1-to-1 and onto the unit probability simplex [101].

A classification of the stability of the steady states in different parameter cases was given in the Chapter 2 Section 2.1. The hyperbolic cases are represented in Figure 3.2, showing their generic dynamics. In the next section, we will prove the following lemma by finding the exact expression for the balance simplex Σ.

Lemma 3.2.1 *When* $(\alpha, \beta) \in \mathbb{R}^2 \setminus \{(\alpha, \beta) : \alpha < 0, \beta < 0, \alpha\beta \geq 1\}$ *the planar system (3.1) has a compact and connected 1-dimensional invariant manifold* Σ *that*

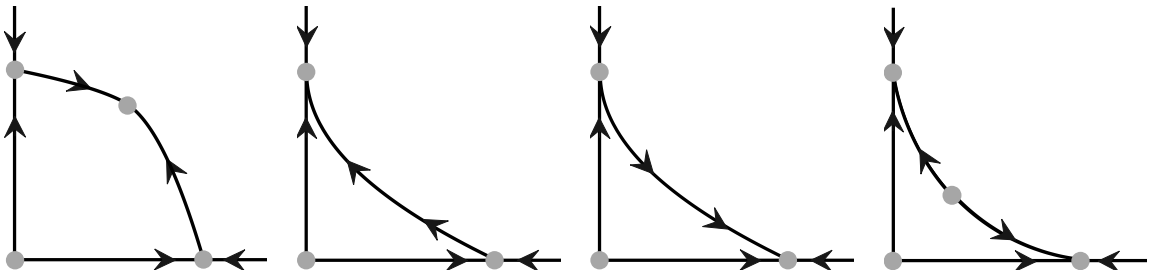

(a) $\alpha, \beta < 1$ * (b) $\alpha > 1, \beta < 1$ (c) $\alpha < 1, \beta > 1$ (d) $\alpha,\ \beta > 1$

Figure 3.2: Phase plots of 2-species scaled Lotka–Volterra systems in the x_1x_2-plane. These four plots cover the generic qualitative dynamics of the system with different interspecific interaction coefficients (α and β). The grey points are the steady states of the system and the arrows show how solution orbits evolve over time. *Note Figure 3.2a does not apply to the strongly co-operative case ($\alpha, \beta < 0$ and $\alpha\beta \geq 1$) where all positive solutions are unbounded.

globally attracts all non-zero solutions, and contains all non-zero steady states and the heteroclinic orbits connecting them.

3.3 Explicit expressions for the balance simplex

In this section we explicitly construct the balance simplex of Lemma 3.2.1 for all $(\alpha, \beta) \in \mathbb{R}^2 \setminus \{(a, b) : a < 0, b < 0, ab \geq 1\}$.

We begin by transforming (3.1) into polar co-ordinates:

$$\dot{\theta} = R\cos\theta\sin\theta[\cos\theta\ (1-\beta) + \sin\theta\ (\alpha - 1)],$$

$$\dot{R} = R[1 - R\cos^2\theta\ (\cos\theta + \alpha\sin\theta) - R\sin^2\theta\ (\sin\theta + \beta\cos\theta)].$$

With some simplification, we can write:

$$\frac{dR}{d\theta} - R\frac{B}{A} = -\frac{4}{A},$$

where $A = (1-\alpha)(\cos\theta - \cos 3\theta) - (1-\beta)(\sin\theta + \sin 3\theta)$ and $B = (3+\beta)\cos\theta +$

$(1-\beta)\cos 3\theta + (3+\alpha)\sin\theta - (1-\alpha)\sin 3\theta$.

To work with rational functions, we use the substitution $T = \tan\theta$. Note that we are only interested in the first quadrant, $\theta \in \left[0, \frac{\pi}{2}\right]$ (i.e. $T \in [0,\infty)$) and $T = \frac{x_2}{x_1}$. Using the chain rule, we can now write

$$\frac{dR}{dT} + R\,\frac{1+\alpha T+\beta T^2+T^3}{T(1+T^2)[(1-\beta)+T(\alpha-1)]} = \frac{\sqrt{1+T^2}}{T[(1-\beta)+T(\alpha-1)]}. \tag{3.2}$$

The differential equation (3.2) can be solved using the following integrating factor:

$$\nu(T) = \frac{T^{\frac{1}{1-\beta}}\Theta(T)^{\xi+1}}{\sqrt{1+T^2}}, \tag{3.3}$$

where $\Theta(T) = 1-\beta-T(1-\alpha)$ and $\xi+1 = \frac{-1+\alpha\beta}{(\alpha-1)(\beta-1)}$, i.e. $\xi = \frac{-2+\alpha+\beta}{(\alpha-1)(\beta-1)}$. Multiplying by this integrating factor, then integrating we obtain formally

$$R(T) = \frac{\int_0^T s^{\frac{\beta}{1-\beta}}\Theta(s)^{\xi}\,ds + C}{\nu(T)}, \tag{3.4}$$

where C is a constant. If $(T, R(T))$ is a local solution of (3.2) passing through the point $(T_0, R(T_0)) = (T_0, R_0)$ where $T_0 \in [0,\infty)$, then $(x_1(t), x_2(t)) := \left(\frac{R(t)}{\sqrt{1+t^2}}, \frac{tR(t)}{\sqrt{1+t^2}}\right)$ is a local solution of (3.1) passing through the point (x_0, y_0) where $x_0 = \frac{R_0}{\sqrt{1+T_0^2}}$ and $y_0 = \frac{T_0R_0}{\sqrt{1+T_0^2}}$. Different choices of T_0, R_0 determine the constant C in (3.4).

We define

$$\begin{aligned}\mu(T) &= \int_0^T s^{\frac{\beta}{1-\beta}}\Theta(s)^{\xi}\,ds \\ &= T^{\frac{1}{1-\beta}}(1-\beta)^{\xi}\int_0^1 s^{\frac{\beta}{1-\beta}}\left(1-\frac{sT}{T^*}\right)^{\xi}\,ds,\end{aligned} \tag{3.5}$$

where $T^* = \frac{\beta-1}{\alpha-1}$ (which may be positive or negative – recall that we restrict $\alpha \neq 1, \beta \neq 1$). Depending on α, β, and the value of T, the integral $\mu(T)$ may not always converge, and this determines the range of values of T for which the local solution

to (3.2) can be extended. Formally, our solution would then be:

$$R(T) = \frac{(1-\beta)^{\xi}\sqrt{1+T^2}\int_0^1 s^{\frac{\beta}{1-\beta}}\left(1-\frac{sT}{T^*}\right)^{\xi}\,ds}{\Theta(T)^{\xi+1}} + \frac{C\sqrt{1+T^2}}{T^{\frac{1}{1-\beta}}\Theta(T)^{\xi+1}}, \tag{3.6}$$

for which the balance manifold is given parametrically in (x_1, x_2) co-ordinates by $\left\{\left(\frac{R(T)}{\sqrt{1+T^2}}, \frac{TR(T)}{\sqrt{1+T^2}}\right) \mid T \in I\right\}$, where $I \subseteq [0,\infty)$ is the interval where (3.6) converges.

To provide an alternative solution form when the solution above fails to converge, it is useful to note a symmetry in this problem. If α and β are swapped, this is equivalent to swapping the index of the two species without changing the dynamics. In the phase plane, this is equivalent to a reflection on $x_1 = x_2$, i.e. the axes are swapped. We can return to our original dynamics by re-indexing the two species, which we can do in the form of the transformation $T \to \frac{1}{T} =: \overline{T}$. With this in mind, we define

$$\begin{aligned}\mu_2\left(\overline{T}\right) &= \int_0^{\overline{T}} s^{\frac{\alpha}{1-\alpha}}\Theta_2(s)^{\xi}\,ds \\ &= \overline{T}^{\frac{1}{1-\alpha}}(1-\alpha)^{\xi}\int_0^1 s^{\frac{\alpha}{1-\alpha}}\left(1-s\overline{T}T^*\right)^{\xi}\,ds, \end{aligned} \tag{3.7}$$

$$\nu_2\left(\overline{T}\right) = \frac{\overline{T}^{\frac{1}{1-\alpha}}\Theta_2(\overline{T})^{\xi+1}}{\sqrt{1+\overline{T}^2}}, \tag{3.8}$$

where $\Theta_2(\overline{T}) := 1-\alpha-\overline{T}(1-\beta)$. Using (3.7) and (3.8) we obtain a second solution to (3.2):

$$R_2(T) = \frac{\mu_2\left(\overline{T}\right)+C_2}{\nu_2\left(\overline{T}\right)} = \frac{\mu_2\left(\frac{1}{T}\right)+C_2}{\nu_2\left(\frac{1}{T}\right)}, \tag{3.9}$$

where C_2 is a constant of integration. For clarity, we will add the subscript '1' to our first solution (and $\Theta(T)$):

$$R_1(T) = \frac{\mu_1(T)+C_1}{\nu_1(T)}. \tag{3.10}$$

	$R_1(T)$	$R_2(T)$
Case 1: $\beta < 1,\ 1 < \alpha < 2 - \beta$	$[0, \infty)$	–
Case 2: $\alpha < 1,\ 1 < \beta < 2 - \alpha$	–	$[0, \infty)$
Case 3: $\alpha, \beta < 1$ and $\alpha\beta < 1$	$[0, T^*]$	$[T^*, \infty)$
Case 4: $\beta < 1,\ 1 < 2 - \beta < \alpha$	$[0, \infty)$	–
Case 5: $\alpha < 1,\ 1 < 2 - \alpha < \beta$	–	$[0, \infty)$

Table 3.1: The valid ranges in T for which we can use the solutions $R_1(T)$ and $R_2(T)$ in different parameter cases α and β. The remaining case (case 6) where both $\alpha,\ \beta > 1$ uses a slightly different solution and will be discussed later in Section 3.4.6. A region plot of these cases can be found in Figure 3.3.

We will explore solutions to (3.2) made from R_1 and R_2 for different parameters α and β in order to find an explicit expression for the balance simplex.

Remark 3.3.1 *We note that solutions R_1, R_2 with appropriate constants C_1 or C_2 can be used to describe all orbits of (3.1), but this is not the focus of our study. Rather we are concerned with the balance simplex which is constructed from special orbits of (3.2), namely heteroclinic orbits.*

The forthcoming analysis derives valid ranges we can use the solutions in different parameter cases (see Figure 3.3) and a summary is given in Table 3.1.

3.4 Construction of the heteroclinic orbits

Now we will determine which constants C_1 and C_2 correspond to the solution connecting all the non-zero steady states by explicitly examining the limits of the solutions $R_1(T)$ and $R_2(T)$. We will make use of two important results on the

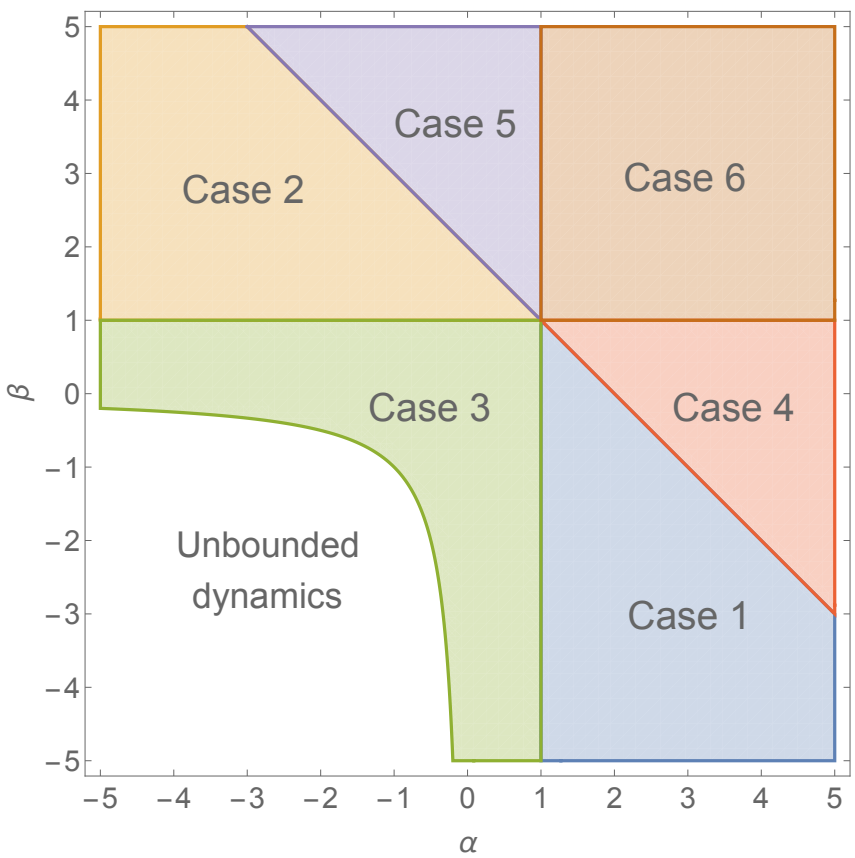

Figure 3.3: The parameter space (α, β) with the different cases shown, each extending to infinity. Note that in the region of unbounded dynamics (both $\alpha, \beta < 0$ and $\alpha\beta \geq 1$), the balance simplex does not exist.

convergence of integrals (*p-integrals* [42]):

I1: $\int_0^1 \frac{1}{x^p}\,dx = \int_0^1 x^{-p}\,dx < \infty$ if and only if $p < 1$ (i.e. $-p > -1$).

I2: $\int_1^\infty \frac{1}{x^p}\,dx = \int_1^\infty x^{-p}\,dx < \infty$ if and only if $p > 1$ (i.e. $-p < -1$).

In what follows we use that when the interior steady state $x^* = \left(\frac{\alpha-1}{\alpha\beta-1}, \frac{\beta-1}{\alpha\beta-1}\right)$ exists, its position with respect to the variable T is given by $T^* = \frac{\beta-1}{\alpha-1} > 0$. For $(\alpha, \beta) \in \mathbb{R}^2 \setminus \{(\alpha, b) : \alpha < 0, \beta < 0, \alpha\beta \geq 1\}$, x^* exists if and only if $T^* > 0$. We write $\overline{T}^* = \frac{1}{T^*}$.

3.4.1 Case 1: $-\infty < \beta < 1$ and $1 < \alpha < 2 - \beta$

Here $\xi > 0$, $\frac{1}{1-\beta} > 0$ and $T^* < 0$, so that there is no interior steady state. In this case we expect the balance simplex to consist of a single heteroclinic orbit connecting $(1, 0)$ and $(0, 1)$. We use the first solution $R_1(T)$ since $\Theta_1(T) > 0$ for $T \in [0, \infty)$. Next we determine the constant C in (3.6) so that the balance simplex passes through $(1, 0)$ at $T = 0$ and $(0, 1)$ at $T = \infty$.

a) $T \to 0$

For the limit of $R_1(T)$ as $T \to 0$, we have a potential problem with the $T^{\frac{1}{1-\beta}}$ in the denominator of the term with the constant $C_1 := C$ in equation (3.6). However, if we set $C_1 = 0$, then we can calculate the limit

$$\lim_{T\to 0} R_1(T) = \frac{(1-\beta)^\xi \cdot \sqrt{1} \cdot (1-\beta)}{(1-\beta+0)^{\xi+1}} = 1, \tag{3.11}$$

which in our original co-ordinates means $(x_1(0), x_2(0)) = (1, 0)$, the axial steady state on the x_1 axis.

b) $T \to \infty$

The leading order of $\nu(T)$ as $T \to \infty$ is $\frac{1}{1-\beta} + \xi > 0$, thus $\nu(T)$ is unbounded $T \to \infty$. Note that $\frac{\beta}{1-\beta} > -1$, so from **I2** and equation (3.5), $\mu(T)$ is also unbounded as $T \to \infty$. We consider the limit of $R_1(T)$ using L'Hôpital's rule:

$$\lim_{T\to\infty} R_1(T) = \lim_{T\to\infty} \frac{\mu_1(T) + C_1}{\nu_1(T)} = \lim_{T\to\infty} \frac{\mu_1'(T)}{\nu_1'(T)} \tag{3.12}$$

where

$$\begin{aligned}
\mu_1'(T) =& T^{\frac{\beta}{1-\beta}}\Theta(T)^{\xi}, \\
\nu_1'(T) =& \frac{1}{\sqrt{1+T^2}}\frac{T^{\frac{\beta}{1-\beta}}}{1-\beta}\Theta_1(T)^{\xi+1} + \frac{1}{\sqrt{1+T^2}}T^{\frac{1}{1-\beta}}(\xi+1)(\alpha-1)\Theta_1(T)^{\xi} \\
& - T^{\frac{1}{1-\beta}}\Theta_1(T)^{\xi+1}\frac{T}{(1+T^2)^{\frac{3}{2}}}.
\end{aligned} \tag{3.13}$$

With some simplifications, we can show:

$$\lim_{T\to\infty} R_1(T) = \lim_{T\to\infty} \frac{\mu_1'(T)}{\nu_1'(T)} = \frac{1}{\frac{1}{1-\beta}(\alpha-1) + (\xi+1)(\alpha-1) - (\alpha-1)} = 1. \tag{3.14}$$

It is worth noting that the limit has this value regardless of the constant of integration C_1. This is expected as the axial state $(0, 1)$ is locally attracting with these parameters.

We can conclude that with the choice of $C_1 = 0$, the solution $R(T) = R_1(T),\ T \in [0, \infty)$ corresponds to the balance simplex in (T, R) co-ordinates, joining both axial steady states.

3.4.2 Case 2: $\beta > 1$ and $-\infty < \alpha < 2 - \beta < 1$

For our domain $T \in [0, \infty)$, $\Theta_1(T) < 0$ which will be complex when raised to the power ξ, however $\Theta_2(\overline{T}) > 0$ here so we consider the second solution, $R_2(T)$, instead.

This parameter space is equivalent to the case where $-\infty < \alpha < 1$ and $1 < \beta < 2-\alpha$; this is Case 1 with α and β exchanged. The solution is thus obtained analogously from Case 1 by exchanging α and β, and the variable T with $\overline{T}$ everywhere in the calculations since we are now using the second solution. The balance simplex Σ is thus given by $R = R_2(T)$ with $C_2 = 0$ which joins the two axial steady states.

3.4.3 Case 3: $-\infty < \alpha, \beta < 1$ and $\alpha\beta < 1$

The inequality $\alpha\beta < 1$ is required for boundedness of all solutions; without it, the balance simplex does not always exist. Here $\xi < -1$, $\frac{1}{1-\beta} > 0$ and $T^* > 0$, so that there is an interior steady state. To construct the balance simplex will need to join together the two solutions R_1 and R_2 at the interior steady state $T = T^*$.

a) $T \to 0$

Near $T = 0$, $\Theta_1(T) > 0$ and we can calculate the limit of $R_1(T)$ as done previously, making the choice of $C_1 = 0$ for boundedness: $\lim_{T\to 0} R_1(T) = 1$.

b) $T \to \infty$, i.e. $\overline{T} \to 0$

For large T, we consider the solution $R_2(T)$ since $\Theta_2\left(\overline{T}\right) > 0$ when $T > T^*$. We can use the analogous calculations in case 3a if we consider $\overline{T}$ small. With the choice of $C_2 = 0$: $\lim_{T\to\infty} R_2(T) = \lim_{\overline{T}\to 0} \frac{\mu_2(\overline{T})}{\nu_2(\overline{T})} = 1$.

c) $T \to T^*$

We first consider this limit from below, $T \to T^*-$, where only the first solution $R_1(T)$ is real. Since $\xi < -1$, $\mu(T)$ behaves like **I1**; we know that $\mu(T)$ is unbounded as $T \to T^*$. The function $\nu(T)$ is also unbounded as $T \to T^*$, again using $\xi < -1$.

This means we can examine this limit of $R_1(T)$ using L'Hôpital's rule. We have:

$$\lim_{T\to T^*-} R_1(T) = \lim_{T\to T^*-} \frac{\mu_1'(T)}{\nu_1'(T)} = \frac{\sqrt{(\alpha-1)^2+(\beta-1)^2}}{1-\alpha\beta}, \tag{3.15}$$

which matches the value $R(T^*) = \sqrt{(x_1^*)^2+(x_2^*)^2}$ obtained from polar co-ordinates at the interior steady state x^*. This is a valid conclusion for any constant of integration C_1, consistent with x^* being attracting. We could also do an analogous calculation for the limit $T \to T^*+$. Here the second solution $R_2(T)$ is real and we would consider the limit $\overline{T} \to \overline{T}^*-$ which gives exactly the same limit value as $R_2(T^*) = R_1(T^*)$.

We conclude that by choosing $C_1 = C_2 = 0$, we have a solution which connects each axial steady state to the interior steady state, thus giving the balance simplex.

3.4.4 Case 4: $-\infty < \beta < 1$ and $1 < 2-\beta < \alpha$

Here $\xi < 0$, $\frac{1}{1-\beta} > 0$ and $T^* < 0$, so that there is no interior steady state. We use the first solution $R_1(T)$.

a) $T \to 0$

Once again, if we set $C_1 = 0$, then we find $\lim_{T\to 0} R_1(T) = 1$, corresponding to $(1, 0)$.

b) $T \to \infty$

It is clear from **I2** and equation (3.5) that $\mu_1(T)$ is unbounded as $T \to \infty$ since the leading order of its integrand is $\frac{\beta}{1-\beta} + \xi = \frac{1}{\alpha-1} - 1 > -1$. The leading order of $\nu_1(T)$ is $\frac{\beta}{1-\beta} + 1 + \xi = \frac{1}{\alpha-1} > 0$ and so $\nu_1(T)$ is also unbounded as $T \to \infty$ and we can again apply L'Hôpital's rule on $R_1(T)$ to conclude $\lim_{T\to\infty} R_1(T) = 1$ for any constant C_1, consistent with $(0, 1)$ being attracting.

Hence with $C_1 = 0$, the solution $R = R_1(T)$ corresponds to the balance simplex joining both axial steady states.

3.4.5 Case 5: $\beta > 1$ and $2 - \beta < \alpha < 1$

Here, we use the second solution, $R_2(T)$, since $\Theta_2(\overline{T}) > 0$. Equivalently, this case is where $\alpha < 1$ and $1 < 2 - \alpha < \beta$ which has been covered analogously in Case 4 with the first solution $R_1(T)$. The balance simplex Σ is thus given by $R = R_2(T)$ with $C_2 = 0$.

3.4.6 Case 6: $\alpha, \beta > 1$

Here $\xi > 0$, $\frac{\beta}{1-\beta} < -1$ and $T^* > 0$, so that there is an interior steady state. As in Case 4 we will join R_1 and R_2 at $T = T^*$.

a) $T \to \infty$

In this case $\Theta_1(T) > 0$ if and only if $T > T^*$. Thus for large T we now consider the modification:

$$R_1^*(T) = \frac{\mu_1^*(T) + C_1}{\nu_1(T)} \tag{3.16}$$

where

$$\mu_1^*(T) = \int_{T^*}^{T} s^{\frac{\beta}{1-\beta}} \Theta_1(s)^{\xi} \, ds. \tag{3.17}$$

The integrand has leading order $\frac{\beta}{1-\beta} + \xi = -1 + \frac{1}{\alpha-1} > -1$ since $\alpha > 1$. This means $\mu_1^*(T)$ is unbounded as $T \to \infty$ using **I2**. The leading order of $\nu_1(T)$ is $\frac{\beta}{1-\beta} + 1 + \xi = \frac{1}{\alpha-1} > 0$ and so $\nu_1(T)$ is also unbounded as $T \to \infty$ and we can apply

L'Hôpital's rule,

$$\lim_{T\to\infty} R_1^*(T) = \lim_{T\to\infty} \frac{\mu_1^*(T) + C_1}{\nu_1(T)} = \lim_{T\to\infty} \frac{\mu_1'(T)}{\nu_1'(T)}. \tag{3.18}$$

This follows exactly the same calculation as in case 1b, thus we can conclude $\lim_{T\to\infty} R_1^*(T) = 1$, regardless of the constant of integration C_1, consistent with $(0,1)$ being attracting.

b) $T \to 0$, i.e. $\overline{T} \to \infty$

For small T (i.e. large $\overline{T}$), since $\Theta_2(\overline{T}) > 0$ when $T < T^*$ we consider the modification:

$$R_2^*(T) = \frac{\mu_2^*\left(\overline{T}\right) + C_2}{\nu_2\left(\overline{T}\right)} = \frac{\mu_2^*\left(\frac{1}{T}\right) + C_2}{\nu_2\left(\frac{1}{T}\right)} \tag{3.19}$$

where

$$\mu_2^*\left(\overline{T}\right) = \int_{\overline{T}^*}^{\overline{T}} s^{\frac{\alpha}{1-\alpha}} \Theta_2(s)^{\xi}\ ds. \tag{3.20}$$

Using the analogous calculations from case 6a, $\mu_2^*\left(\overline{T}\right)$ is unbounded as $\overline{T} \to \infty$, and the same is true for $\nu_2\left(\overline{T}\right)$. Thus we can apply L'Hôpital's rule to conclude that $R_2^*(T)$ converges to 1 as $T \to 0$, i.e. as $\overline{T} \to \infty$, regardless of the constant C_2, consistent with $(1,0)$ being attracting.

c) $T \to T^*$

Another point we must examine is $T^* > 0$ since $\Theta_1(T^*) = 0$ and $\xi > 0$. We first examine the limit from above ($T \to T^*+$) where $R_1^*(T)$ remains real. It is clear that $\nu_1(T^*) = 0$ and $\lim_{T\to T^*+} \mu_1^*(T) = 0$.

Since $R_1^*(T) = \frac{\mu_1^*(T)+C_1}{\nu_1(T)}$, if $C_1 \neq 0$, then $R_1^*(T)$ is unbounded as $T \to T^*+$. Setting

$C_1 = 0$, we can use L'Hôpital's rule to examine the limit of $R_1^*(T)$ as $T \to T^*+$. This follows the calculation from case 3c, but we must be careful with the sign of $\alpha - 1$ when simplifying and bringing terms into the square root:

$$\lim_{T \to T^*+} R_1^*(T) = \lim_{T \to T^*+} \frac{\mu_1'(T)}{\nu_1'(T)} = \frac{\sqrt{(\alpha-1)^2 + (\beta-1)^2}}{\alpha\beta - 1}, \tag{3.21}$$

which matches the value of $R(T^*) = \sqrt{(x_1^*)^2 + (x_2^*)^2}$ at the interior steady state x^*. Since we expect x^* to lie on the balance simplex, $C_1 = 0$ is indeed the correct constant for the balance simplex.

We can also do an analogous calculation for the limit of $R_2^*(T)$ as $T \to T^*-$ (i.e. as $\overline{T} \to \overline{T}^*+$), which gives exactly the same limit value with the choice of $C_2 = 0$.

Thus, for the case where both $\alpha, \beta > 1$ we use the modified solution $R_1^*(T)$ with $C_1 = 0$ in the range $T \in [T^*, \infty)$ and $R_2^*(T)$ with $C_2 = 0$ in $T \in [0, T^*]$ for the balance simplex.

3.5 Our solution is Σ, a balance simplex

Recall that the general solution R to (3.2) was found by transforming the scaled Lotka–Volterra system (3.1) into polar co-ordinates, then using the substitution $T = \tan\theta$. The constants C_1 and/or C_2 were set to 0 to find the balance simplex. This gives a simple parametric form of our solution, for example, for $R_1(T)$:

$$\begin{aligned} x_1 &= \frac{1}{\sqrt{1+T^2}} R_1(T), \\ x_2 &= \frac{T}{\sqrt{1+T^2}} R_1(T). \end{aligned} \tag{3.22}$$

Let $R(T)$, $T \in [0, \infty)$, be our complete solution to (3.2), equal to $R_1(T)$ or $R_2(T)$ in the appropriate ranges of T, with the constants of integration C_1 and/or C_2 set to 0. We have seen that parametrically $(x_1, x_2) = \left(\frac{1}{\sqrt{1+T^2}} R(T), \frac{T}{\sqrt{1+T^2}} R(T)\right)$ and the

function $R(T)$ is injective. We can therefore map our solution to the unit simplex using $(x_1, x_2) \mapsto (u, 1-u)$ where $u = \frac{x_1}{x_1+x_2} = \frac{1}{1+T}$ is the relative frequency of species 1. Thus our solution is homeomorphic to the unit 1-simplex by radial projection.

We have seen that in the 2-species scaled Lotka–Volterra system (3.1) where the dynamics are bounded and steady states are hyperbolic, non-zero orbits are attracted to non-zero steady states (e.g. Figure 3.2 and Chapter 2) which all lie on our solution. The solution is also a heteroclinic orbit which is invariant to the flow of the system. Thus our solution is Σ, a balance simplex, satisfying Definition 3.2.1.

3.6 Simplifications that use the Gaussian hypergeometric function

The Gaussian hypergeometric function (GHF) [6,7,90] is defined for $a, b, c, z \in \mathbb{C}$ by

$$ {}_2F_1(a, b; c; z) = \sum_{k=0}^{\infty} \frac{(a)_k (b)_k}{(c)_k k!} z^k, \tag{3.23} $$

where the Pochhammer symbol means $(x)_0 = 1$ and $(x)_k = x(x+1)\cdots(x+k-1)$ for a positive integer k. This power series in z is defined when c is not equal to a non-positive integer and converges if $|z| < 1$.

The GHF also has the following integral representation which converges if $|z| < 1$ and $\Re(c) > \Re(b) > 0$ [6]:

$$ {}_2F_1(a, b; c; z) = \frac{\Gamma(c)}{\Gamma(b)\Gamma(c-b)} \int_0^1 t^{b-1}(1-t)^{c-b-1}(1-tz)^{-a}\, dt \tag{3.24} $$

where Γ is the Gamma function:

$$\Gamma(z) = \int_0^\infty x^{z-1}e^{-x}\,dx, \tag{3.25}$$

which converges absolutely when $\Re(z) > 0$. We now show that we can actually write our solutions R_1, R_2, R_1^* and R_2^* in terms of GHFs.

We will also make use of Euler's transformation of the hypergeometric function [6, pp. 64], derived from the substitution $t \to \frac{1-t}{1-tz}$ in the integral representation (3.24):

$${}_2F_1(a,b;c;z) = (1-z)^{c-a-b}\,{}_2F_1(c-a,c-b;c;z). \tag{3.26}$$

We can now write the integral μ_1 (3.5) for $\beta < 1$ in the following way, using $a = -\xi$, $b = \frac{1}{1-\beta} > 0$, $c = \frac{2-\beta}{1-\beta} > 0$, and also that $\frac{\Gamma[c]}{\Gamma[b]\Gamma[c-b]} = \frac{\Gamma[b+1]}{\Gamma[b]\Gamma[1]} = b = \frac{1}{1-\beta}$,

$$\begin{aligned}
\mu_1(T) &= T^{\frac{1}{1-\beta}}(1-\beta)^\xi \int_0^1 s^{\frac{\beta}{1-\beta}}\left(1-\frac{sT}{T^*}\right)^\xi ds \\
&= T^{\frac{1}{1-\beta}}(1-\beta)^{\xi+1}\,{}_2F_1\left[-\xi, \frac{-1}{\beta-1}; \frac{\beta-2}{\beta-1}; \frac{T}{T^*}\right] \\
&= T^{\frac{1}{1-\beta}}\Theta_1(T)^{\xi+1}\,{}_2F_1\left[\frac{\alpha}{\alpha-1}, 1; \frac{\beta-2}{\beta-1}; \frac{T}{T^*}\right],
\end{aligned} \tag{3.27}$$

giving the general solution for $\beta < 1$:

$$R_1(T) = \sqrt{1+T^2}\,{}_2F_1\left[\frac{\alpha}{\alpha-1}, 1; \frac{\beta-2}{\beta-1}; \frac{T}{T^*}\right] + \frac{C_1\sqrt{1+T^2}}{T^{\frac{1}{1-\beta}}\Theta_1(T)^{\xi+1}}. \tag{3.28}$$

Similarly, recalling that we use $\overline{T}$ to denote $\frac{1}{T}$,

$$\mu_2\left(\overline{T}\right) = \overline{T}^{\frac{1}{1-\alpha}}\Theta_2(\overline{T})^{\xi+1}\,{}_2F_1\left[\frac{\beta}{\beta-1}, 1; \frac{\alpha-2}{\alpha-1}; \overline{T}T^*\right], \tag{3.29}$$

giving the general solution for $\alpha < 1$:

$$R_2(T) = \sqrt{1+\overline{T}^2}\ {}_2F_1\left[\frac{\beta}{\beta-1}, 1; \frac{\alpha-2}{\alpha-1}; \overline{T}T^*\right] + \frac{C_2\sqrt{1+\overline{T}^2}}{\overline{T}^{\frac{1}{1-\alpha}}\Theta_2\left(\overline{T}\right)^{\xi+1}}. \tag{3.30}$$

Remark 3.6.1 *The third argument of ${}_2F_1$ in μ_1 (respectively μ_2) is a non-positive integer when β (respectively α) belongs to the set:*

$$\begin{aligned}\mathcal{K} &= \left\{\frac{k-2}{k-1} \mid k \text{ is a non-positive integer}\right\} \\ &= \left\{\frac{k-1}{k} \mid k \text{ is a negative integer}\right\}.\end{aligned} \tag{3.31}$$

note that $\mathcal{K} \subset (1, 2]$. From Table 3.1, we can see that we only use μ_1 in the case where $\beta < 1$, thus $\beta \notin \mathcal{K}$ and the GHF in equation (3.28) is well defined. Similarly, μ_2 is only used in cases where $\alpha < 1$.

The integrals μ_1^* (3.17) and μ_2^* (3.20) (from case 6 where both $\alpha, \beta > 1$) can also be written in terms of GHFs:

$$\begin{aligned}\mu_1^*(T) &= \int_{T^*}^{T} s^{\frac{\beta}{1-\beta}}\Theta_1(s)^{\xi}\ ds \\ &= (\alpha-1)^{\xi}\int_0^1 \left[s(T-T^*)+T^*\right]^{\frac{\beta}{1-\beta}}\left[s(T-T^*)\right]^{\xi}(T-T^*)\ ds \\ &= (\alpha-1)^{\xi}(T-T^*)^{\xi+1}T^{*\frac{\beta}{1-\beta}}\int_0^1 s^{\xi}\left(1-s\left(\frac{T^*-T}{T^*}\right)\right)^{\frac{\beta}{1-\beta}}\ ds \\ &= \frac{(\alpha-1)^{\xi}(T-T^*)^{\xi+1}T^{*\frac{\beta}{1-\beta}}}{\xi+1}\,{}_2F_1\left[\frac{\beta}{\beta-1}, \xi+1; \xi+2; \frac{T^*-T}{T^*}\right].\end{aligned}$$

Applying Euler's transformation, we have

$$\begin{aligned}{}_2F_1\left[\frac{\beta}{\beta-1}, \xi+1; \xi+2; \frac{T^*-T}{T^*}\right] &= {}_2F_1\left[\xi+1, \frac{\beta}{\beta-1}; \xi+2; \frac{T^*-T}{T^*}\right] \\ &= \left(\frac{T}{T^*}\right)^{\frac{1}{1-\beta}}\ {}_2F_1\left[\frac{\alpha}{\alpha-1}, 1; \xi+2; \frac{T^*-T}{T^*}\right].\end{aligned}$$

Hence the general solution for $T > T^*$ when $\alpha, \beta > 1$ is

$$\begin{aligned} R_1^*(T) &= \frac{\mu_1^*(T) + C_1}{\nu(T)} \\ &= \frac{\alpha - 1}{\alpha\beta - 1}\sqrt{1 + T^2}\ {}_2F_1\left[\frac{\alpha}{\alpha - 1}, 1; \xi + 2; \frac{T^* - T}{T^*}\right] + \frac{C_1\sqrt{1 + T^2}}{T^{\frac{1}{1-\beta}}\Theta_1(T)^{\xi+1}}. \end{aligned} \tag{3.32}$$

Similarly,

$$\begin{aligned} \mu_2^*\left(\overline{T}\right) &= \int_{\overline{T}^*}^{\overline{T}} s^{\frac{\alpha}{1-\alpha}}\Theta_2\left(s\right)^{\xi}\ ds \\ &= \frac{(\beta - 1)^{\xi}(\overline{T} - \overline{T}^*)^{\xi+1}\overline{T}^{*\frac{\alpha}{1-\alpha}}}{\xi + 1}\ {}_2F_1\left[\frac{\alpha}{\alpha - 1}, \xi + 1; \xi + 2; \frac{\overline{T}^* - \overline{T}}{\overline{T}^*}\right]. \end{aligned} \tag{3.33}$$

and so after applying the Euler transformation, the general solution for $T < T^*$ is

$$\begin{aligned} R_2^*(T) &= \frac{\mu_2^*(\overline{T}) + C_2}{\nu_2(\overline{T})} \\ &= \frac{\beta - 1}{\alpha\beta - 1}\sqrt{1 + \overline{T}^2}\ {}_2F_1\left[\frac{\beta}{\beta - 1}, 1; \xi + 2; \frac{\overline{T}^* - \overline{T}}{\overline{T}^*}\right] + \frac{C_2\sqrt{1 + \overline{T}^2}}{\overline{T}^{\frac{1}{1-\alpha}}\Theta_2(\overline{T})^{\xi+1}}. \end{aligned} \tag{3.34}$$

Remark 3.6.2 *For both μ_1^* and μ_2^* the third argument of their GHFs is a non-positive integer k when*

$$\alpha = \frac{k(1 - \beta) + \beta}{k(1 - \beta) - 1 + 2\beta}. \tag{3.35}$$

Note that the numerator and denominator are both positive since $\beta > 1$ and k is a non-positive integer. Using $\beta - 1 > 0$ we can also see that $k(1 - \beta) + \beta < k(1 - \beta) - 1 + 2\beta$ implying $\alpha < 1$ in (3.35). Thus when using μ_1^* and μ_2^*, their GHFs are always defined since we only use them in the case where both $\alpha, \beta > 1$.

3.7 Summary of explicit solutions

Recall that $T^* = \frac{\beta-1}{\alpha-1}$ and note that $\xi+2 = \frac{2\alpha\beta-\alpha-\beta}{(\alpha-1)(\beta-1)}$. When writing ${}_2F_1$ here, we are referring to the Gaussian hypergeometric function, with its analytic continuation.

1. $-\infty < \beta < 1,\ \alpha > 1$:

$$(x_1(T), x_2(T)) = {}_2F_1\left[\frac{\alpha}{\alpha-1}, 1; \frac{\beta-2}{\beta-1}; \frac{T}{T^*}\right] \times (1, T), \quad T \in [0, \infty).$$

2. $-\infty < \alpha < 1,\ \beta > 1$:

$$(x_1(T), x_2(T)) = {}_2F_1\left[\frac{\beta}{\beta-1}, 1; \frac{\alpha-2}{\alpha-1}; \frac{T^*}{T}\right] \times \left(\frac{1}{T}, 1\right), \quad T \in [0, \infty).$$

3. $-\infty < \alpha, \beta < 1$ and $\alpha\beta < 1$:

$$(x_1(T), x_2(T)) = \begin{cases} {}_2F_1\left[\frac{\alpha}{\alpha-1}, 1; \frac{\beta-2}{\beta-1}; \frac{T}{T^*}\right] \times (1, T), & T \in [0, T^*] \\ {}_2F_1\left[\frac{\beta}{\beta-1}, 1; \frac{\alpha-2}{\alpha-1}; \frac{T^*}{T}\right] \times \left(\frac{1}{T}, 1\right), & T \in [T^*, \infty]. \end{cases}$$

4. $\alpha > 1,\ \beta > 1$:

$$\begin{aligned} &(x_1(T), x_2(T)) \\ &= \begin{cases} \frac{\beta-1}{\alpha\beta-1}\, {}_2F_1\left[\frac{\beta}{\beta-1}, 1; \xi+2; 1-\frac{T^*}{T}\right] \times \left(\frac{1}{T}, 1\right), & T \in [0, T^*] \\ \frac{\alpha-1}{\alpha\beta-1}\, {}_2F_1\left[\frac{\alpha}{\alpha-1}, 1; \xi+2; 1-\frac{T}{T^*}\right] \times (1, T), & T \in [T^*, \infty). \end{cases} \end{aligned}$$

3.8 Example plots for different species-species interactions

Some phase plots with example parameters for α and β showing the balance simplex can be found in Figures 3.4 and 3.5. Recall that the system (3.1) always has axial steady states at (0,1) and (1,0).

1. *Competition* $(\alpha, \beta > 0)$ is shown in Figures 3.4a, 3.4b and 3.5b. Here Σ coincides with the carrying simplex which is known to be C^1-continuous on the interior $\mathbb{R}^2_{>0}$ [63]. From [4,85] it is known that the carrying simplex of the competitive system (3.1) is convex when $\alpha + \beta < 2$ (weakly competitive), concave when $\alpha + \beta > 1$ (strongly competitive) and a straight line if $\alpha + \beta = 1$.

2. *Predation* $(\alpha\beta < 0)$ is shown in Figures 3.4d and 3.5a. Note that this model is not the same as the classic predator-prey model, since the origin is repelling. We are taking all intrinsic growth rates to be positive – suggesting that the predator has a secondary food source which it switches to when it primary food source is scarce (known as 'prey-switching', see for example [87] and references within).

3. *Cooperation* $(\alpha, \beta < 0)$ is shown in Figure 3.4c. As is well-known [37, 47], the effect of cooperation is to enhance the population densities of both species beyond that of their respective carrying capacities, as seen here. The most notable feature in the balance simplex is that there is now a cusp at the interior steady state, thus showing by example that, although the individual heteroclinic orbits forming Σ are as smooth as the vector field, they may not join smoothly at an interior steady state. Therefore, we can conclude that the balance simplex for this model is at least continuous and piecewise analytic. In Figure 3.5a, we provide an example of a non-competitive system where the

balance simplex is analytic (not just piecewise).

3.9 Special cases

3.9.1 Rational function as the integrand

For any non-zero integers n_1, n_2 (of any sign), let $\alpha = \frac{n_2-1}{n_2}$ and $\beta = \frac{n_1-1}{n_1}$. From our original integral $\mu(T)$ (3.5), we find that:

$$\mu(T) = \int T^{n_1-1} \left(1 - \frac{n_1-1}{n_1} - T\left(1 - \frac{n_2-1}{n_2}\right)\right)^{-n_1-n_2} dT. \tag{3.36}$$

Note that n_1-1 and $-n_1-n_2$ are integers meaning the integrand is a rational function which we can integrate in the standard way and use the same original integrating factor $\nu(T)$ (3.3) to plot our solution $R(T)$.

3.9.2 Case $\alpha = 1$ and $\beta \notin \mathcal{K} \cup \{1\}$

If either $\alpha = 1$ or $\beta = 1$ we have a different integral to start with and the interior steady state x^* does not exist. Note the case where both are equal to 1 has a line of interior steady states which is also the carrying simplex, see Figure 3.7b.

Suppose, without loss of generality, that $\alpha = 1$ and $\beta \notin \mathcal{K} \cup \{1\}$ (see (3.31) for the definition of $\mathcal{K}$). We now have:

$$\frac{dR}{dT} + R\,\frac{1+T+\beta T^2+T^3}{T(1+T^2)(1-\beta)} = \frac{\sqrt{1+T^2}}{T(1-\beta)}. \tag{3.37}$$

The integrating factor is:

$$\nu_3(T) = \frac{T^{\frac{1}{1-\beta}}}{\sqrt{1+T^2}} e^{\frac{T}{1-\beta}}. \tag{3.38}$$

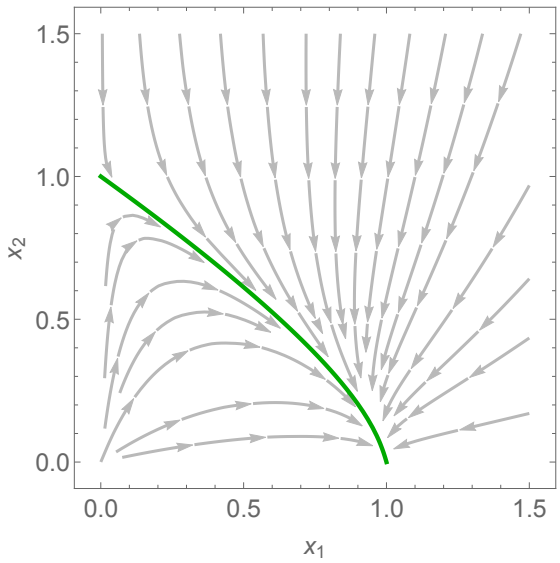

(a) $\alpha = 0.2,\ \beta = 1.3$ (case 2)

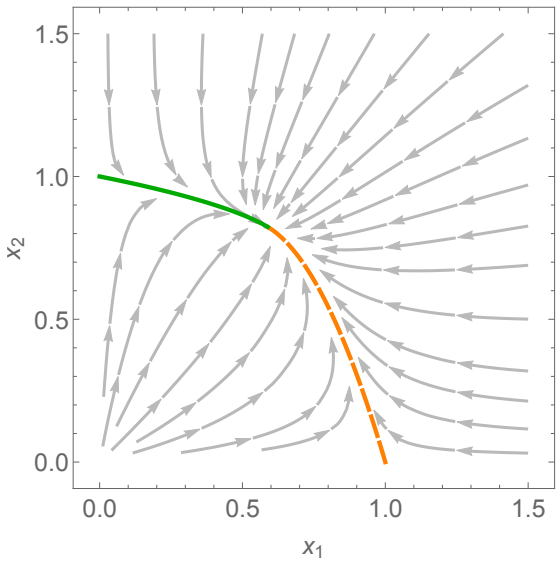

(b) $\alpha = 0.5,\ \beta = 0.3$ (case 3)

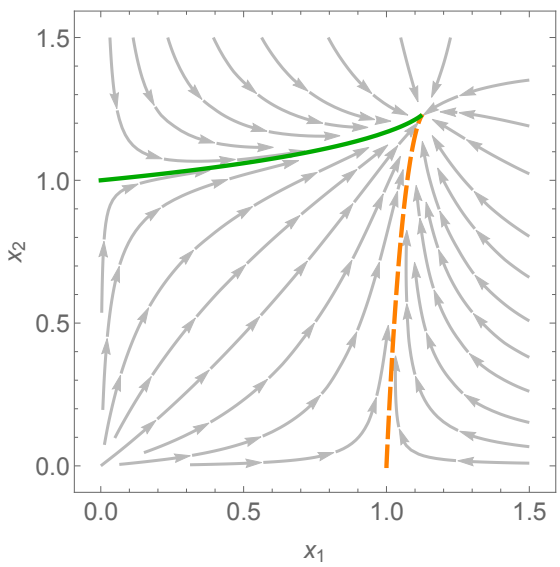

(c) $\alpha = -0.1,\ \beta = -0.2$ (case 3)

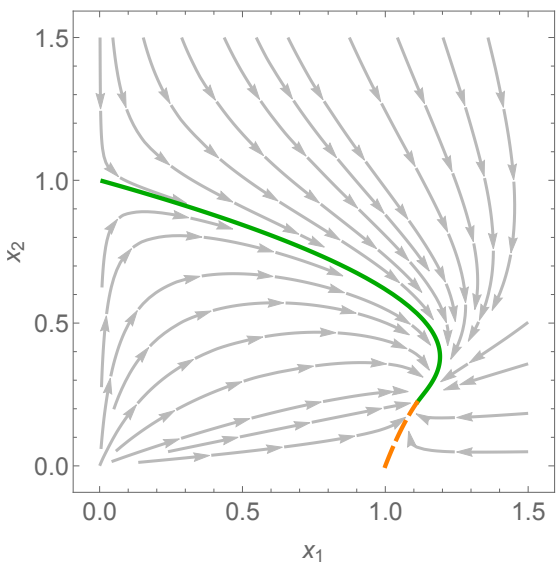

(d) $\alpha = -0.5,\ \beta = 0.7$ (case 3)

Figure 3.4: Phase plots of 2-species scaled Lotka–Volterra systems with different interspecific interaction coefficients (α and β). Here Figures 3.4a and 3.4b are competitive systems, 3.4c is a co-operative system and 3.4d is an example of predation. In these plots, the solutions $R_1(T)$ (dashed, orange) and $R_2(T)$ (solid, green) only meet at the interior steady state x^*. Recall that there are always axial steady states at (0,1) and (1,0).

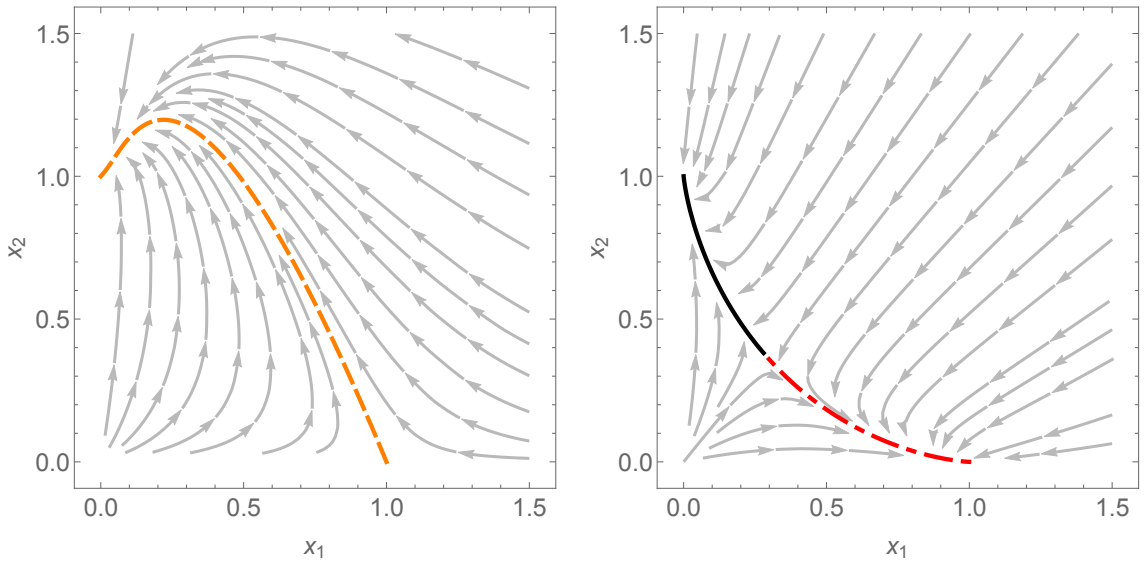

(a) $\alpha = 1.2,\ \beta = -0.9$ (case 1) (b) $\alpha = 1.9,\ \beta = 2.2$ (case 6)

Figure 3.5: Phase plots of 2-species scaled Lotka–Volterra systems with different interspecific interaction coefficients (α and β). Here, 3.5a is an example of predation where we only need to use one solution, $R_1(T)$ (dashed, orange). Figure 3.5b is a strongly competitive system, using the solutions $R_1^*(T)$ (solid, black) and $R_2^*(T)$ (dashed and dotted, red).

Now:

$$\begin{aligned}
\mu_3(T) &= \frac{1}{1-\beta}\int e^{\frac{-T}{\beta-1}}\, T^{\frac{-\beta}{\beta-1}}\, dT \\
&= C - \frac{1}{1-\beta}\int_T^\infty e^{\frac{-t}{\beta-1}}\, t^{\frac{-\beta}{\beta-1}}\, dt \\
&= C + (\beta-1)^{\frac{-\beta}{\beta-1}}\int_{\frac{T}{\beta-1}}^\infty e^{-\tau}\, \tau^{\frac{-\beta}{\beta-1}}\, d\tau \\
&= C + (\beta-1)^{\frac{-\beta}{\beta-1}}\,\Gamma\left[\frac{1}{1-\beta}, \frac{T}{\beta-1}\right]
\end{aligned} \tag{3.39}$$

where we have kept the constant of integration C in the definition of μ_3 and Γ here is the incomplete gamma function: $\Gamma[s,x] = \int_x^\infty t^{s-1}e^{-t}\,dt$. By analytic continuity, Γ can be defined for any x (even negative) except when s is a non-positive integer [7, vol II]. For our case, this is when $\beta \in \mathcal{K}$. Note that the case $\frac{1}{1-\beta} = 0$ is not possible. Thus when $\alpha = 1$ and $\beta \notin \mathcal{K} \cup \{1\}$, we have the general solution:

$$R(T) = \frac{\mu_3(T)}{\nu_3(T)}. \tag{3.40}$$

An example of this case is plotted in Figure 3.6a. Note that when $\alpha = 1$, the steady state $(0, 1)$ is non-hyperbolic.

3.9.3 Case $\alpha = 1$ and $\beta \in \mathcal{K}$

If $\alpha = 1$ and $\beta \in \mathcal{K}$ suppose $\beta = \frac{k_1 - 1}{k_1}$, where k_1 is a negative integer. Recall that $\mathcal{K} \subset (1, 2]$. From (3.37), our integral is:

$$\mu_4(T) = k_1 \int e^{k_1 T}\, T^{k_1 - 1}\, dT = C - k_1 \int_T^\infty e^{k_1 t}\, t^{k_1 - 1}\, dt. \tag{3.41}$$

By repeated integration by parts we have

$$\begin{aligned}
\mu_4(T) &= C - k_1 e^{k_1 t}\, \frac{t^{k_1}}{k_1}\bigg|_T^\infty + k_1 \int_T^\infty e^{k_1 t}\, t^{k_1}\, dt \\
&= C - k_1 e^{k_1 t}\, \frac{t^{k_1}}{k_1}\bigg|_T^\infty + k_1 e^{k_1 t}\, \frac{t^{k_1+1}}{k_1+1}\bigg|_T^\infty - \frac{k_1^2}{k_1+1} \int_T^\infty e^{k_1 t}\, t^{k_1+1}\, dt \\
&= C - k_1 e^{k_1 t}\, \frac{t^{k_1}}{k_1}\bigg|_T^\infty + k_1 e^{k_1 t}\, \frac{t^{k_1+1}}{k_1+1}\bigg|_T^\infty - \frac{k_1^2}{k_1+1} e^{k_1 t}\, \frac{t^{k_1+2}}{k_1+2}\bigg|_T^\infty \\
&\quad + \frac{k_1^3}{(k_1+1)(k_1+2)} \int_T^\infty e^{k_1 t}\, t^{k_1+2}\, dt.
\end{aligned} \tag{3.42}$$

Note that when we evaluate the terms at ∞ and T, the ∞ part is equal to zero (since $k_1 < 0$), and the T part will have a minus sign. We use the following notation:

$$\mathfrak{K}_i = \frac{k_1^i}{(k_1+1)\cdots(k_1+i)} \tag{3.43}$$

and let $n = -1 - k_1$ so that $k_1 + n = -1$.

$$\begin{aligned}
\mu_4(T) = C &+ e^{k_1 T}\, T^{k_1} - \mathfrak{K}_1\, e^{k_1 T}\, T^{k_1+1} + \ldots + (-1)^i \mathfrak{K}_i\, e^{k_1 T}\, T^{k_1+i} \\
&+ \ldots + (-1)^n \mathfrak{K}_n\, e^{k_1 T}\, T^{k_1+n} + (-1)^n \int_T^\infty \mathfrak{K}_n\, k_1\, e^{k_1 t}\, \frac{t^{k_1+n}}{k_1+n}\, dt
\end{aligned} \tag{3.44}$$

where

$$(-1)^n \int_T^\infty \mathfrak{K}_n\, k_1\, e^{k_1 t}\, \frac{t^{k_1+n}}{k_1+n}\, dt = (-1)^{n+1} \int_T^\infty \mathfrak{K}_n\, k_1\, e^{k_1 t}\, \frac{1}{t}\, dt$$
$$= (-1)^{n+1} \int_{-k_1 T}^\infty \mathfrak{K}_n\, k_1\, e^{-\tau}\, \frac{1}{\tau}\, d\tau$$
$$= (-1)^n \mathfrak{K}_n\, k_1\, Ei(k_1 T). \tag{3.45}$$

Here $Ei(z) = -\int_{-z}^\infty e^{-t} t^{-1} dt$ is the exponential integral. Note that we have the same integrating factor, ν_3 (3.38), as our previous case, thus when $\alpha = 1$ and $\beta \in \mathcal{K}$, we have the general solution

$$R(T) = \frac{\mu_4(T)}{\nu_3(T)}. \tag{3.46}$$

For example with $\alpha = 1$ and $\beta = \frac{5}{4}$ (so that $k_1 = -4$).

$$\mu_4(T) = \frac{e^{-4T}}{T^4} - \frac{4e^{-4T}}{3T^3} + \frac{16e^{-4T}}{6T^2} - \frac{64e^{-4T}}{6T} - \frac{256 Ei(-4T)}{6} \tag{3.47}$$

which is plotted in the Figure 3.6b.

3.9.4 Case $\alpha + \beta = 2$

It is known that for the competitive 2-species scaled Lotka–Volterra system, the curvature of the carrying simplex depends on the term $\alpha + \beta - 2$ [4]. The sign of this can affect whether the carrying simplex is convex or concave. As we have mentioned, when $\alpha = \beta = 1$, there is a line of interior steady states and this line ($x_2 = 1 - x_1$) is the carrying simplex (Figure 3.7b).

In other cases, we can still use the solutions we have derived (Section 3.7). So we

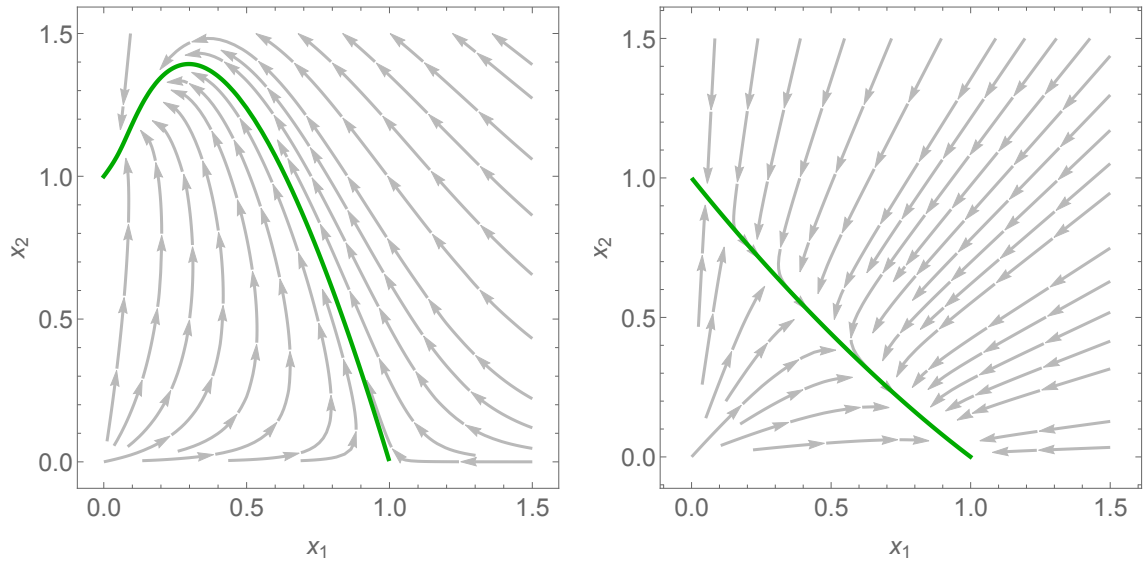

(a) $\alpha = 1,\ \beta = -1.32$ ($\beta \notin \mathcal{K} \cup \{1\}$, $C = 0.274$)

(b) $\alpha = 1,\ \beta = 1.25$ ($\beta \in \mathcal{K}$, $C = 0$)

Figure 3.6: Phase plots of 2-species scaled Lotka–Volterra systems where one of the interspecfic interaction coefficients, α (without loss of generality), is equal to 1. The solid green curve is the balance simplex, connecting both axial steady states.

assume $\alpha + \beta = 2$ and $\alpha, \beta \neq 1$, note that:

$$1 - \alpha = \beta - 1 \tag{3.48}$$

$$\frac{\alpha}{\alpha - 1} = \frac{\beta - 2}{\beta - 1}. \tag{3.49}$$

The hypergeometric function used for first solution to the balance simplex simplifies to

$${}_2F_1\left[\frac{\alpha}{\alpha - 1}, 1; \frac{\beta - 2}{\beta - 1}; \frac{T(\alpha - 1)}{\beta - 1}\right] = \sum_{n=0}^{\infty} (-T)^n. \tag{3.50}$$

Thus in the cases which use this first solution, $x_1 = 1 - T + T^2 - T^3 + \ldots$ and $x_2 = Tx_1 = T - T^2 + T^3 - \ldots = 1 - x_1$ (since x_1 converges). Thus the balance simplex is precisely the line $x_2 = 1 - x_1$. An example is shown in Figure 3.7a where $\alpha = 2.23$ and $\beta = -0.23$. The same holds for the hypergeometric function from the second solution, so we can conclude that even in non-competitive cases, if $\alpha + \beta = 2$, the balance simplex is the line $x_2 = 1 - x_1$.

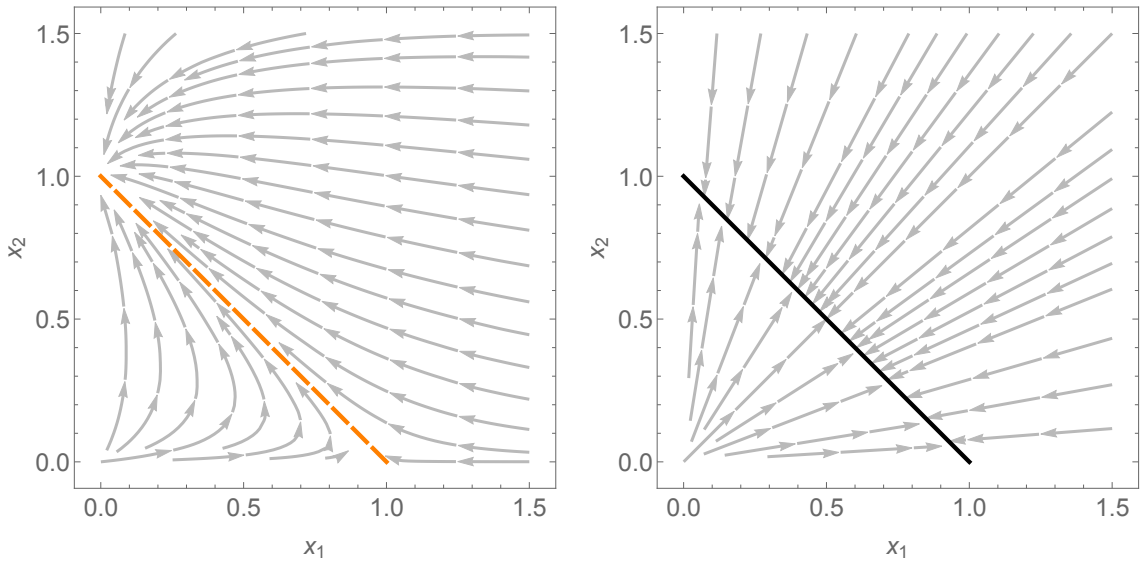

(a) $\alpha = 2.32,\ \beta = -0.32$ (b) $\alpha = 1,\ \beta = 1$

Figure 3.7: Phase plots of 2-species scaled Lotka–Volterra systems where $\alpha + \beta = 2$. In these cases, the balance simplex is the line $x_2 = 1 - x_1$.

3.10 Discussion

We have introduced the concept of a balance simplex Σ to describe a manifold where growth from small population densities and decay from large densities balance, and derived explicit formulae for Σ for the 2-species scaled Lotka–Volterra equations (3.1) when the dynamics are bounded. These expressions are valid even in non-competitive cases, showing that an analogous concept of the carrying simplex introduced by Hirsch [35] exists outside of competitive systems, although not all of the properties still hold. For example, carrying simplices are unordered, meaning if $x, y \in \Sigma$ and $x \geq y$ then $x = y$. This clearly does not hold for the non-competitive system shown in Figure 3.4d.

All non-zero solutions tend to the balance simplex which therefore contains all limit sets. In our planar system, as is well-known in the competitive case (e.g. [37]) this immediately implies that every orbit is convergent (since we have discounted unbounded orbits).

Our explicit solutions confirm that for (3.1), Σ maps radially 1-to-1 and onto the probability simplex and the same is found in more general competitive models [35].

For models with more general functional forms for the per-capita growth rate, injectivity of the radial projection may fail, and in that case we call Σ the balance simplex, further discussed in Chapter 6. In particular, this lack of injectivity can occur in predator-prey systems when there is an interior stable spiral [18]. Practically, injectivity of the radial projection means that if a sample of the population is taken and an approximation of the balance simplex is known, the actual population densities and total population size can be estimated if the system is close to balance.

Carrying simplices of planar competitive Lotka–Volterra systems have a curvature that is single-signed. In planar and higher dimensional Lotka–Volterra systems, the sign of this Gaussian curvature can be indicative of global stability of interior fixed points [4, 101]. In fact, for the planar case this curvature depends solely on the sign of a simple expression of the parameters [4, 85, 99]. For our scaled Lotka–Volterra system in the competitive case, this expression is $\alpha + \beta - 2$. This difference in convexity properties can be seen in Figures 3.4b and 3.5b where $\alpha + \beta - 2 = -1.2$ and 2.1 respectively. We have also seen in Section 3.9.4 that when $\alpha + \beta = 2$, even for non-competitive systems, the balance simplex is always the straight line $1 - x_1$.

For non-competitive scaled Lotka–Volterra systems (with only hyperbolic steady states), we initially believed that each heteroclinic orbit would have a constant sign of curvature. However, examining a perturbation of the system in Figure 3.6a (i.e. considering $\alpha = 1.01, \beta = -1.32$ which is part of Case 1) the shape of the balance simplex remains similar in that its curvature changes sign near (0,1).

We expect balance simplices (as the common boundary of repulsion of the origin and infinity) to appear in higher dimensional population models. In a 3-species Lotka–Volterra system where the origin and infinity are repellers, the presence of a balance simplex would also have strong implications for the long-term dynamics. If the resulting balance simplex is sufficiently smooth, then the flow on the balance simplex is 2-dimensional and hence amenable to treatment by the Poincaré-Bendixson

Theorem [84] and similar tools. In particular chaos would not be possible in a 3-species system with a sufficiently regular balance simplex.

Chapter 4

A Parametric Series Solution for some 3-Species Scaled Lotka–Volterra Systems

In this chapter we explore the balance simplex Σ for the 3-species case. We do not expect to be able to find an explicit solution, so we work towards a series solution which we want to match exactly to the (now known) 2-species solutions on the boundaries.

We know that the carrying simplex exists for the competitive case [35]. The structure of the carrying simplex for the 3-species system has been studied by several authors. Zeeman and Zeeman [100, 102], and Baigent [5] both studied how the curvature of the carrying simplex can affect the stability of an existing interior steady state. Mierczyński's work on carrying simplices focuses on exploring the smoothness at the boundaries and corners (where the axial steady states lie) [62].

We work towards proving the existence of the balance simplex, however the work in this chapter will only be applicable to the parameter space where the dynamics are bounded and $\alpha_{ij} < 1$ and $\alpha_{ij}\alpha_{ji} < 1$, $i \neq j$, $i, j \in \{1, 2, 3\}$. Physically this excludes the case where species are strongly competitive or strongly co-operative. It also excludes any cases where one species is heavily predated on by another. Recall that by the balance simplex Σ, we mean an invariant surface which divides $\mathbb{R}^3_{\geq 0}$ into two distinct regions. It separates points with the α-limit of the origin, from those with the α-limit of infinity. All points on Σ have an α-limit which is neither the origin nor infinity, thus all non-zero steady states lie on Σ.

4.1 A series solution

We consider the three-species scaled Lotka–Volterra equations:

$$\begin{aligned}
\frac{dx_1}{dt} &= x_1(1 - x_1 - \alpha_{12}x_2 - \alpha_{13}x_3), \\
\frac{dx_2}{dt} &= x_2(1 - \alpha_{21}x_1 - x_2 - \alpha_{23}x_3), \\
\frac{dx_3}{dt} &= x_3(1 - \alpha_{31}x_1 - \alpha_{32}x_2 - x_3).
\end{aligned} \tag{4.1}$$

For the two-species case in Chapter 3, we found solutions in the form $x_1 = G(T),\ x_2 = TG(T)$ where $T = \frac{x_2}{x_1} \in [0, \infty)$. The function $G(T)$ takes the form of a hypergeometric function, and may need to be defined piecewise in some cases or multiplied by T^{-1} and constants.

We proceed with this idea for the 3-species case and consider $x_1 = G(T_1, T_2)$, $x_2 = T_1 G(T_1, T_2)$ and $x_3 = T_2 G(T_1, T_2)$ where $T_1 = \frac{x_2}{x_1}, T_2 = \frac{x_3}{x_1} \in [0, \infty)$. We expect to find G through a series solution, rather than an exact, analytic representation. Considering $\frac{dx_1}{dt} = \frac{dG}{dt}$ we have:

$$\frac{dT_1}{dt}\frac{\partial G}{\partial T_1} + \frac{dT_2}{dt}\frac{\partial G}{\partial T_2} = G(1 - G - \alpha_{12}T_1 G - \alpha_{13}T_2 G). \tag{4.2}$$

From $\frac{dx_2}{dt}$ we have:

$$\begin{aligned}\frac{dT_1}{dt}\left(G + T_1\frac{\partial G}{\partial T_1}\right) + T_1\frac{dT_2}{dt}\frac{\partial G}{\partial T_2} &= G\frac{dT_1}{dt} + T_1\frac{dG}{dt} \\ &= T_1 G(1 - \alpha_{21}G - T_1 G - \alpha_{23}T_2 G). \end{aligned}\tag{4.3}$$

Substituting $\frac{dG}{dt}$ as (4.2) into (4.3) and rearranging, we find

$$\frac{dT_1}{dt} = T_1 G\left[(1 - \alpha_{21}) + T_1(\alpha_{12} - 1) + T_2(\alpha_{13} - \alpha_{23})\right]. \tag{4.4}$$

Similarly, considering $\frac{dG}{dt}$ and $\frac{dx_3}{dt}$ gives:

$$\frac{dT_2}{dt} = T_2 G\left[(1 - \alpha_{31}) + T_1(\alpha_{12} - \alpha_{32}) + T_2(\alpha_{13} - 1)\right]. \tag{4.5}$$

By substituting (4.4) and (4.5) into (4.2), we can solve G as a series solution of the form

$$G(T_1, T_2) = \sum_{i,j=0}^{\infty} c_{i,j} T_1^i T_2^j, \tag{4.6}$$

with the condition $G(0,0) = 1$, meaning that the point $(1,0,0)$ lies on $\{G, T_1G, T_2G\}$ (which will form part of the balance simplex Σ). For $i, j \geq 1$:

$$\begin{aligned}
c_{0,0} &= 1 \\
c_{i,0} &= \frac{i(\alpha_{12}-1)+1}{i(\alpha_{21}-1)-1} c_{i-1,0} \\
c_{0,j} &= \frac{j(\alpha_{13}-1)+1}{j(\alpha_{31}-1)-1} c_{0,j-1} \\
c_{i,j} &= -\frac{[\alpha_{12}+(i-1)(\alpha_{12}-1)+j(\alpha_{12}-\alpha_{32})]}{i(1-\alpha_{21})+j(1-\alpha_{31})+1} c_{i-1,j} \\
&\quad - \frac{[\alpha_{13}+i(\alpha_{13}-\alpha_{23})+(j-1)(\alpha_{13}-1)]}{i(1-\alpha_{21})+j(1-\alpha_{31})+1} c_{i,j-1}.
\end{aligned} \tag{4.7}$$

With some rearranging and simplifying,

$$c_{i,0} = \frac{\left(\frac{\alpha_{12}}{\alpha_{12}-1}\right)_i}{\left(\frac{\alpha_{21}-2}{\alpha_{21}-1}\right)_i} \left(\frac{\alpha_{12}-1}{\alpha_{21}-1}\right)^i, \tag{4.8}$$

where we have used the Pochhammer symbol, $(x)_n = x(x+1)\cdots(x+n-1)$ for $n \geq 1$ and $(x)_0 = 1$. We now consider the case where $T_2 = 0$, i.e. the 2-species subcase with x_1 and x_2.

$$G(T_1, 0) = \sum_{i=0}^{\infty} \frac{\left(\frac{\alpha_{12}}{\alpha_{12}-1}\right)_i}{\left(\frac{\alpha_{21}-2}{\alpha_{21}-1}\right)_i} \left(\frac{\alpha_{12}-1}{\alpha_{21}-1}\right)^i T_1^i \tag{4.9}$$

$$= {}_2F_1\left[\frac{\alpha_{12}}{\alpha_{12}-1}, 1; \frac{\alpha_{21}-2}{\alpha_{21}-1}; \frac{T_1}{T_1^*}\right], \tag{4.10}$$

where $T_1^* = \frac{\alpha_{21}-1}{\alpha_{12}-1}$. This matches the x_1 co-ordinate of our first solution for the balance simplex in the 2-species case (with $\alpha = \alpha_{12}$ and $\beta = \alpha_{21}$) which is used when:

1. $\alpha_{12} > 1$ and $\alpha_{21} < 1$, in which case the known integral solution is valid for $T_1 \in [0, \infty)$.

2. $-\infty < \alpha_{12}, \alpha_{21} < 1$ and $\alpha_{12}\alpha_{21} < 1$, in which case the known integral solution

is valid for $T_1 \in [0, T_1^*]$.

However, we know that as the form of an infinite series (4.9), $G(T_1, 0)$ may not converge when $T_1 \geq |T_1^*|$, so we will focus on the second case above (in Chapter 3, this refers to case 3, see Table 3.1).

Similarly, on the x_1x_3-plane:

$$\begin{aligned} G(0, T_2) &= \sum_{j=0}^{\infty} \frac{\left(\frac{\alpha_{13}}{\alpha_{13}-1}\right)_j}{\left(\frac{\alpha_{31}-2}{\alpha_{31}-1}\right)_j} \left(\frac{\alpha_{13}-1}{\alpha_{31}-1}\right)^j T_2^j \\ &= {}_2F_1\left[\frac{\alpha_{13}}{\alpha_{13}-1}, 1; \frac{\alpha_{31}-2}{\alpha_{31}-1}; \frac{T_2}{T_2^*}\right] \end{aligned} \tag{4.11}$$

where $T_2^* = \frac{\alpha_{31}-1}{\alpha_{13}-1}$. In its series form, we know this converges for $T_2 \in [0, T_2^*)$ when $\alpha_{13}, \alpha_{31} < 1$ and $\alpha_{13}\alpha_{31} < 1$ which is what we will also assume.

In these cases, the convergence of T_1 and T_2 at the 2-species boundary interior steady states (T_1^* and T_2^*, respectively) holds due to Gauss' theorem:

Theorem 4.1.1 (Gauss' Theorem [6]) *When* $\Re(c-a-b) > 0$*,*

$${}_2F_1[a, b; c; 1] = \frac{\Gamma[c]\Gamma[c-a-b]}{\Gamma[c-a]\Gamma[c-b]}, \tag{4.12}$$

where ${}_2F_1$ *refers to the Gaussian hypergeometric function in its series form.*

The condition $\Re(c-a-b) > 0$ holds if $\alpha_{12}\alpha_{21} < 1$ and $\alpha_{12}, \alpha_{21} < 1$ for (4.9), and if $\alpha_{13}\alpha_{31} < 1$ and $\alpha_{13}, \alpha_{31} < 1$ for (4.11). Note that G does not necessarily converge in the whole interior of the domain $(T_1, T_2) \in [0, T_1^*] \times [0, T_2^*]$, convergence is only guaranteed on its boundaries where T_1 or $T_2 = 0$.

If we want to use the parametric surface $\{G, T_1G, T_2G\}$ (with the analogous coefficients) for the other two axial steady states ($(0,1,0)$ and $(0,0,1)$) by rotation, we need to ensure they also follow the same parameter case and use the first known solution on the boundaries.

Remark 4.1.2 *We consider only the following parameter space for the interaction matrix A of the system* (4.1)*:*

$$\begin{aligned}\mathcal{A} =&\{A \in \mathbb{R}^{3\times 3} \,|\, \alpha_{ii} = 1, \alpha_{ij} < 1, \alpha_{ij}\alpha_{ji} < 1, i \neq j, i, j \in \{1, 2, 3\} \\ &\textit{and the dynamics of (4.1) are bounded } \}\end{aligned} \tag{4.13}$$

This means each 2-species subsystem has an interior steady state which is attracting. The 3-species interior steady state may or may not exist.

Note the condition that the dynamics of (4.1) are bounded is not implied by the preceding inequalities. In the co-operative case, each pair of species will be weakly co-operative (meaning the dynamics on the boundaries are bounded), however the full system can still be unbounded. Consider the case where $\alpha_{ij} = -0.6$ for all $i \neq j$. The interior steady state of the full system does not exist, and since all species are co-operating, the dynamics are unbounded.

In Figure 4.1, we consider a competitive 3-species system where $0 < \alpha_{ij} < 1$. The orange surface is the parametric surface $\{G, T_1G, T_2G\}$ (up to order 100 in T_1 and T_2) starting from the axial steady state $(1, 0, 0)$ in the domain $(T_1, T_2) \in [0, T_1^*] \times [0, T_2^*]$. The red and light blue surfaces were found by rotating the system (in terms of re-indexing each species and the corresponding interaction coefficients) and applying the series solution G with these new parameters and co-ordinates (so this G has different coefficients). The darker patches in the red surface are where the numerical solution (in navy and shown separately in Figure 4.1b) lies slightly above the surface. We can also see an exposed navy region in the interior where the numerical solution is not covered by the domains of the parametric surfaces. If we try extending the domains, G (for all three cases) becomes very large in magnitude and sometimes negative, thus we have a problem with convergence to the numerical solution. In fact, even without extending, the orange surface does not converge entirely on its

domain to the numerical solution. This means that in this case, the union of these surfaces is not a good approximation for the carrying simplex as it does not form a simply connected surface (recall that a surface is called simply connected if every closed curve on the surface can be contracted to a point without leaving the surface).

In Figure 4.1c, we have used the series G only up to degree 20 in T_1 and T_2. By doing this, the parametric surfaces can be plotted slightly further beyond the aforementioned domains, whilst still resembling the numerical and boundary solutions. This tells us that the parametric surfaces $\{G, T_1G, T_2G\}$ does not require many terms to give us an idea of how Σ should appear. This also covers up the previously exposed region although the overlapping regions do not match exactly (some parts lie above or below other surfaces).

Figure 4.2 shows a fully co-operative system. In this case, the basic numerical solution from `Mathematica` does not work (numerical instabilities appear in the majority of the plot), and our parametric surfaces $\{G, T_1G, T_2G\}$ still gives us a good idea of the shape of the balance simplex. In Figure 4.2b, we see that the edges of each surface is not smooth, this is due to the plot itself in `Mathematica`. Where the surfaces intersect is where we expect the interior edges of the balance simplex to be. The parts above these edges can be ignored.

4.2 Existence of the balance simplex when $A \in \mathcal{A}$

We only consider the parameter case we have been working on, $\mathcal{A}$ (4.13). On the boundaries, this corresponds to case 3 in our 2-species solution classification (Chapter 3).

In the 3-species model, it is useful to recall the transformation to the total population size $N = x_1 + x_2 + x_3$ and the proportions of each species, $u_i = \frac{x_i}{N},\ i = 1, 2, 3$

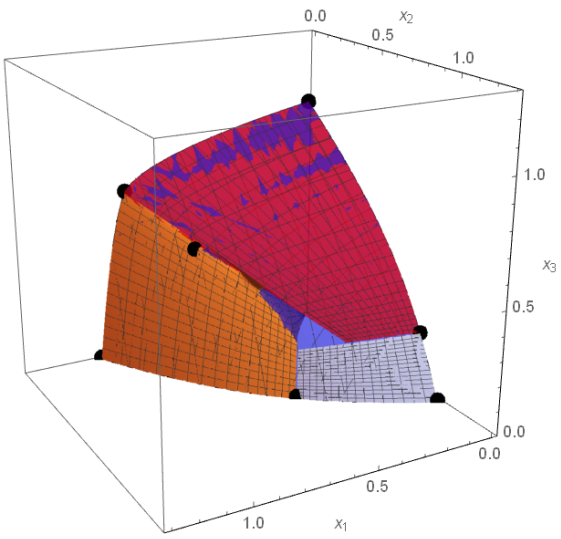

(a) The parametric surface $\{G, T_1G, T_2G\}$ (order 100 in T_1, T_2)

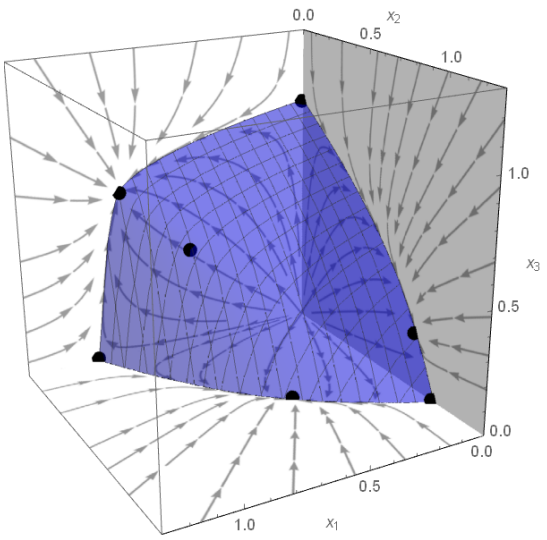

(b) The numerical solution for Σ

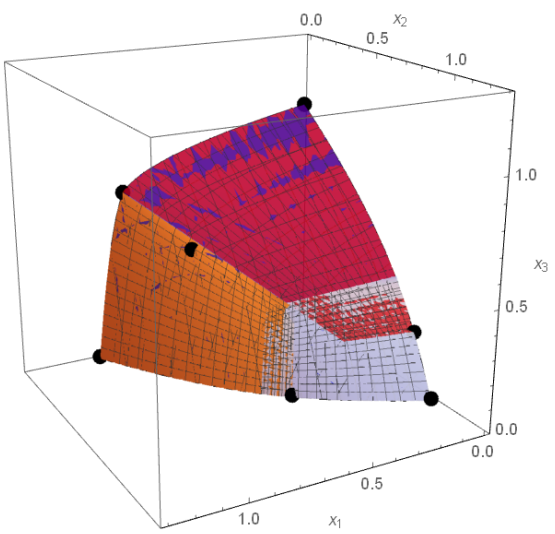

(c) The parametric surface $\{G, T_1G, T_2G\}$ (order 20 in T_1, T_2)

Figure 4.1: The parametric surface $\{G, T_1G, T_2G\}$ (or the equivalent rotation) from each axial steady state in yellow, red and light blue. The navy surface in all three figures is the numerical solution for Σ. The black points are the non-zero steady states.
Parameters: $\alpha_{12} = 0.75, \alpha_{13} = 0.18, \alpha_{21} = 0.62, \alpha_{23} = 0.54, \alpha_{31} = 0.32, \alpha_{32} = 0.87$.

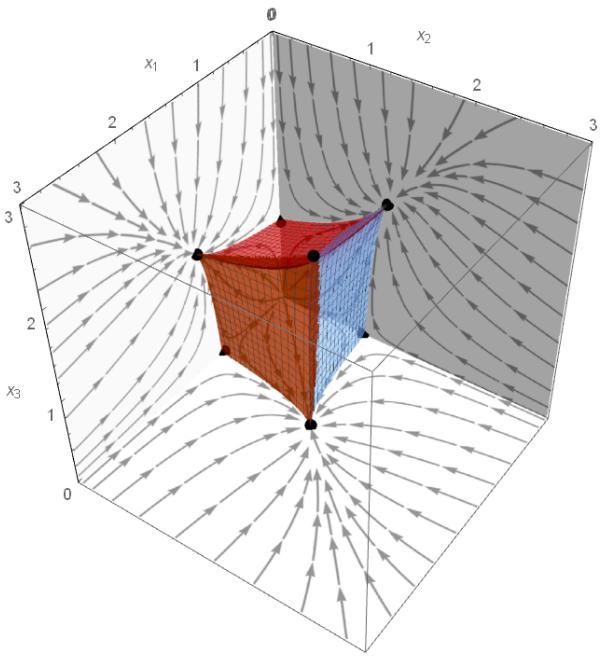

(a)

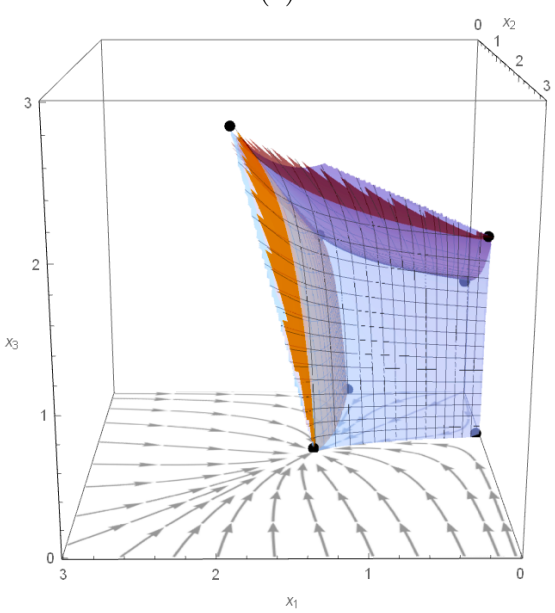

(b)

Figure 4.2: Different views of the same parametric surface $\{G, T_1G, T_2G\}$ (or the equivalent rotation) from each axial steady state where G is up to the order 100 in T_1, T_2. Where the surfaces intersect is where we expect the edges of the balance simplex to be.
Parameters: $\alpha_{12} = -0.25, \alpha_{13} = -0.18, \alpha_{21} = -0.22, \alpha_{23} = -0.14, \alpha_{31} = -0.32, \alpha_{32} = -0.57$.

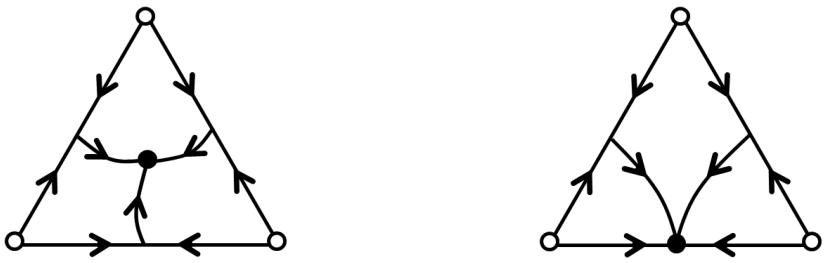

(a) Case 7 (b) Case 35

Figure 4.3: The relevant cases from Bomze's classification [10,11], showing the generic dynamics of the species proportions, u. Each vertex represents the case where only one species exists. In cases 7 and 35, there is a steady state which globally attracts everything from the interior of this simplex.

(Chapter 2, Section 2.2). After rescaling time by N, the dynamics are given by:

$$\frac{dN}{dt} = 1 - Nu^T Au, \tag{4.14}$$

$$\frac{du_1}{dt} = u_1 \left(u^T Au - (Au)_1 \right), \tag{4.15}$$

$$\frac{du_2}{dt} = u_2 \left(u^T Au - (Au)_2 \right), \tag{4.16}$$

where $A = [\alpha_{ij}]$ is the interaction matrix and $u = (u_1, u_2, u_3)^T$ is the vector of species proportions. The u dynamics are independent of the dynamics of the total population size N. When the former is known, the latter is in the form:

$$N = \exp\left[-\int_0^t u^T Au \, ds \right] \left(\int_0^t \exp\left[\int_0^r u^T Au \, ds \right] dr + N_0 \right). \tag{4.17}$$

Recall that for $A \in \mathcal{A}$, each 2-species subsystem has an interior steady state which is globally attracting in the interior that subsystem. The interior steady state of the full 3-species system, x^*, does not always exist. With this, we can easily identify that the u dynamics for the 3-species system will be case 7 or 35 from Bomze's classification [10, 11] (see Figure 4.3).

In our 3-species system, we assume the dynamics are bounded and that the origin and infinity are repelling. This means $\frac{dN}{dt} > 0$ for N small, and $\frac{dN}{dt} < 0$ for N large, thus $N^* = (u_s^T Au_s) > 0$ is attracting for N (where u_s is the globally attracting state

for u in case 7 or 35). Note that by rescaling time by N, these equations do not show that $N = 0$ is a steady state. However, the rescaling does not effect any other qualitative dynamics or the positions of the other steady states in (u, N).

Our aim in this section is to prove the existence of the balance simplex Σ in the 3-species system when the interaction matrix $A \in \mathcal{A}$. By construction, $\{G, T_1G, T_2G\}$ satisfies the dynamics of the system near $(T_1, T_2) = (0, 0)$ where $G(0, 0) = 1$ (which is equivalent to the axial steady state (1,0,0) in the x-co-ordinates). It also matches exactly with the series form of the known solutions on the 2-species boundaries when $T_1 \in [0, T_1^*]$ and $T_2 \in [0, T_2^*]$.

Taking the domain $T_1 \in [0, T_1^*]$ and $T_2 \in [0, T_2^*]$, we have seen that $\{G, T_1G, T_2G\}$ may not converge in the whole domain (e.g. parts of the interior). However, since the vector field of the system (4.1) is analytic (and thus analytic in a compact, convex region near (1,0,0) in the x-co-ordinates), the solution is analytic and unique near (1,0,0) [8] (also follows from the ODE version of the Cauchy–Kovalevskaya Theorem [23]). Therefore the solution of (4.1) can be represented by $\{G, T_1G, T_2G\}$ in a neighbourhood of $(1, 0, 0)$. This means we know $\{G, T_1G, T_2G\}$ converges near $(1, 0, 0)$ and we can plot it.

We can repeat this process for the other two axial steady states $(0, 1, 0)$ and $(0, 0, 1)$ (since all 2-species subsystems belong to the same case) by rotating the parameters and system, an example is shown in Figure 4.4a. These neighbourhoods near the axial steady states can be taken arbitrarily small.

Lemma 4.2.1 *The 3-species system (4.1) has no non-trivial periodic orbits or non-trivial closed orbits when $A \in \mathcal{A}$.*

Proof: As we have discussed, the species proportions follow the dynamics of $\frac{du_1}{dt}$ and $\frac{du_2}{dt}$ on a unit simplex as either case 7 or case 35 in Bomze's classification (Figure 4.3). Using this classification there are no non-trivial periodic orbits, or any non-trivial closed orbits (e.g. homoclinic orbits). □

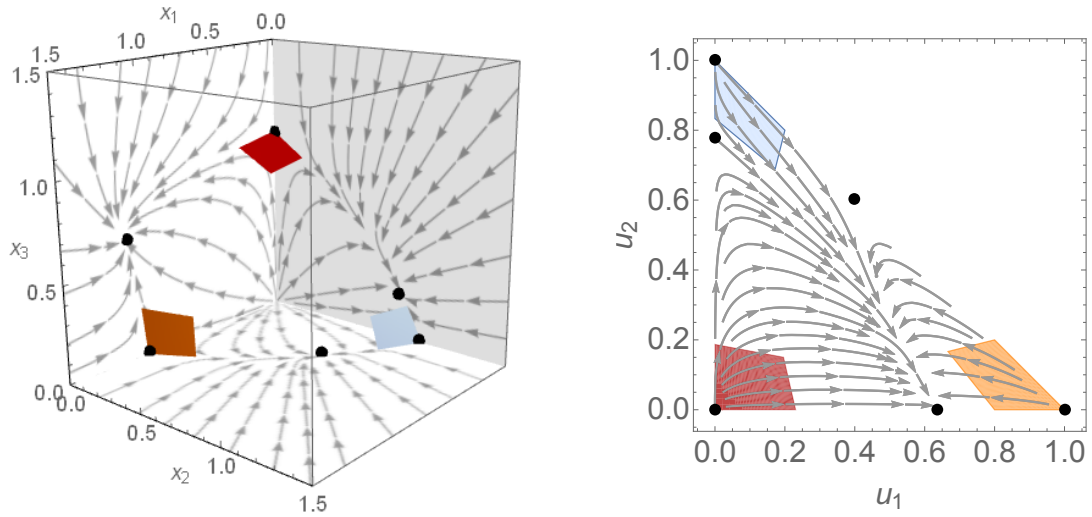

(a) E in (x_1, x_2, x_3) co-ordinates

(b) The projection of E in the u_1u_2-plane, E_u

Figure 4.4: In Figure 4.4a, the surface E is the solution $\{G, T_1G, T_2G\}$ (or the equivalent rotation) near the axial steady states where it is guaranteed to converge. For the purposes of this plot, we have used G up to degree 100 in T_1 and T_2, but in the theory, E uses the full infinite series G. These regions can be taken arbitrarily close to the axial steady states. In Figure 4.4b, the orbits shown are the u-dynamics and follows case 35 of Bomze's classification.
Parameters: $\alpha_{12} = 0.75$, $\alpha_{13} = -0.18$, $\alpha_{21} = 0.62$, $\alpha_{23} = 0.54$, $\alpha_{31} = 0.32$, $\alpha_{32} = 0.87$.

Lemma 4.2.2 *The 3-species balance simplex of (4.1) exists as a piecewise analytic surface when $A \in \mathcal{A}$.*

Proof: Since we assume the dynamics of (4.1) are bounded, we know infinity is repelling. This means we can consider the system in a compact domain (which must contain all steady states of the system) rather than the whole of $\mathbb{R}^3_{\geq 0}$. For example, for the co-operative system in Figure 4.2 we can consider the compact domain $[0, 3]^3$. Since the vector field is C^1-continuous with bounded derivatives on this compact domain, we know it is Lipschitz in the x variables on this domain [8]. This means solutions exist, are unique and vary continuously with initial conditions [8]. The same can be done with the system in (u, N)-co-ordinates, where the total population size N is bounded.

Recall our disjoint surface E which satisfies the dynamics of the system (4.1) (Figure 4.4a). When considering E in the u-simplex, we will call it E_u (Figure 4.4b).

Take any point on the interior boundary of E, say x_0. With this initial value, we can calculate the corresponding value in (u, N)-co-ordinates: (u_0, N_0). We know that u_0 lies in the interior of the u-simplex. Additionally, from Bomze's classification (Figure 4.3), we know the solution $u(u_0, t)$ will converge to the steady state in the u-simplex, denoted by u_s, which globally attracts the interior. Thus the dynamics of the species proportions are known and the total population $N(u, t)$ can be solved for with the initial condition $N(u_0, 0) = N_0$.

From the Lipschitz property and analyticity of the vector field (of the (u, N) system in a compact domain), the solution N is unique, varies continuously with initial conditions u_0 and is analytic along orbits [8]. We know N will converge to $N_s := (u_s^T A u_s)^{-1} > 0$. Putting this solution back in the x-co-ordinates gives an orbit from x_0 converging to $x_s := u_s N_s$, which is the steady state that globally attracts the interior $\mathbb{R}^3_{>0}$. Since N varies continuously with the initial condition u_0, as we take conditions u_0 around the interior of E_u, the solution trajectories will form a surface in both the (u, N)-co-ordinates and the x-co-ordinates (we know N remains non-zero). From Bomze's classification (Figure 4.3) and the Stable Manifold Theorem [69], we know these orbits in the x-co-ordinates represent the unstable manifolds of the axial steady states which are 2-dimensional (recall the axial steady states are stable on the axis they lie on).

Thus at any interior point on these unstable manifolds, we know the solution, and that the orbits converge to x_s. Again, using the continuity of solutions with initial conditions, it follows that the boundary of these unstable manifolds (relative to $\mathbb{R}^3_{\geq 0}$) are the heteroclinic orbits from the boundary 2-species interior steady states to x_s. Taking the union of these surfaces, all the non-zero steady states, and the heteroclinic orbits starting from the non-axial, non-zero steady states, we identify the balance simplex Σ.

This surface is indeed simply connected. From Bomze's classification, we know

there cannot be periodic orbits or closed orbits in $\mathbb{R}^3_{\geq 0}$. As we mentioned, the surface in question is continuous, thus if it is not simply connected, there would be a closed orbit on the surface satisfying the dynamics which is not possible. □

4.3 The carrying simplex when $\alpha_{ij} = \alpha = n/(n+1)$

In this section, we explore whether we can find an explicit solution for the 3-species case when the system is simplified, namely we impose that all interaction coefficients are equal, $\alpha_{ij} = \alpha$. Recall that our series solution is based on G (4.6), which has coefficients $c_{i,j}$ (4.7).

Lemma 4.3.1 *When all interaction coefficients $\alpha_{ij} = \alpha = \frac{n}{n+1}$; $n \in \mathbb{N}$, G is polynomial with a finite number of terms.*

Proof: We will examine the coefficients of G,

$$\begin{aligned} c_{n+1,0} = c_{0,n+1} &= \frac{\left(\frac{\alpha}{\alpha-1}\right)_{n+1}}{\left(\frac{\alpha-2}{\alpha-1}\right)_{n+1}} \\ &= \frac{\alpha(\alpha+(\alpha-1))\cdots(\alpha+n(\alpha-1))}{(\alpha-2)(\alpha-2+(\alpha-1))\cdots(\alpha-2+n(\alpha-1))}. \end{aligned} \tag{4.18}$$

When $\alpha = \frac{n}{n+1}$, $c_{n+1,0} = c_{0,n+1} = 0$. Note that this also implies $c_{m,0} = c_{0,m} = 0$ for all $m > n+1 \in \mathbb{N}$. Now consider

$$\begin{aligned} c_{n+1,j} &= -\frac{\alpha+n(\alpha-1)}{(1-\alpha)(n+1+j)+1}c_{n,j} - \frac{(\alpha+(j-1)(\alpha-1))}{(1-\alpha)(n+1+j)+1}c_{n+1,j-1} \\ &= 0 - \frac{(\alpha+(j-1)(\alpha-1))}{(1-\alpha)(n+1+j)+1}c_{n+1,j-1}, \end{aligned} \tag{4.19}$$

where the value of α simplifies the first term to 0. Following this recursion in j, we find that $c_{n+1,j}$ is a multiple of $c_{n+1,0} = 0$, therefore $c_{n+1,j} = 0$ for any $j \in \mathbb{N}$. By

symmetry, we can also conclude that $c_{i,n+1} = 0$ for any $i \in \mathbb{N}$. Now consider

$$c_{n+2,j} = 0 - \frac{(\alpha + (j-1)(\alpha - 1))}{(1-\alpha)(n+2+j)+1} c_{n+2,j-1}. \tag{4.20}$$

Again, following the recursion, we find that $c_{n+2,j}$ is a multiple of $c_{n+2,0} = 0$. This pattern continues and we can conclude that $c_{m,j} = 0$ for any $j > 0$ and $m > n+1$. By symmetry, $c_{i,m} = 0$ for any $i > 0$ and $m > n+1$. Therefore G is a finite polynomial with the highest order term of $T_1^n T_2^n$ when $\alpha = \frac{n}{n+1}$. □

G is symmetric in terms of T_1 and T_2 and has $(n+1)^2$ terms. For example, if $\alpha = \frac{2}{3}$, then $G = 1 - \frac{T_1}{2} - \frac{T_2}{2} + \frac{2T_1T_2}{5} + \frac{T_1^2}{10} + \frac{T_2^2}{10} - \frac{T_1^2T_2}{10} - \frac{T_1T_2^2}{10} + \frac{T_1^2T_2^2}{35}$.

In the simple case where $\alpha = \frac{1}{2}$, we have that $G = 1 - \frac{T_1}{3} - \frac{T_2}{3} + \frac{T_1T_2}{6}$. The parametric form of the surface is then $\{x_1, x_2, x_3\} = \{G, T_1G, T_2G\}$. We can eliminate T_1 and T_2 to find that the surface is a graph of a function:

$$x_3 = \frac{2x_1(3x_1^2 - 3x_1 + x_2)}{x_2 - 2x_1}. \tag{4.21}$$

This surface is an exact solution (see Figure 4.5), not an approximation, of our dynamics. Indeed, it satisfies the PDE derived from our system (4.1):

$$\begin{aligned} 0 = {} & x_1(1 - x_1 - \alpha x_2 - \alpha x_3)\frac{\partial x_3}{\partial x_1} + x_2(1 - \alpha x_1 - x_2 - \alpha x_3)\frac{\partial x_3}{\partial x_2} \\ & - x_3(1 - \alpha x_1 - \alpha x_2 - x_3). \end{aligned} \tag{4.22}$$

As with our other surfaces in the more general case, this gives one third of the carrying simplex, specifically the region near the axial steady state $(1, 0, 0)$ which is unaffected by the singularity along $x_2 = 2x_1$. To find the other parts, we just rotate the co-ordinates in the form (4.21) since the system is symmetric.

When $\alpha = \frac{n}{n+1}$, $n > 1$ it is not possible to write the surface as a graph of a function as there will be terms involving higher powers of x_3. Another way of

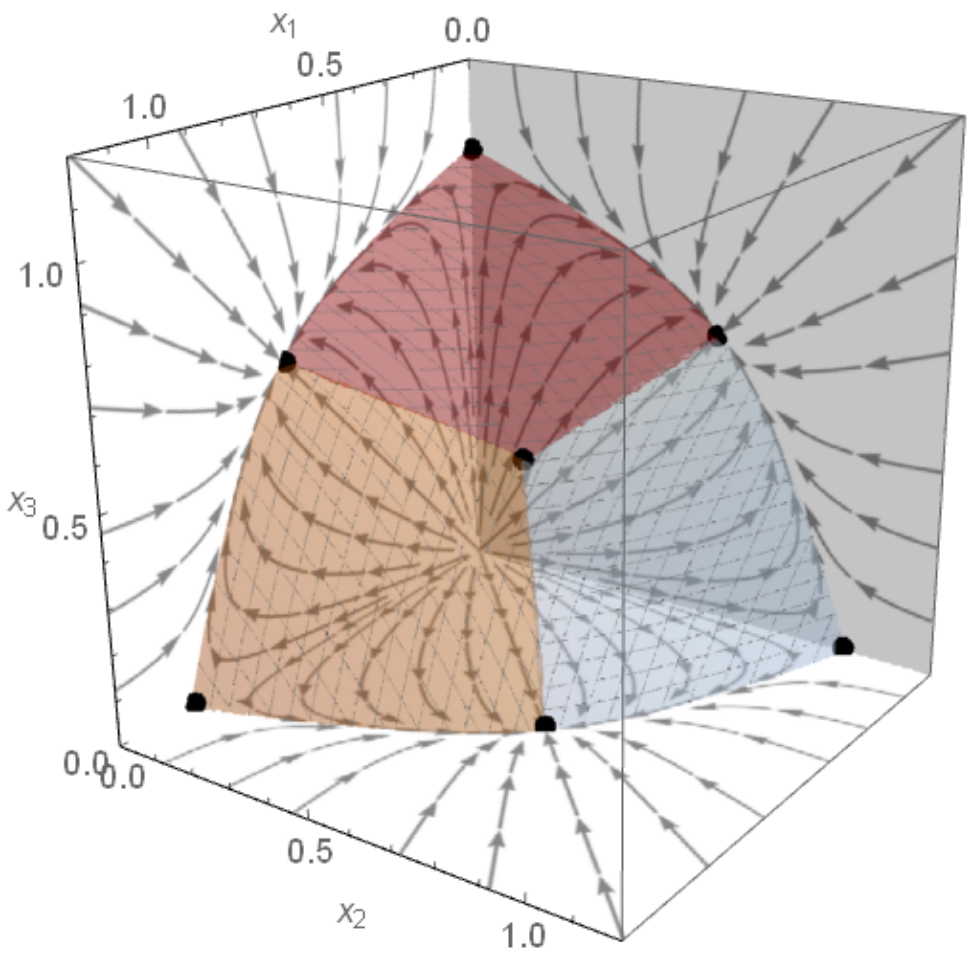

Figure 4.5: The carrying simplex of (4.1) where all parameters are equal to $\frac{1}{2}$. The orange surface is defined by (4.21), and the other two surfaces similarly by rotation. Using $\{G, T_1G, T_2G\}$ instead in these regions gives the same result.

verifying the surface satisfies the dynamics of our system is by computing its normal vector

$$n = \frac{\partial}{\partial T_1}\{G, T_1G, T_2G\} \times \frac{\partial}{\partial T_2}\{G, T_1G, T_2G\}. \tag{4.23}$$

Calculating the dot product of n with the vector field of the system (written in terms of T_1 and T_2) gives zero if the surface is tangent to the vector field. This is a simple way to verify the surface is indeed invariant to the flow of the system. In general, without specifying n, it is not easy to show this dot product is zero algebraically, due to the form of $c_{i,j}$.

In the figures of the previous sections, the plots of the parametric surfaces were approximations as they were finite versions of an infinite series with seemingly no analytic form. In this case, we are able to plot the surfaces exactly and it is precisely the carrying simplex, however it only applies to a small number of competitive cases.

4.4 The structure of c_{ij}

In our series solution G (4.6), the coefficients are given by $c_{i,j}$. When $i, j \geq 1$,

$$c_{i,j} = R_{i,j}c_{i-1,j} + U_{i,j}c_{i,j-1}, \tag{4.24}$$

where

$$\begin{aligned} R_{i,j} &= -\frac{[\alpha_{12} + (i-1)(\alpha_{12}-1) + j(\alpha_{12}-\alpha_{32})]}{i(1-\alpha_{21}) + j(1-\alpha_{31}) + 1}, \\ U_{i,j} &= -\frac{[\alpha_{13} + i(\alpha_{13}-\alpha_{23}) + (j-1)(\alpha_{13}-1)]}{i(1-\alpha_{21}) + j(1-\alpha_{31}) + 1}. \end{aligned} \tag{4.25}$$

In this subsection, we explore what the form of $c_{i,j}$ will look like when we iterate it back towards the explicitly known boundary values $c_{i,0}$ and $c_{0,j}$ (see (4.8)).

Consider a rectangular grid of nodes. From the node (i, j), we assign the path from $(i-1, j)$ to (i, j) with the value $R_{i,j}$ (if $i > 0$) and the path from $(i, j-1)$ to (i, j) with $U_{i,j}$ (if $j > 0$). For longer paths, the value assigned will be the product of these.

Remark 4.4.1 *We will only consider paths which travel upwards and rightwards, and not along the boundary where i or $j = 0$. For example, there will be no such paths from $(0, 0)$ to any other node.*

Definition 4.4.1 Consider the node (i, j) where $i, j \neq 0$. For each of the boundary nodes $(g, 0),\ g \leq i$, assign the value $c_{g,0}$ (from (4.8)). Similarly for the boundary nodes $(0, h),\ h \leq j$, assign the value $c_{0,h}$. Consider the value of all possible paths starting from the boundary nodes, multiplied by the value at that boundary node. Let $P_{i,j}$ be the sum of these terms.

For example, from Figure 4.6:

$$\begin{aligned}
P_{1,1} &= R_{1,1}c_{0,1} + U_{1,1}c_{1,0}\,, \\
P_{2,1} &= R_{2,1}R_{1,1}c_{0,1} + R_{2,1}U_{1,1}c_{1,0} + U_{2,1}c_{2,0}\,, \\
P_{1,2} &= R_{1,2}c_{0,2} + U_{1,2}R_{1,1}c_{0,1} + U_{1,2}U_{1,1}c_{1,0}\,, \\
P_{2,2} &= R_{2,2}R_{1,2}c_{0,2} + R_{2,2}U_{1,2}R_{1,1}c_{0,1} + U_{2,2}R_{2,1}R_{1,1}c_{0,1} \\
&\quad + R_{2,2}U_{1,2}U_{1,1}c_{1,0} + U_{2,2}R_{2,1}U_{1,1}c_{1,0} + U_{2,2}U_{2,1}c_{2,0}\,.
\end{aligned} \tag{4.26}$$

It will be useful to note that we can also write

$$P_{2,2} = U_{2,2}P_{2,1} + R_{2,2}U_{1,2}P_{1,1} + R_{2,2}R_{1,2}c_{0,2}\,, \tag{4.27}$$

which considers the interior nodes which lie under and to the left of $(2, 2)$ (i.e. (2,1) and (1,1)). It also considers the value of the path from the boundary node on the

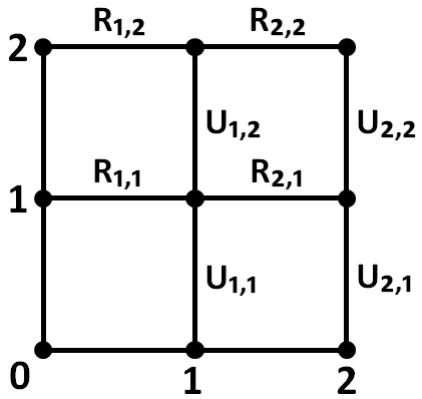

Figure 4.6: A 2×2 grid of nodes, with the path values $U_{i,j}$ and $R_{i,j}$, $1 \leq i, j \leq 2$.

same row as $(2, 2)$.

At a node, the only option for movement is to move either upwards or rightwards. From $(1, 1)$ to (i, j), all paths will take $i + j - 2$ steps. Since we know $i - 1$ of these steps must be towards the right, the number of paths from $(1, 1)$ to (i, j) is given by

$$\binom{i+j-2}{i-1} = \frac{(i+j-2)!}{(j-1)!\,(i-1)!}. \tag{4.28}$$

Since the first step from the boundary is unique, to find the number of paths to (i, j), where $i, j > 0$, we can sum the number of paths from $(1, 1), (1, 2), \ldots, (1, j)$ and $(1, 1), (2, 1), (3, 1), \ldots, (i, 1)$. The node (1,1) is counted twice as it is the only node with two 1-step paths from the boundary. Thus the number of paths to the node (i, j) is given by

$$\sum_{k=0}^{j-1} \binom{i+j-2-k}{i-1} + \sum_{k=0}^{i-1} \binom{i+j-2-k}{j-1}. \tag{4.29}$$

For example, the number of paths to (2,2) from the boundary is:

$$\sum_{k=0}^{1} \binom{2-k}{1} + \sum_{k=0}^{1} \binom{2-k}{1} = 6. \tag{4.30}$$

We now prove that the coefficients of G are the terms $P_{i,j}$ from Definition 4.4.1.

Lemma 4.4.2 *$c_{m,n} = P_{m,n}$ for all $m, n \in \mathbb{N}$.*

Proof: We prove this by induction.

There are only two paths to the node $(1,1)$ from the boundary. We find that $P_{1,1} = U_{1,1}c_{1,0} + R_{1,1}c_{0,1}$. Comparing this to the definition of $c_{1,1}$ (4.24), we conclude that $c_{1,1} = P_{1,1}$.

We now assume that $c_{m,n} = P_{m,n}$, and that $c_{i,j} = P_{i,j}$ holds for all (i,j) such that $(i,j) \leq (m,n)$ (using our notation from vector ordering).

By definition,

$$\begin{aligned} c_{m,n+1} &= U_{m,n+1}c_{m,n} + R_{m,n+1}c_{m-1,n+1} \\ &= U_{m,n+1}P_{m,n} + R_{m,n+1}(U_{m-1,n+1}P_{m-1,n} + R_{m-1,n+1}c_{m-2,n+1}) \\ &= U_{m,n+1}P_{m,n} + R_{m,n+1}U_{m-1,n+1}P_{m-1,n} \\ &\quad + R_{m,n+1}R_{m-1,n+1}(U_{m-2,n+1}P_{m-2,n} + R_{m-2,n+1}c_{m-3,n+1}). \end{aligned}$$

We keep iterating the $c_{m-k,n+1}$ term (at the end) by increasing $k > 0$ to m and using the definition of $c_{i,j}$ and our induction hypothesis. This gives

$$\begin{aligned} c_{m,n+1} = U_{m,n+1}P_{m,n} &+ R_{m,n+1}U_{m-1,n+1}P_{m-1,n} \\ &+ R_{m,n+1}R_{m-1,n+1}U_{m-2,n+1}P_{m-2,n} + \dots \\ &+ R_{m,n+1}R_{m-1,n+1}\cdots R_{2,n+1}U_{1,n+1}P_{1,n} \\ &+ R_{m,n+1}R_{m-1,n+1}\cdots R_{2,n+1}R_{1,n+1}c_{0,n+1}\,. \end{aligned} \tag{4.31}$$

In this form, it is exactly analogous to the example shown in equation (4.27). Indeed, we are considering the terms $P_{i,n}$ from the nodes (i,n) for $1 \leq i \leq m$, and the value of the horizontal path from (0,n+1) to $(m, n+1)$, multiplied by $c_{0,n+1}$. Recall that $P_{i,n}$ contains the values of all paths from the boundary nodes to (i,n). In (4.31), each $P_{i,n}$ is multiplied by the value of the path travelling one step upwards ($U_{i,n+1}$) and then $m-i$ steps right-wards (the R terms). With the aforementioned horizontal path,

this accounts for all possible paths from the boundary to $(m, n+1)$. We conclude that $c_{m,n+1} = P_{m,n+1}$.

By swapping U and N, and the order of the indices, we can also conclude that $c_{m+1,n} = P_{m+1,n}$. Thus this lemma is proven by induction. □

Thus we have shown that the coefficients of G, $c_{i,j}$, can be determined by considering the values along the paths from the boundary nodes, along with the values at these boundary nodes which are known, $c_{i,0}$ and $c_{0,j}$.

4.5 Asymptotic completeness

In this section, we prove that the balance simplex Σ satisfies the condition of being asymptotically complete, given by Hirsch for carrying simplices.

Definition 4.5.1 ([36]) $\Sigma \subset \mathbb{R}^3_{\geq 0}$ is called asymptotically complete if every non-zero point $x \in \mathbb{R}^3_{\geq 0}$ is asymptotic with some point $y \in \Sigma$ under the flow, i.e. $\lim_{t\to\infty}|\varphi_t(x) - \varphi_t(y)| = 0$.

In our work thus far, we mentioned how Σ globally (and asymptotically) attracts all non-zero initial points, $x \in \mathbb{R}^3_{\geq 0}$. In this case, one could pick the ω-limit of x (a steady state, shown in the upcoming lemma, Lemma 4.5.1) and conclude that the orbits from these two points satisfy the condition in Definition 4.5.1. However, this is a trivial case which is not useful if we want to reduce the dynamics of the system to a hypersurface without losing information (as done by the carrying simplex [35, 36]). We will avoid this case unless the dynamics are truly trivial (discussed at the end of this section in Corollary 4.5.3).

The assumption we make is that the balance simplex exists as a unique, simply connected surface which divides $\mathbb{R}^3_{\geq 0}$ into two distinct regions: one containing points with the α-limit of the origin, and the other containing points with the α-limit of

infinity. This holds for systems in the parameter space we have been discussing in this chapter.

We first establish the following:

Lemma 4.5.1 *For the system (4.1) with parameters such that the dynamics are bounded and steady states are hyperbolic, there are no non-trivial periodic orbits, thus the ω-limit of every point is a steady state.*

Proof: Consider Bomze's classification of the dynamics of the species proportions on the u-simplex for 3 species [10, 11]. The only cases where non-trivial periodic orbits exist implies that there are infinitely many of them. Thus the steady state contained in them is a centre which is not hyperbolic (it follows that the corresponding steady state in the x-co-ordinate will also be non-hyperbolic) [31,37]. We also see that in the cases where all steady states are hyperbolic, all initial frequencies tend to a steady state and since the N dynamics are taken to be bounded, the ω-limit of every point $x \in \mathbb{R}^3_{\geq 0}$ is a steady state. □

Now we can prove the following theorem (which also works in the 2-species case as we have shown there are no non-trivial periodic orbits for that system either, Chapter 2 Corollary 2.4.4).

Theorem 4.5.2 *Consider the system (4.1) with parameters such that the dynamics are bounded, the steady states are hyperbolic, and the balance simplex Σ exists. Then Σ is asymptotically complete.*

Proof: Consider any initial non-zero point x_0 in $\mathbb{R}^3_{\geq 0}$. This point can be written as $u_0 N_0$ where u_0 is the vector of species proportions and $N_0 > 0$ is the total population size. We take a ray from the origin through x_0, labelled R_0. Let x_Σ denote a point which lies on $R_0 \cap \Sigma$, which can be written as $u_0 N_\Sigma$, $N_\Sigma > 0$. Note that x_Σ exists due to Σ existing and being simply connected.

Recall that the dynamics for u ((4.15) and (4.16)) are independent of N. For

u_0, the orbit $u(u_0, t)$ asymptotically tends to a steady state, say u_s, as there are no non-trivial periodic orbits (Lemma 4.5.1). Now consider the ray from the origin through a point with the species proportions u_s, labelled R_s. Recall that we assume the N dynamics are bounded. On R_s the dynamics are given by:

$$\frac{dN}{dt} = 1 - u_s^T A u_s N. \tag{4.32}$$

Using boundedness this means that the constant $u_s^T A u_s > 0$; we find that the N dynamics has an attracting steady state $N_s := (u_s^T A u_s)^{-1}$ (globally attracting on $R_s \setminus \{0\}$). This means $\lim_{t\to\infty} \varphi_t(u_0 N_0) = u_s N_s$ and $\lim_{t\to\infty} \varphi_t(u_0 N_\Sigma) = u_s N_s$. The point $u_s N_s$ is a non-zero steady state thus it lies on Σ.

We have shown that the orbit starting from $x_0 = u_0 N_0$ is asymptotically attracted to the orbit starting from $x_\Sigma = u_0 N_\Sigma \in \Sigma$, which remains on Σ due to its invariance.

□

Corollary 4.5.3 *Suppose the dynamics of the 3-species scaled Lotka–Volterra system (4.1) are bounded, all steady states are hyperbolic, and the balance simplex Σ exists. Consider any non-zero steady state $x_s = u_s N_s$, where $N_s = (u_s^T A u_s)^{-1} > 0$ and label the ray from the origin through this steady state by R_s. Then for any non-zero point on $x \in R_s$, $\varphi_t(x) \in R_s$ for all $t \in \mathbb{R}$ and $\lim_{t\to\infty} \varphi_t(x) = x_s$.*

Proof: The fact that the ray R_s is invariant to the flow of the system follows from u_s being a steady state in the u dynamics. The global attraction of x_s along $R_s \setminus \{0\}$ follows from the previous proof. □

4.6 Conclusions

In this chapter, we first proved the existence of the balance simplex Σ in a 3-species scaled Lotka–Volterra system when the dynamics are bounded and the inter-

specific interaction coefficients satisfy $\alpha_{ij} < 1$ and $\alpha_{ij}\alpha_{ji} < 1$, $i \neq j$, $i, j \in \{1, 2, 3\}$. This means that each 2-species subsystem has an interior steady state which is attracting. Physically, it excludes the case where species are strongly competitive or strongly co-operative. It also excludes the case where one species is heavily predated on by another.

We were able to find a series solution for the 3-species case which matches exactly the known 2-species solution (in series form) on the boundaries. Since this series solution satisfies the dynamics of the system, we were able to prove the existence of the balance simplex by taking a small extension of this solution from each axial steady state into $\mathbb{R}^3_{>0}$ and taking the surface formed by evolving the points on this extension over time.

The series solution $\{G, T_1G, T_2G\}$ is based around the axial steady state $(1, 0, 0)$ and the only restriction used when finding the series G was that the axial steady state lies on the surface, i.e. $G(0, 0) = 1$. By rotation, we were able to find the series solutions for the other two axial steady states. As we have mentioned, the combined piecewise solution itself is not generally the balance simplex and it does not always converge on the interior (see Figure 4.1a). Since the boundary condition of the known 2-species solution was not actually used to find the coefficients of G, we have not been able to find a series for the other parameter cases, even when starting a series solution about a different point from $(T_1, T_2) = (0, 0)$.

In the special case where $a_{ij} = \frac{n}{n+1}$ for any $i, j \in \{1, 2, 3\}$, $n \in \mathbb{N}$, the series G is finite (i.e. a polynomial), and $\{G, T_1G, T_2G\}$ is the exact expression for one third of the carrying simplex.

In Section 4.5, we prove that when Σ exists for a 3-species scaled Lotka–Volterra system with hyperbolic steady states and bounded dynamics, Σ is asymptotically complete (see Definition 4.5.1) in a non-trivial way, the result can also be applied to the 2-species case. We also show that any ray from the origin to a non-zero steady

state is invariant to the flow (Corollary 4.5.3).

In the next chapter, we continue to work with the 3-species scaled Lotka–Volterra system (4.1) and prove the existence of Σ when the interaction matrix A is strictly copositive.

Chapter 5

Existence of the Balance Simplex in a 3-Species Scaled Lotka–Volterra System When the Interaction Matrix A Is Strictly Copositive

In this chapter, we prove the existence of the balance simplex Σ when the interaction matrix $A = [\alpha_{ij}]$ of the 3-species scaled Lotka–Volterra system is strictly copositive. This result will appear in an upcoming paper. Recall that the system is given by:

$$\begin{aligned}
\frac{dx_1}{dt} &= x_1(1 - x_1 - \alpha_{12}x_2 - \alpha_{13}x_3),\\
\frac{dx_2}{dt} &= x_2(1 - \alpha_{21}x_1 - x_2 - \alpha_{23}x_3),\\
\frac{dx_3}{dt} &= x_3(1 - \alpha_{31}x_1 - \alpha_{32}x_2 - x_3).
\end{aligned} \tag{5.1}$$

The real matrix A is called strictly copositive when $x^TAx > 0$ for $x \neq 0$, $x \in \mathbb{R}^3_{\geq 0}$ [30]. Physically, this means that the average fitness of the whole population is always positive, regardless of the composition of the population [37]. Since $2x^TAx = x^T(A + A^T)x$, it suffices to discuss whether the symmetric matrix $\frac{(A+A^T)}{2}$ is strictly copositive when discussing the strict copositivity of A.

5.1 Strict copositivity

Lemma 5.1.1 (Hadeler [30]) *The real symmetric matrix* $B = \begin{pmatrix} 1 & \alpha & \beta \\ \alpha & 1 & \gamma \\ \beta & \gamma & 1 \end{pmatrix}$ *is strictly copositive if and only if* $\min\{\alpha, \beta, \gamma\} > -1$ *and at least one of the following two conditions hold:*

$$\alpha + \beta + \gamma + 1 > 0 \tag{5.2}$$

$$1 + 2\alpha\beta\gamma - \alpha^2 - \beta^2 - \gamma^2 > 0. \tag{5.3}$$

We denote the 2-dimensional unit probability simplex by $\Delta = \{u \in \mathbb{R}^3_{\geq 0} \,|\, u_1 + u_2 + u_3 = 1\}$, the dynamics of the replicator system for 3 strategies and the matrix

game A is given by [37]:

$$\begin{aligned}\frac{du_1}{dt} &= u_1\left((Au)_1 - u^TAu\right),\\ \frac{du_2}{dt} &= u_2\left((Au)_2 - u^TAu\right).\end{aligned} \tag{5.4}$$

Theorem 5.1.2 *If (i) the interaction matrix A is strictly copositive, (ii) all steady states of the system (5.4) are isolated and hyperbolic, then the 3-species scaled Lotka–Volterra system (5.1) has a balance simplex Σ which is piecewise analytic and there is a continuous function $\Psi : \Delta \to [0,\infty)$ such that $\Sigma = \{\Psi(u)u \,|\, u \in \Delta\}$.*

Recall the dynamics of the (u_1, u_2, N) system where u_1 and u_2 are the proportions of species 1 and 2 (respectively) and N is the total population size (equations (4.14)-(4.16) from Chapter 4 which have time rescaled by N). The reason for considering A to be strictly copositive is because this implies the dynamics remain bounded, indeed we have that $u^TAu > 0$ thus $\frac{dN}{dt}$ remains bounded. Along with condition (ii), this means that there are no non-trivial periodic orbits (see Lemma 4.5.1 from Chapter 4). Thus every orbit of the u-dynamics in Δ converges (in forwards and backwards time).

If we consider the (u_1, u_2, N)-dynamics (Chapter 2, Section 2.2) without rescaling time t by N yet as we typically have, but instead reversing it (now denoted by s and with the population density now denoted by M) we have the system

$$\frac{dM}{ds} = M(Mu^TAu - 1), \tag{5.5}$$

$$\frac{du_1}{ds} = u_1M\left((Au)_1 - u^TAu\right), \tag{5.6}$$

$$\frac{du_2}{ds} = u_2M\left((Au)_2 - u^TAu\right). \tag{5.7}$$

With the time reversed, the origin of this system in the x-co-ordinates is an attractor,

thus we will be discussing the basin of attraction of the origin, $\mathcal{B}(0)$, and denote its boundary relative to $\mathbb{R}^3_{\geq 0}$ by $\partial\mathcal{B}(0)$.

Consider some initial point $u_0 \in \Delta$ and $M_0 > 0$. We introduce the invertible function $\tau : [0,\infty) \to [0,\infty)$ by $\tau(s) = \int_0^s M(u_0, M_0, \sigma)\, d\sigma$. We will be rescaling time using τ. In the limit of this integral, there are two possibilities:

$$(a) \quad \int_0^\infty M(u_0, M_0, \sigma)\, d\sigma < \infty, \tag{5.8}$$

$$(b) \quad \int_0^\infty M(u_0, M_0, \sigma)\, d\sigma = \infty. \tag{5.9}$$

In case (a), since M remains positive and smooth for $M_0 > 0$ (the vector field is analytic), we must have that $\lim_{s\to\infty} M(u_0, M_0, s) = 0$. Thus in this case, $u_0 M_0 \in \mathcal{B}(0)$.

We now consider case (b). With the time scaling τ, the system is:

$$\frac{d\overline{M}}{d\tau} = \overline{M}\,\overline{\theta} - 1, \tag{5.10}$$

$$\frac{d\overline{u}_1}{d\tau} = \overline{u}_1 \left((A\overline{u})_1 - \overline{\theta} \right), \tag{5.11}$$

$$\frac{d\overline{u}_2}{d\tau} = \overline{u}_2 \left((A\overline{u})_2 - \overline{\theta} \right), \tag{5.12}$$

where $\overline{\theta} = \overline{u}(u_0,\tau)^T A \overline{u}(u_0,\tau)$. Note that $\overline{u}_1$ and $\overline{u}_2$ follow the replicator dynamics (5.4) on Δ. By explicit integration, we find that

$$\overline{M}(u_0, M_0, \tau) = \exp\left[\int_0^\tau \overline{\theta}(u_0,\sigma)\, d\sigma\right] \left(M_0 - \int_0^\tau \exp\left[-\int_0^\rho \overline{\theta}(u_0,\sigma)\, d\sigma \right] d\rho \right). \tag{5.13}$$

We define $\psi : \Delta \times [0,\infty) \to [0,\infty)$ by

$$\psi(u_0,\tau) = \int_0^\tau \exp\left[-\int_0^\rho \overline{\theta}(u_0,\sigma)\, d\sigma \right] d\rho. \tag{5.14}$$

Since A is strictly copositive, $\overline{\theta} \geq \delta > 0$. Thus for all $u_0 \in \Delta$,

$$\psi(u_0, \tau) \leq \int_0^\tau \exp\left[-\int_0^\rho \delta \, d\sigma\right] d\rho = \frac{1}{\delta}\left(1 - \exp[-\delta\tau]\right) < \frac{1}{\delta}. \tag{5.15}$$

For a fixed $u_0 \in \Delta$, $\psi(u_0, \tau)$ is an increasing function of τ bounded above by $\frac{1}{\delta}$ hence we may pass to the limit

$$\lim_{\tau\to\infty} \psi(u_0, \tau) = \int_0^\infty \exp\left[-\int_0^\rho \overline{\theta}(u_0, \sigma) \, d\sigma\right] d\rho < \frac{1}{\delta}. \tag{5.16}$$

We define $\Psi : \Delta \to [0, \infty)$ by the pointwise limit

$$\Psi(u_0) = \lim_{\tau\to\infty} \psi(u_0, \tau), \quad u_0 \in \Delta. \tag{5.17}$$

For $\tau_2 > \tau_1$,

$$\begin{aligned} \max_{u_0\in\Delta} |\psi(u_0, \tau_2) - \psi(u_0, \tau_1)| &= \max_{u_0\in\Delta} \int_{\tau_1}^{\tau_2} \exp\left[-\int_0^\rho \overline{\theta}(u_0, \sigma) \, d\sigma\right] d\rho \\ &\leq \frac{1}{\delta}\left(\exp[-\delta\tau_1] - \exp[-\delta\tau_2]\right). \end{aligned} \tag{5.18}$$

The right hand side (5.18) can be made arbitrarily small for sufficiently large τ_1 and τ_2, say $\tau_2 > \tau_1 > T$ independent of u_0. In other words, $\psi(\cdot, \tau)$ is a uniformly Cauchy sequence of continuous functions on Δ which converges uniformly to a continuous function on Δ as $\tau \to \infty$, thus Ψ is continuous on Δ [71, Thm 7.12]. Note that the uniform convergence of $\psi(\cdot, \tau)$ also follows from (5.18), consider taking the limit $\tau_2 \to \infty$ first.

Recall that we are discussing case (b) (5.9) so $\tau(s) \to \infty$ as $s \to \infty$. Since A is strictly copositive, $\overline{\theta} > 0$ thus $\int_0^\tau \overline{\theta}(u_0, s) \, ds \to \infty$ as $\tau \to \infty$. Recalling the expression for $\overline{M}$ (5.13), if $M_0 > \Psi(u_0)$ then $\overline{M}(u_0, M_0, \tau) \to \infty$ as $\tau \to \infty$ meaning that $u_0 M_0 \in \mathcal{B}(\infty)$. If $M_0 < \Psi(u_0)$, we have $\overline{M}(u_0, M_0, \tau) \to -\infty$ as $\tau \to \infty$ but we

know that $\overline{M} \geq 0$. This contradiction means this scenario does not happen in case (b) but in case (a) instead, meaning $u_0 M_0 \in \mathcal{B}(0)$.

Recall that basins of attraction (and repulsion) are open [83], thus $\mathcal{B}(0)$ and $\mathcal{B}(\infty)$ are open in $\mathbb{R}^3_{\geq 0}$. Now consider a point $u_0 M_0 \in \partial\mathcal{B}(\infty)$, since $u_0 M_0 \notin \mathcal{B}(\infty)$ this implies $M_0 \leq \Psi(u_0)$. We can find a sequence of points in $\mathcal{B}(\infty)$ which converges to $u_0 M_0$. We write this sequence in the form $\{u_i M_i\}_{i\in\mathbb{N}}$, where all $u_i \in \Delta$, $M_i \in \mathbb{R}$. It follows that u_i converges to u_0 and M_i converges to M_0 (since all non-zero points in this form have a unique representation). Every point of this sequence is not in $\mathcal{B}(0)$ and thus satisfies $M_i \geq \Psi(u_i)$. Using the continuity of Ψ, it follows that the limit point $u_0 M_0 \in \partial\mathcal{B}(\infty)$ satisfies $M_0 = \Psi(u_0)$. Similarly, we find that any point $u_0 M_0 \in \partial\mathcal{B}(0)$ also satisfies $M_0 = \Psi(u_0)$.

Now consider a point $u_0 M_0$ which satisfies $M_0 = \Psi(u_0)$. We can find a sequence $\{M_i\}_{i\in\mathbb{N}}$ in $\mathbb{R}$ which converges to M_0 from above (i.e. $M_i > M_0 = \Psi(u_0)$ for all $i \in \mathbb{N}$), meaning the points $u_0 M_i \in \mathcal{B}(\infty)$ for all $i \in \mathbb{N}$. Similarly, we can find a sequence $\{\widetilde{M}_i\}_{i\in\mathbb{N}}$ in $\mathbb{R}$ which converges to M_0 from below (i.e. $\widetilde{M}_i < M_0 = \Psi(u_0)$ for all $i \in \mathbb{N}$) implying $u_0\widetilde{M}_i \in \mathcal{B}(0)$ for all $i \in \mathbb{N}$. Since the basins of attraction are open in $\mathbb{R}^3_{\geq 0}$, we can conclude that $u_0 M_0 \in \partial\mathcal{B}(0)$ and $u_0 M_0 \in \partial\mathcal{B}(\infty)$ both hold.

The results from the previous two paragraphs allow us to conclude that $\partial\mathcal{B}(0) = \partial\mathcal{B}(\infty)$. We denote this set by Σ and by definition it is the balance simplex. Therefore taking any $u_0 \in \Delta$ we can find the point $u_0 M_0$ which is on the balance simplex by taking:

$$M_0 = \Psi(u_0) = \int_0^\infty \exp\left[-\int_0^\rho \overline{\theta}(u_0, \sigma)\, d\sigma\right] d\rho. \tag{5.19}$$

Note that this point is unique, meaning the balance simplex can be radially projected 1-to-1 and onto the unit simplex Δ.

The replicator dynamics on Δ have been classified by Bomze [10, 11]. Let E

denote the set of steady states of the $\overline{u}$-dynamics (5.11), (5.12) (which we assume are hyperbolic). Recall that all orbits in Δ converge to an equilibrium (Lemma 4.5.1 from Chapter 4), thus we know that

$$\Delta = \bigcup_{p_i \in E} W^s(p_i), \tag{5.20}$$

where $p_i \in E$ is a steady state and $W^s(p_i)$ is its stable manifold. The vector field on Δ is analytic, so by the Stable Manifold Theorem [69], each $W^s(p_i)$ is an analytic manifold. Mapping each $u_0 \in W^s(p_i)$ to $u_0\Psi(u_0) \in \Sigma$ gives the stable manifold of $p_i\Psi(p_i)$ which is a steady state of the 3-species Lotka–Volterra system. We can conclude that each $W^s(p_i\Psi(p_i))$ is an analytic manifold, thus Σ is (at least) a piecewise analytic surface.

The reason for choosing the union of stable manifolds (and not the unstable manifolds) for Δ and each non-zero steady state $p_i\Psi(p_i)$ of (5.1) follows from Corollary 4.5.3 in Chapter 4. In this context with time reversed, $p_i\Psi(p_i)$ is repelling on the ray from the origin through $p_i\Psi(p_i)$. So if we had taken the unstable manifolds, we would not identify Σ.

Finally, after reversing time (back to t) and considering the basins of repulsions and unstable manifolds instead, the statement of Theorem 5.1.2 is now proven.

5.2 Comparison with the parameter space from Chapter 4

Note that the parameter space where A is strictly copositive is not the same space we have been discussing previously in Chapter 4,

$$\mathcal{A} = \{A \in \mathbb{R}^{3\times 3} \,|\, \alpha_{ii} = 1, \alpha_{ij} < 1, \alpha_{ij}\alpha_{ji} < 1, i \neq j, i, j \in \{1, 2, 3\}$$

and the dynamics of (5.1) are bounded}. (5.21)

An example is

$$A = \begin{pmatrix} 1 & 2 & -\frac{1}{2} \\ \frac{1}{2} & 1 & -\frac{1}{2} \\ \frac{1}{2} & \frac{1}{2} & 1 \end{pmatrix}, \tag{5.22}$$

$$\frac{A + A^T}{2} = \begin{pmatrix} 1 & \frac{3}{2} & 0 \\ \frac{3}{2} & 1 & 0 \\ 0 & 0 & 1 \end{pmatrix}, \tag{5.23}$$

which is strictly copositive as it satisfies the first condition in Lemma 5.1.1, however $A \notin \mathcal{A}$ since $a_{12} > 1$. In this case the 2-species subsystem with species 1 and 2 does not have an interior steady state, indeed $\left(\frac{\alpha_{12}-1}{\alpha_{12}\alpha_{21}-1}, \frac{\alpha_{21}-1}{\alpha_{12}\alpha_{21}-1}\right) \notin \mathbb{R}^2_{\geq 0}$. The other interior steady states of the 2-species subsystems are saddle points.

It is also clear $\mathcal{A}$ not contained in the space where A is strictly copositive, consider

$$A = \begin{pmatrix} 1 & 0.5 & 0.5 \\ 0.6 & 1 & -2.6 \\ 0.3 & 0.5 & 1 \end{pmatrix}, \tag{5.24}$$

$$\frac{A + A^T}{2} = \begin{pmatrix} 1 & 0.55 & 0.4 \\ 0.55 & 1 & -1.05 \\ 0.4 & -1.05 & 1 \end{pmatrix}, \tag{5.25}$$

which is not strictly copositive it does not satisfy Lemma 5.1.1. Indeed $(0,1,1)^T.A.(0,1,1) = -0.1 < 0$. However $A \in \mathcal{A}$; the dynamics of (5.1) with A are bounded since the interior steady state x^* is globally attracting on the interior. Indeed, the other steady states are repelling with respect to the interior and infinity

is repelling, we can also conclude this by considering the (u, N) dynamics (where the corresponding proportion vector steady state u^* is globally attracting on the interior of the u-simplex) and recalling Corollary 4.5.3 from Chapter 4 (regarding the attraction of all non-zero solutions on the ray from the origin through any non-zero steady state).

The intersection of these two parameter spaces is not empty, consider the co-operative system from Figure 4.2 in Chapter 4. The interaction matrix from this system is also strictly copositive:

$$A = \begin{pmatrix} 1 & -0.25 & -0.18 \\ -0.22 & 1 & -0.14 \\ -0.32 & -0.57 & 1 \end{pmatrix}, \tag{5.26}$$

$$\frac{A + A^T}{2} = \begin{pmatrix} 1 & -0.235 & -0.25 \\ -0.235 & 1 & -0.355 \\ -0.25 & -0.355 & 1 \end{pmatrix}, \tag{5.27}$$

satisfying the first condition in Lemma 5.1.1. From Figure 4.2 it is clear that Σ is not completely analytic, but is piecewise analytic when considering the fact that it is composed of the basins of repulsion of the non-zero steady states of a system which has an analytic vector field.

Note that there are interaction matrices A which are not strictly copositive and $A \notin \mathcal{A}$, consider:

$$A = \begin{pmatrix} 1 & -2.5 & 0.2 \\ 0.45 & 1 & 1.1 \\ 0.2 & 0.4 & 1 \end{pmatrix}. \tag{5.28}$$

A is not strictly copositive since $\{1, 1, 0\}^T.A.\{1, 1, 0\} = -0.05$, and $\alpha_{23} > 1$ meaning $A \notin \mathcal{A}$. Note that the dynamics of the system (5.1) (with this interaction matrix)

are still bounded. The non-zero steady states are the three axial steady states, $s_1 = (0.83, 0, 0.83)$ and $s_2 = (1.65, 0.26, 0)$ (to two decimal places). The steady state s_1 is a stable node, whilst the other steady states are all repelling with respect to the interior $\mathbb{R}^3_{\geq 0}$. By considering the (u, N) dynamics, the corresponding species proportion steady state of s_1 is given by $u_s = (0.5, 0, 0.5)$ which is globally attracting on the interior of the u-simplex. Again, recalling Corollary 4.5.3 from Chapter 4 and the fact that the boundary dynamics are bounded, we can conclude s_1 is globally attracting on the interior $\mathbb{R}^3_{>0}$ and the dynamics of the system are bounded.

5.3 Conclusions

In this chapter, we have proved that the balance simplex exists for the 3-species scaled Lotka–Volterra system (5.1) when the interaction matrix A is strictly copositive (Theorem 5.1.2), meaning the average fitness in the system is always positive. In this case, $\Sigma = \{\Psi(u)u \,|\, u \in \Delta\}$ for a continuous scalar function Ψ, defined by (5.17). Thus Σ can be radially projected 1-to-1 and onto the unit simplex Δ. Σ is also the union of piecewise analytic manifolds which are the unstable manifolds of all non-zero steady states. Note that Theorem 5.1.2 covers the carrying simplex for competitive scaled Lotka–Volterra systems (5.1); all the elements A are positive thus A is strictly copositive.

In the proof of Theorem 5.1.2, we considered the dynamics of the total population density and the species proportions, however we scaled and reversed time to get the system (5.10)-(5.12). The reason for reversing time was convenience. When time is reversed, we know that for any point not on Σ, its forward orbit will tend to the origin or infinity, regardless of what steady state its backwards orbit was from. So for this system we were able to discuss the integrals along forward orbits.

In Section 5.2, we compared the parameter space where A is strictly copositive,

to the space discussed in the previous chapter $\mathcal{A}$ (see 5.21). We found that the intersection of these spaces is not empty, and neither is completely contained in the other.

In the next chapter, we focus on finding a reliable method for plotting an approximation of the balance simplex in a range of parameter cases.

Chapter 6

Plotting the Balance Simplex of a 3-Species Scaled Lotka–Volterra System as a Zero Set

In this chapter, we again consider the 3-species scaled Lotka–Volterra system, namely:

$$\begin{aligned}\frac{dx_1}{dt} &= x_1(1 - x_1 - \alpha_{12}x_2 - \alpha_{13}x_3) =: F_1,\\ \frac{dx_2}{dt} &= x_2(1 - \alpha_{21}x_1 - x_2 - \alpha_{23}x_3) =: F_2,\\ \frac{dx_3}{dt} &= x_3(1 - \alpha_{31}x_1 - \alpha_{32}x_2 - x_3) =: F_3.\end{aligned} \tag{6.1}$$

We suspect the balance simplex exists in this 3-dimensional system when the dynamics are bounded and steady states are hyperbolic, as we have seen in the 2-species case. We want to explore how we can visualise the balance simplex in a wide range of parameter cases. Recall that the balance simplex Σ is a unique, simply connected surface which divides $\mathbb{R}^3_{\geq 0}$ into two distinct regions: one containing points with the α-limit of the origin, and the other containing points with the α-limit of infinity. Σ is invariant to the flow of (6.1), thus it contains all non-zero steady states.

Whilst one should be able to plot an approximation of Σ using numerical methods and discretisation [27, 93], we focus on a more theoretical approach. In this chapter, we plot the balance simplex as the zero set of a function $\phi(x_1, x_2, x_3)$. The equation it satisfies will resemble that which is satisfied by a Darboux polynomial [22], however ϕ will be a power series.

6.1 Background

Cairó and Llibre [14] have studied the Darboux integrability [22] for the 3-species Lotka–Volterra equations. By determining whether a system is integrable or not, one can determine if the system will exhibit chaotic behaviour or if it is possible to characterise the long-term behaviour of the model. The study of Darboux integrability can help determine the number of invariant algebraic surfaces a system has.

The following definitions can be found in [14]

Definition 6.1.1 A Darboux polynomial for the 3-species neutral Lotka–Volterra system is $\phi(x_1, x_2, x_3)$, which is not identically zero and satisfies

$$\frac{\partial \phi}{\partial x_1} F_1 + \frac{\partial \phi}{\partial x_2} F_2 + \frac{\partial \phi}{\partial x_3} F_3 = m\phi \tag{6.2}$$

for some polynomial m, called the cofactor of ϕ.

Since the vector field of (6.1) is quadratic, the cofactor m must be at most of degree 1 in $x = (x_1, x_2, x_3)$.

Definition 6.1.2 For a Darboux polynomial $\phi(x)$, its zero set $\{x \in \mathbb{R}^3_{\geq 0} \,|\, \phi(x) = 0\}$ is called an invariant algebraic surface. We refer to this zero set as $\phi^{-1}(0)$.

The invariance of $\phi^{-1}(0)$ to the flow of the system follows from (6.2); the normal of $\phi^{-1}(0)$ is orthogonal to the vector field, thus the surface $\phi^{-1}(0)$ is formed of orbits of the system. Basic examples of invariant algebraic surfaces for (6.1) would be the planes $x_1 = 0$, $x_2 = 0$ and $x_3 = 0$. Another reason why Darboux polynomials are studied is due to being related to the integrability of a system.

Definition 6.1.3 The function $H(x_1, x_2, x_3, t) : \mathbb{R}^3_{\geq 0} \times \mathbb{R} \to \mathbb{R}$ is called an invariant of the system (6.1) if H is constant on all orbits of the system. If additionally H is independent of time, it is called a first integral of the system, in this case it is also a Darboux polynomial for the system with the cofactor 0.

Definition 6.1.4 A 3-dimensional vector field F is called integrable if it has two independent first integrals, H_1 and H_2, i.e. the vectors ∇H_1 and ∇H_2 are linearly independent in the space where the two first integrals are defined.

If F is integrable with two independent first integrals H_1 and H_2, then its orbits are determined by intersecting the invariant sets $H_1 = h_1$ and $H_2 = h_2$ where h_1

and h_2 vary in $\mathbb{R}$ [3, 14]. This means the dynamics of an integrable system are well understood and not chaotic.

There are several papers giving different examples of first integrals for the 3-species Lotka–Volterra system in specific parameter cases, e.g. [1, 13, 28]. In this next section we focus on a method for plotting the balance simplex for the 3-species scaled Lotka–Volterra system which we intend to work in most cases.

6.2 The balance simplex as a zero set

For the 3-species competitive Lotka–Volterra system, Zeeman and LaMar developed `CSimplex` [51], a module for the program `Geomview`, which allowed the carrying simplex to be plotted. The carrying simplex was computed as the steady solution $u(x_1, x_2, t)$ (when it exists) of the quasilinear partial differential equation

$$\frac{\partial u}{\partial t} = F_3 - F_1\frac{\partial u}{\partial x_1} - F_2\frac{\partial u}{\partial x_2} \tag{6.3}$$

for $(x_1, x_2, t) \in (0, 1)^2 \times (0, \infty)$, with initial conditions $u(x_1, x_2, 0) = 1 - x_1 - x_2$.

For non-competitive systems, we do not expect the balance manifold to always be a graph of a function; we have seen in the 2-species case where a cusp forms for co-operating species. We instead consider a function $\phi(x_1, x_2, x_3, t) : \mathbb{R}^4_{\geq 0} \to \mathbb{R}$, of which we examine the zero set, $\phi^{-1}(0)$, in the steady case. We consider

$$\frac{d\phi}{dt} = \frac{\partial \phi}{\partial t} + \nabla\phi \cdot F = m\phi \tag{6.4}$$

where $F = (F_1, F_2, F_3)^T$ and m is a scalar function, both dependent on $x = (x_1, x_2, x_3)^T$. For now, we assume m is of degree 1. The initial condition is $\phi(x_1, x_2, x_3, 0) = 1 - x_1 - x_2 - x_3$. Since Σ is invariant to the flow, we want to find

a steady solution, thus we are left with:

$$\nabla\phi \cdot F = m\phi. \tag{6.5}$$

The level surface $\phi^{-1}(0)$ is a solution to the dynamics $\nabla\phi \cdot F = 0$ which means it is tangent to the vector field F at every point. By choosing a suitable m, we can identify the balance manifold, formed of heteroclinic orbits connecting the non-zero steady states.

6.3 The cofactor m

In this subsection we briefly discuss the effect of m has in equation (6.5). If $m = 0$ then the equation is simply $\nabla\phi \cdot F = 0$, the solution of which would be tangent to the vector field everywhere. However, this does not exclude the trivial solution $\phi \equiv 0$ which will appear if we try to solve this as a series solution.

We consider a basic 1-dimensional PDE where the solution ϕ is an exact solution, rather than a polynomial or power series. In this case, m does not need to be of degree 0 (i.e. a constant). The 1-species scaled Lotka–Volterra system is a logistic equation (and competitive):

$$\frac{dx}{dt} = x(1-x), \tag{6.6}$$

where $x \in \mathbb{R}_{\geq 0}$. For given m the solution $\phi_m(x,t)$ this gives the PDE:

$$\frac{d\phi_m}{dt} = \frac{\partial\phi_m}{\partial t} + x(1-x)\frac{\partial\phi_m}{\partial x} = m\phi_m \tag{6.7}$$

with the initial condition $\phi_m(x,0) = 1 - x$. If $m = 0$, the explicit solution is

$$\phi_0(x,t) = \frac{e^t(x-1)}{e^t(x-1) - x}. \tag{6.8}$$

We want to examine the steady solution. As $t \to \infty$, $\phi_0(x,t)$ converges to the horizontal line $\phi_0(x) = 1$ with a discontinuity at $x = 1$, where $\phi_0(1) = 0$. For finite t, $\phi_0(x,t)$ has an asymptote at $x = (1 - e^{-t})^{-1}$. The zero set of $\phi_0(x,t)$ for any t is $x = 1$, which is precisely the carrying simplex in this 1-dimensional case. In this sense, ϕ_0 is fine as the zero set identifies correctly the carrying simplex, however as a function itself, ϕ_0 has a singularity and the limit function is discontinuous.

We consider different functions for m and write $\exp := e$ for readability:

$$\phi_{-x}(x,t) = 1 - x, \tag{6.9}$$

$$\phi_{-x^2}(x,t) = (1-x)\exp\left[\left(1 + ((x-1)\exp[t] - x)^{-1}\right)x\right]. \tag{6.10}$$

The function $\phi_{-x}(x,t)$ is steady, analytic and has $x = 1$ as its zero set. The function $\phi_{-x^2}(x,t)$ also identifies $x = 1$ as the carrying simplex. The limit function as $t \to \infty$ is $\phi_{-x^2}(x) = (1-x)\exp[x]$ which is analytic.

In Figure 6.1, we can see a plot of ϕ_m for various cofactors m. In all the examples we have tested, if $m = -x^n$; $n > 1$, then the limit function is $\phi_{-x^n}(x) = (1 - x)\exp[x + \frac{x^2}{2} + \ldots + \frac{x^{n-1}}{n-1}]$. In this sense, we can think of m in this form having the effect of smoothing out the previous discontinuous limit function into a limit function which is analytic and has a zero at the same position ($x = 1$).

6.4 The series solution ϕ

We now return to discussing the equation $\nabla\phi \cdot F = m\phi$ (6.5) where F is the vector field of the 3-species scaled Lotka–Volterra system (6.1). This equation is the same

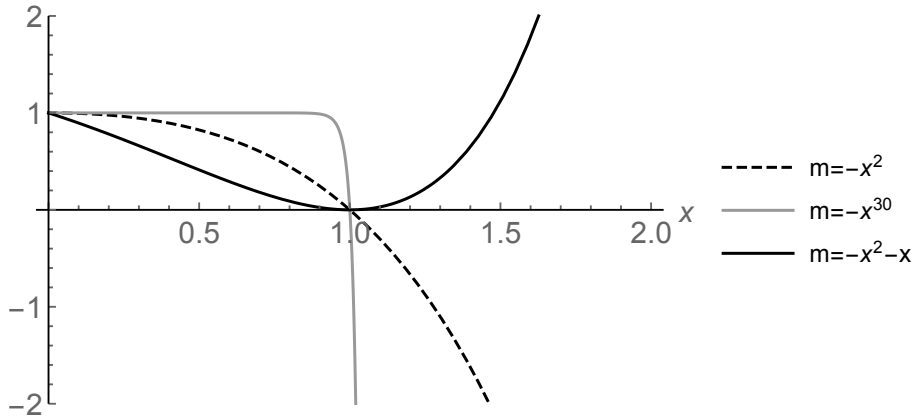

Figure 6.1: Plots of the limit set $\phi_m(x)$ with $m = -x^2, -x^{30}, -x^2 - x$. Recall that $\phi_0(x) = 1$ (with a discontinuity $\phi_0(1) = 0$), and $\phi_{-x}(x) = 1 - x$ (both not included in this plot).

as (6.2) which is satisfied by a Darboux polynomial, however, we do not consider ϕ to be a polynomial but instead a power series of the form:

$$\phi(x_1, x_2, x_3) = \sum_{n=0}^{\infty} \phi_n(x_1, x_2, x_3) \tag{6.11}$$

where ϕ_0 is a constant, and ϕ_n $(n \geq 1)$ is homogeneous and of degree n.

Lemma 6.4.1 *For a homogeneous function ϕ_n of degree n, the following holds: $\nabla\phi_n \cdot x = n\phi_n$.*

Proof: By definition, $\phi_n(\lambda x) = \lambda^n \phi_n(x)$ for all $\lambda \in \mathbb{R}$ and $x \in \mathbb{R}^3_{\geq 0}$. Differentiating with respect to λ using the chain rule gives:

$$x_1 \frac{\partial \phi_n}{\partial x_1} + x_2 \frac{\partial \phi_n}{\partial x_2} + x_3 \frac{\partial \phi_n}{\partial x_3} = n\lambda^{n-1}\phi_n(x). \tag{6.12}$$

Setting $\lambda = 1$ proves the statement. □

For now, we will assume ϕ converges so that we can take the gradient operator inside the sum. Equation (6.5) then becomes:

$$\sum_{n=0}^{\infty} \nabla\phi_n \cdot (x - \mathrm{diag}[x]Ax) = m \sum_{n=0}^{\infty} \phi_n, \tag{6.13}$$

where A is the 3×3 matrix with the interaction coefficients α_{ij}, and diag$[x]$ is a diagonal matrix with entries x (with all other entries 0). Taking m to be degree 1 in x, there are no terms of degree zero on either side of (6.13), so comparing terms of degree 1:

$$\nabla\phi_1 \cdot x = m\phi_0 = \phi_1, \tag{6.14}$$

and of degree 2:

$$\begin{aligned} & \nabla\phi_2 \cdot x - \nabla\phi_1 \cdot \text{diag}[x]Ax = m\phi_1 \\ \Rightarrow \quad & 2\phi_2 = \phi_0\nabla m \cdot \text{diag}[x]Ax + \phi_0 m^2. \end{aligned} \tag{6.15}$$

This pattern continues and we find that (formally):

$$\phi = \phi_0 \left(1 + \sum_{k=1}^{\infty} \frac{1}{k!}(m + \text{diag}[x]Ax \cdot \nabla)^{k-1}\, m\right) \tag{6.16}$$

where the exponent $(k-1)$ means the operator is applied $k-1$ times. We are looking for the set $\phi^{-1}(0)$ so we can set $\phi_0 = 1$. Consider $m = -(x_1 + x_2 + x_3)$ which gives the first two terms of ϕ as $1 - x_1 - x_2 - x_3$, of which the zero level set is the unit simplex. Note that with this, we can simplify $\text{diag}[x]Ax \cdot \nabla(m^n) = -nm^{n-1}x^TAx$ but the other terms from applying the operator do not simplify as easily.

First, we examine ϕ on the x_1-axis:

$$\begin{aligned} \phi(x_1, 0, 0) &= 1 - \sum_{k=1}^{\infty} \frac{1}{k!}\left(-x_1 + x_1^2\frac{d}{dx_1}\right)^{k-1} x_1 \\ &= 1 - x_1 + x_1^2 - x_1^2 + 0 + \ldots \\ &= 1 - x_1. \end{aligned} \tag{6.17}$$

We know that the axial steady state $(1, 0, 0)$ always lies on the balance manifold of

the system (6.1) and we can see that here $\phi(1,0,0) = 0$, the same is true for the two other axial steady states $(0,1,0)$ and $(0,0,1)$.

Unfortunately, ϕ does not simplify as easily on the boundary planes $x_1 = 0$, $x_2 = 0$ or $x_3 = 0$. Indeed:

$$\begin{aligned}
&\phi(x_1, x_2, 0) \\
&= 1 - \sum_{k=1}^{\infty} \frac{1}{k!} \left(-x_1 - x_2 + x_1(x_1 + \alpha_{12}x_2)\frac{\partial}{\partial x_1} + x_2(\alpha_{21}x_1 + x_2)\frac{\partial}{\partial x_2} \right)^{k-1} (x_1 + x_2) \\
&=: 1 - \sum_{k=1}^{\infty} \phi_k. \qquad (6.18)
\end{aligned}$$

We have that:

$$\begin{aligned}
\phi_1 &= x_1 + x_2, \\
\phi_2 &= \frac{1}{2!} x_1 x_2 (\alpha_{12} + \alpha_{21} - 2), \\
\phi_3 &= \frac{1}{3!} x_1 x_2 (\alpha_{12} + \alpha_{21} - 2)(\alpha_{21}x_1 + \alpha_{12}x_2), \\
\phi_4 &= \frac{1}{4!} x_1 x_2 (\alpha_{12} + \alpha_{21} - 2)[(\alpha_{21}x_1 + \alpha_{12}x_2)^2 + \alpha_{21}x_1^2 + 2\alpha_{12}\alpha_{21}x_1x_2 + \alpha_{12}x_2^2].
\end{aligned}$$

After this, the terms become more complex and do not seem to follow a pattern, however we have the factor of $(\alpha_{12} + \alpha_{21} - 2)$ in each ϕ_i, $i > 1$. We know that this factor can change the convexity of the carrying simplex in 2-species competitive systems [4], and here it can change the sign of ϕ_i. In the case where $\alpha_{12} + \alpha_{21} = 2$, the set $\phi^{-1}(0)$ is $1 - x_1 - x_2 = 0$. This matches the 2-species balance simplex in this case, which we have discussed in Chapter 3, Section 3.9.4.

Since we can only plot this surface for finite sums, we set:

$$\phi = 1 - \sum_{k=1}^{K} \frac{1}{k!} (-x_1 - x_2 - x_3 + \mathrm{diag}[x]Ax \cdot \nabla)^{k-1} (x_1 + x_2 + x_3). \qquad (6.19)$$

6.5 Plotting the zero set with finite K

At first (for $K = 1$), we have the unit simplex. This starts to deform as we increase K to resemble what we expect the balance simplex to be, in the sense that on the boundary planes it matches very closely to the plot of our known solution for the 2-species balance simplex. This close resemblance occurs in most cases when $K > 25$. However, in some cases the part of the surface outside of $\mathbb{R}^3_{\geq 0}$ folds in on itself, giving the appearance of two surfaces in the first orthant, see Figure 6.2.

In the examples we have seen of this case with two surfaces, the lower surface resembles what we would expect from the balance simplex. The upper 'folded' part does not follow the solution trajectories, meaning it is not invariant under the flow. Increasing the value of K after 25 does not change the surfaces significantly but does affect the computation time for the plot greatly. Whilst it seems the upper surface does move towards the lower surface with larger K, we have not managed to prove they converge in the limit. This issue can also happen in the 2-species case with this method.

In Figure 6.3, we examine two competitive systems, in which we know the carrying simplex exists. Figure 6.3a has two distinct surfaces (with respect to the first orthant) and took 16 hours to run. Figure 6.3b has only one surface. This example took 4 hours to run with the same value of K, we assume this difference is due to having only one surface appearing. The parameters are chosen such that the carrying simplex of both of these systems have a different sign of convexity. For our plots in the convex case (where all 2-species subsystems satisfy $\alpha_{ij} + \alpha_{ji} - 2 > 0$, $i \neq j$, $i, j \in \{1, 2, 3\}$), we have always found only one surface for $\phi^{-1}(0)$, e.g. Figure 6.3b. For the concave case ($\alpha_{ij} + \alpha_{ji} - 2 < 0$), we have always found two surfaces for $\phi^{-1}(0)$, e.g. Figure 6.3a.

In Figure 6.4, we consider a non-competitive system, with the same parameters as in Figure 6.2 but with a greater value of K. We can see again there are two surfaces,

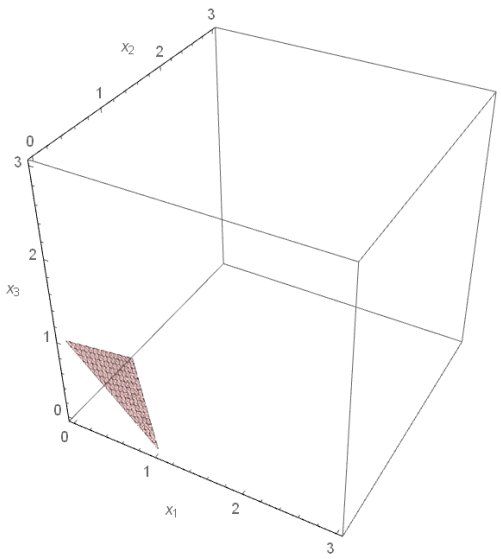

(a) $K = 1$ (unit simplex)

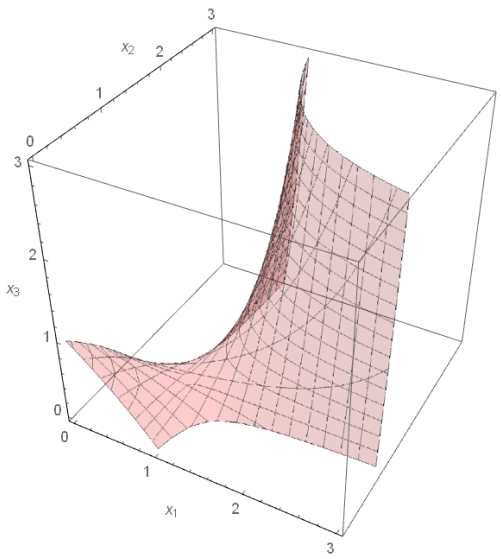

(b) $K = 2$

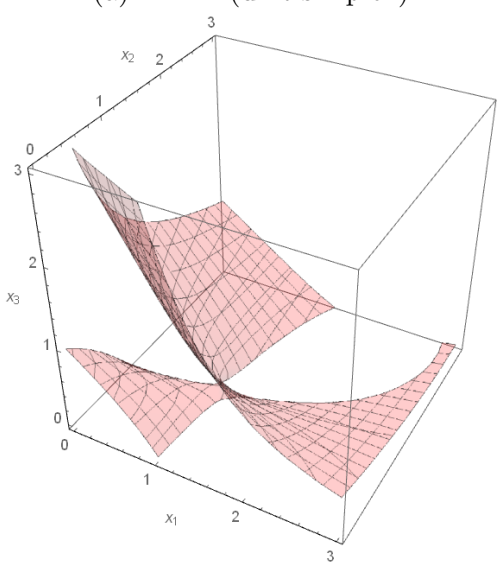

(c) $K = 6$

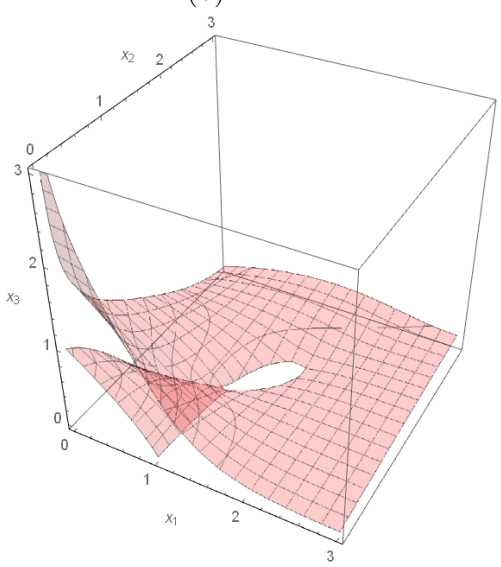

(d) $K = 11$

Figure 6.2: Plots of the surface $\phi^{-1}(0)$ with different values of K in a non-competitive system. We have the appearance of two surfaces, with the lower surface resembling what we would expect from the balance simplex, as it matches closely the dynamics on the 2-species boundaries. A cusp and loop is formed on the lower plane due to the co-operating species, we know the 2-species balance simplex is not smooth at this steady state.
Parameters: $\alpha_{12} = -0.1, \alpha_{13} = 0.41, \alpha_{21} = -0.2, \alpha_{23} = 1.21, \alpha_{31} = 1.21, \alpha_{32} = 0.41$.

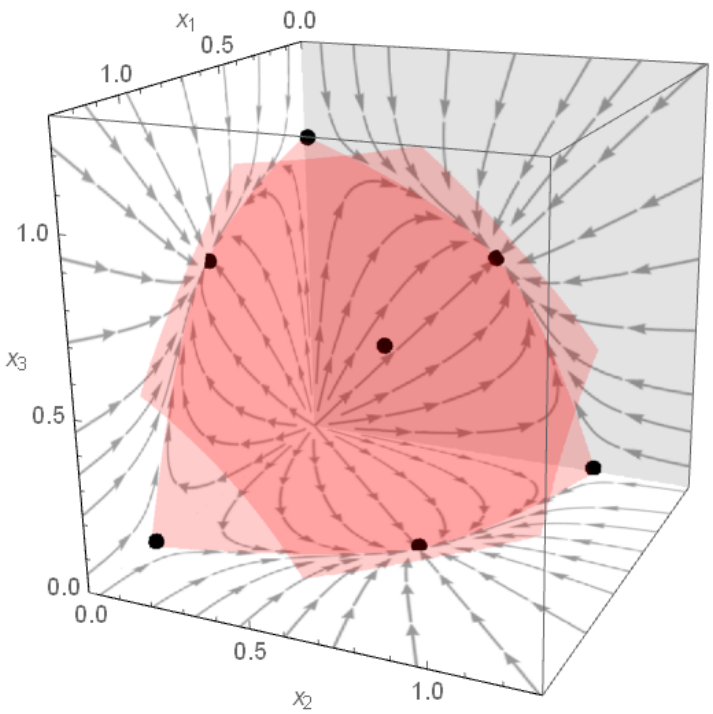

(a) Concave competitive system: $\alpha_{12} = 0.4, \alpha_{13} = 0.5, \alpha_{21} = 0.4, \alpha_{23} = 0.5, \alpha_{31} = 0.4, \alpha_{32} = 0.5$.

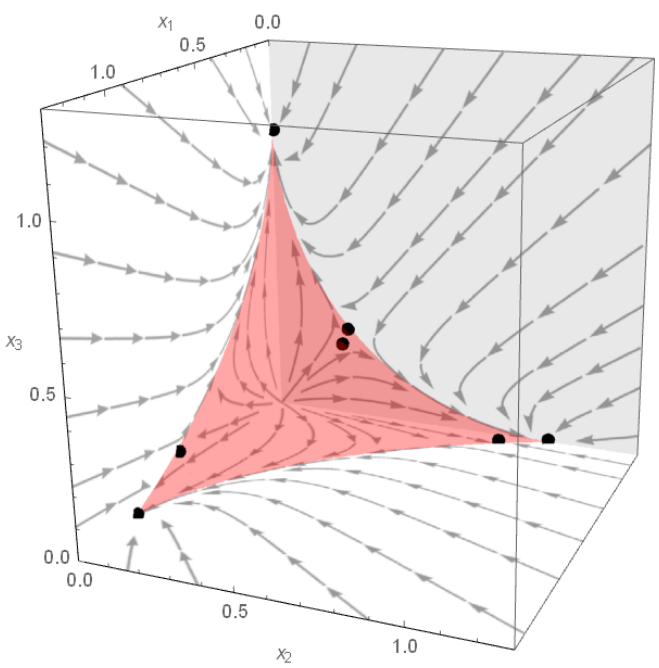

(b) Convex competitive system: $\alpha_{12} = 1.1, \alpha_{13} = 2.41, \alpha_{21} = 2.2, \alpha_{23} = 2.3, \alpha_{31} = 1.21, \alpha_{32} = 2.5$

Figure 6.3: Two competitive examples of the surface $\phi^{-1}(0)$, $K = 81$, with different convexity, the black points are the non-zero steady states.

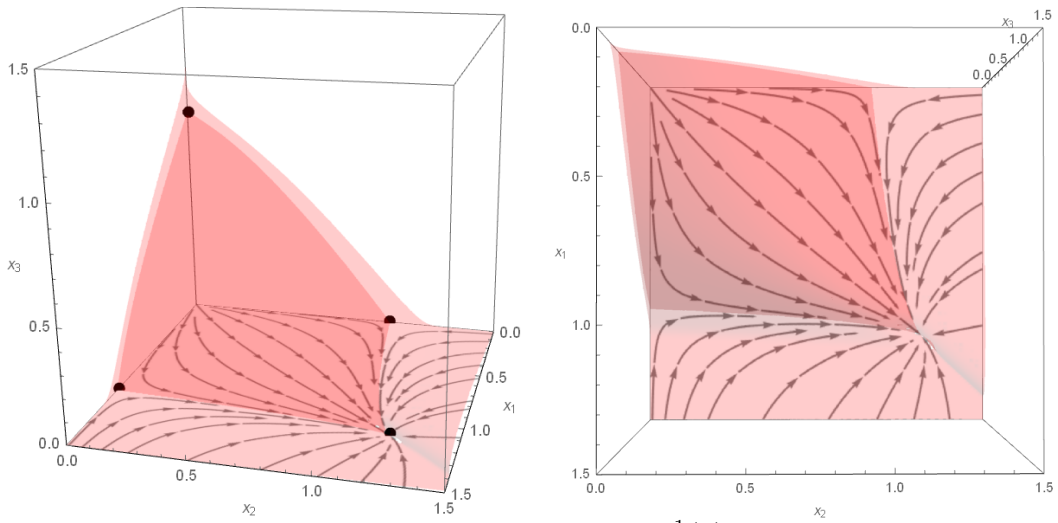

Figure 6.4: Different views of the same surface $\phi^{-1}(0)$, with $K = 81$, taking 13 hours to run.
Parameters: $\alpha_{12} = -0.1, \alpha_{13} = 0.41, \alpha_{21} = -0.2, \alpha_{23} = 1.21, \alpha_{31} = 1.21, \alpha_{32} = 0.41$.

of which the bottom resembles what we would expect of the balance simplex. Note the cusp at the interior steady state of the 2-species co-operating subsystem. Part of a loop also forms near this point (shown more clearly in Figure 6.2d) which gets smaller as K increases. From this method it is not clear whether the lack of C^1-continuity on the bottom plane continues into $\mathbb{R}^3_{>0}$ or if it is just at this 2-species (co-operative) boundary.

In Figure 6.5, we see another non-competitive system. In this case, each pair of species have a predator-prey type relationship (one of the interaction coefficients is positive whilst the other is negative). The $\phi^{-1}(0)$ set gives two surfaces but we have removed the upper surface in the plot. The lower surface sufficiently matches the balance simplex on each 2-species boundary, shown in Figure 6.5a. In Figure 6.5b, some solution trajectories are plotted and the surface $\phi^{-1}(0)$ seems to lie on the boundary (relative to $\mathbb{R}^3_{\geq 0}$) of the basin of repulsion of the origin, $\partial\mathcal{R}(0)$.

In Figure 6.6, we can see a fully co-operative 3-species system (which was also discussed in Chapter 4, Figure 4.2). The $\phi^{-1}(0)$ surface has a cusp on each 2-species plane as well as one in $\mathbb{R}^2_{>0}$ at the interior steady state. The edges of the surface in $\mathbb{R}^2_{>0}$ are the 'loops' (see Figure 6.2d) which are not part balance simplex. Increasing

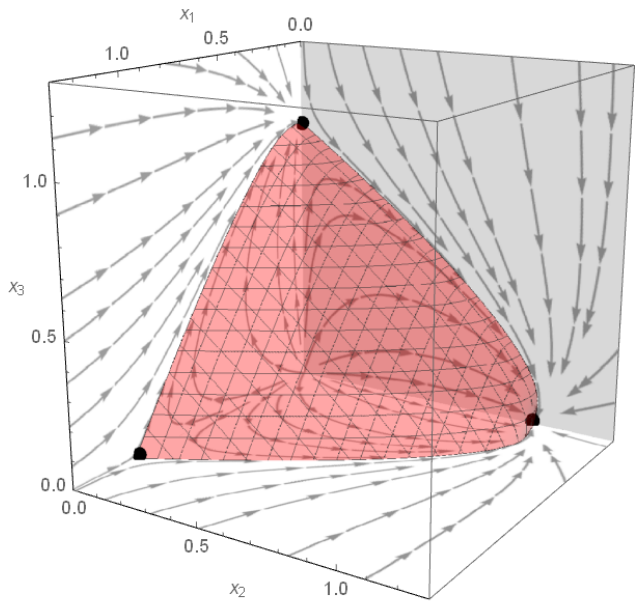

(a) The lower surface of $\phi^{-1}(0)$

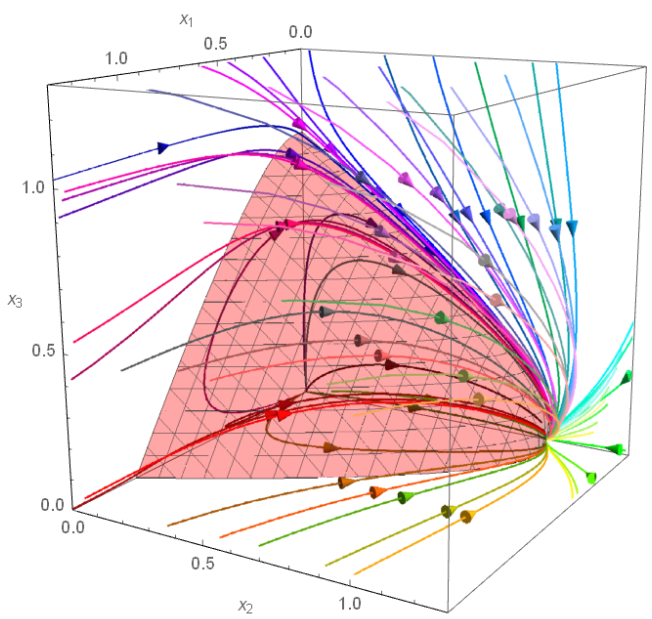

(b) Solution orbits

Figure 6.5: The surface $\phi^{-1}(0)$, $K = 26$, where we have only kept the lower surface. The only non-zero steady states are the axial steady states. The system is non-competitive: $\alpha_{12} = 1.23, \alpha_{13} = 1.56, \alpha_{21} = -0.26, \alpha_{23} = -0.23, \alpha_{31} = -0.13, \alpha_{32} = 1.46$.

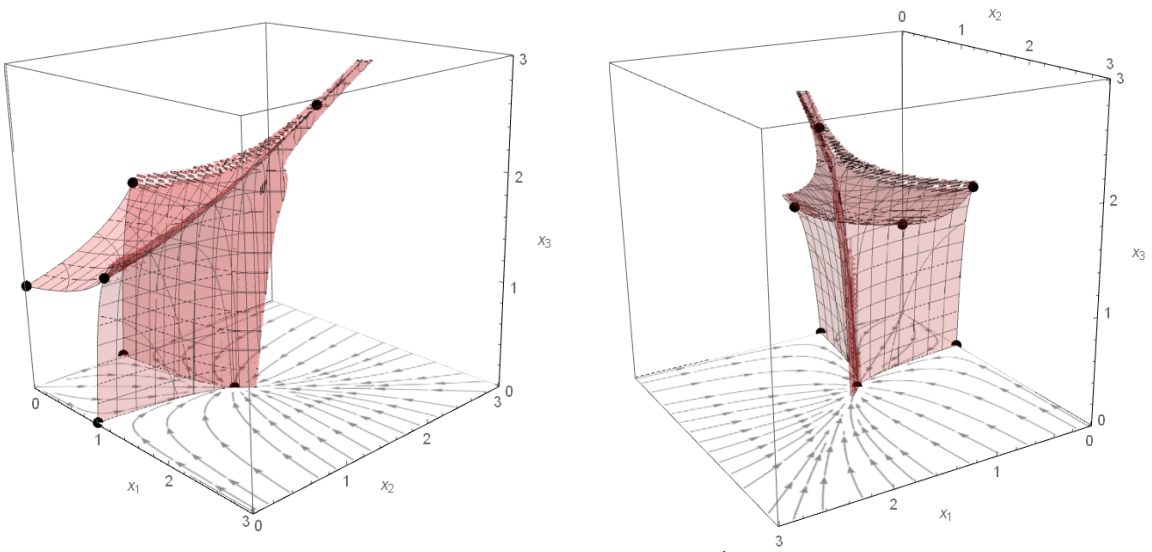

Figure 6.6: Different views of the same surface $\phi^{-1}(0)$, with $K = 22$, for a fully co-operative (and bounded) system. Once again, $\phi^{-1}(0)$ matches closely with the balance simplex in the 2-species subsystems.

K or the `PlotPoints` in `Mathematica` can cause the edges and loops of the plot to become unclear so we have shown this system with a lower K. By following the analogous 2-species case (and our plot for this system in Chapter 4, Figure 4.2, using the series solution G), we expect the 3-species balance simplex to be composed of three smooth slightly curved kite-shaped surfaces, with each edge being a heteroclinic orbit between two non-zero steady states.

Figure 6.7a shows a competitive case where the carrying simplex has regions with a relatively strong curvature. Specifically, in the species 1 and 2 subsystem (the bottom plane) $\alpha_{12} = 3$ and $\alpha_{21} = 5$, which are much larger than the parameters we have typically used in our plots. On this plane, the carrying simplex is very curved, particularly near the axial steady states. Typically, in the other cases, if $K = 25$ then the lower surface will sufficiently match the boundary dynamics in that none of the plotted boundary orbits will cross this surface (of course, in theory some orbits will still cross the surface as it is only an approximation, these just may not be shown in the `Mathematica` plot). In this case however, we had to use a higher value of K ($K = 45$) before the lower surface was sufficiently accurate. We believe this is due to the strong curvature in some regions of the carrying simplex.

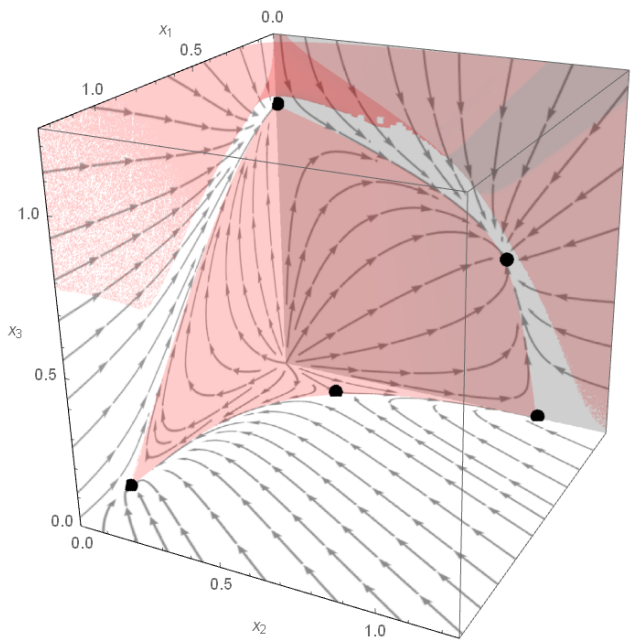

(a) $K = 51$

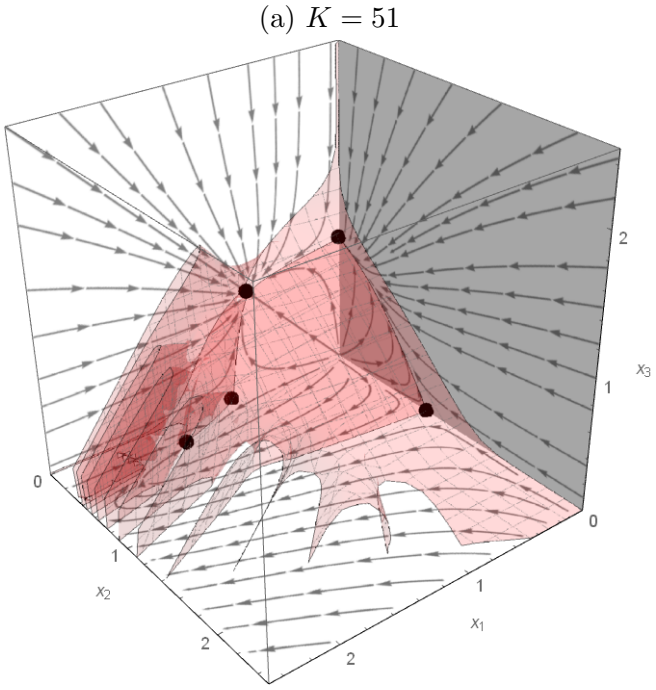

(b) $K = 25$

Figure 6.7: Plots of the surface $\phi^{-1}(0)$. In subfigure (a), the parameters are $\alpha_{12} = 3, \alpha_{13} = 1.3, \alpha_{21} = 5, \alpha_{23} = 0.23, \alpha_{31} = 0.2, \alpha_{32} = 0.5$. In subfigure (b), the parameters are from matrix A (6.21)

In Figure 6.7b, we recall a case (the matrix 5.23 from Chapter 5) where A is not strictly copositive and $A \notin \mathcal{A}$, the parameter space from Chapter 4:

$$\begin{aligned}\mathcal{A} =&\{A \in \mathbb{R}^{3\times 3} \,|\, \alpha_{ii} = 1, \alpha_{ij} < 1, \alpha_{ij}\alpha_{ji} < 1, i \neq j, i, j \in \{1, 2, 3\} \\ &\text{and the dynamics of (6.1) are bounded}\}. \end{aligned} \tag{6.20}$$

The interaction matrix A is

$$A = \begin{pmatrix} 1 & -2.5 & 0.2 \\ 0.45 & 1 & 1.1 \\ 0.2 & 0.4 & 1 \end{pmatrix}. \tag{6.21}$$

This system (6.1) with this matrix A is part of a case where we have not yet proven the balance simplex exists. From the boundary dynamics and boundedness of the system (discussed in Chapter 5), we expect the balance simplex to still exist in this case. The zero set $\phi^{-1}(0)$ is shown in Figure 6.7b, there are two surfaces and some numerical issues appearing. On the boundaries, species 1 and 3 are competing, species 2 and 3 are also competing, and species 1 and 2 are in a predator-prey type relationship. This last subsystem represents the bottom plane where the 2-species balance simplex has a region of strong curvature and an interior steady state which is globally attracting on the interior of that plane. Near this region, we see folds starting to form where the surface $\phi^{-1}(0)$ is not accurate. This does not improve with increasing K.

For the plots in Figure 6.8, we consider another case where $A \notin \mathcal{A}$ and A is not strictly copositive. The interaction matrix A is

$$A = \begin{pmatrix} 1 & 1.05 & -0.9 \\ -0.7 & 1 & -0.8 \\ -0.8 & -0.9 & 1 \end{pmatrix}. \tag{6.22}$$

Note that $\alpha_{12} > 1$ and A is not co-positive since $\{1,1,1\}^T.A.\{1,1,1\} = -0.05$. On the boundaries, species 1 and 3 are co-operating, species 2 and 3 are also co-operating, and species 1 and 2 are in a predator-prey type relationship. There are 5 non-zero steady states on the boundaries, and 1 interior steady state. Some orbits starting from the basin of repulsion of the origin $\mathcal{R}(0)$ are shown in Figure 6.8b.

The interior steady state $x^* = (0.25, 7.625, 8.0625)$ is hyperbolic and attracting, all other steady states are unstable with respect to the interior $\mathbb{R}^3_{>0}$. We can conclude that x^* is globally attracting on the interior by considering the (u, N) dynamics (where the corresponding proportion vector steady state u^* is globally attracting on the interior of the u-simplex) and recalling Corollary 4.5.3 from Chapter 4. From the boundary dynamics (Figure 6.8a) and the boundedness of orbits, we would expect the balance simplex to exist.

In Figure 6.8c we can see the surface $\phi^{-1}(0)$ with $K = 26$. The plot of this surface does not work very well on the interior $\mathbb{R}^3_{>0}$ and does not produce a clearer image with large K or with more `PlotPoints` in `Mathematica`. To improve the clarity of this plot, we have removed some regions of the surface which has numerical instabilities. These regions are near where x_3 is small, and x_1 and x_2 are large (thus not close to $\mathcal{R}(0)$). The issue with this case may be how the 2-species co-operative carrying simplices resembles a line near their interior steady state, causing the balance simplex of the full system to be sharp near those regions. Additionally, with how far from the origin these steady states are (relative to our previous examples), this may cause problems with the convergence of ϕ. Figure 6.8d shows the orbits along with $\phi^{-1}(0)$. The orbits intersect the cone-like shapes from $\phi^{-1}(0)$.

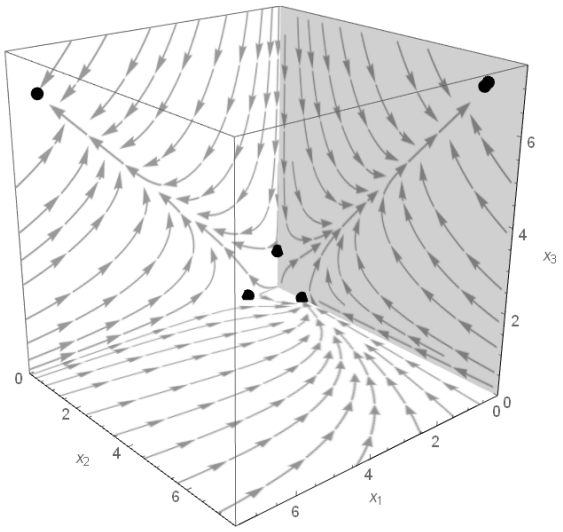

(a) Boundary dynamics (zoomed in)

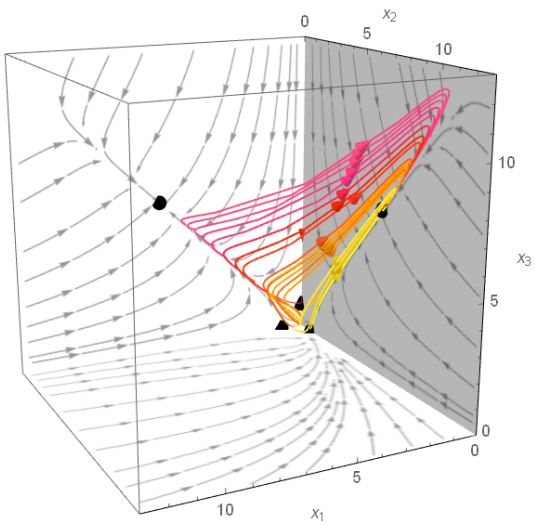

(b) Orbits starting from inside $\mathcal{R}(0)$

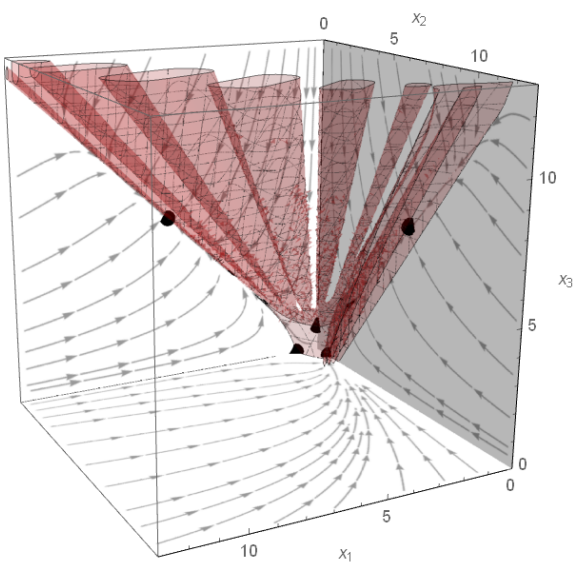

(c) $\phi^{-1}(0)$ with $K = 26$

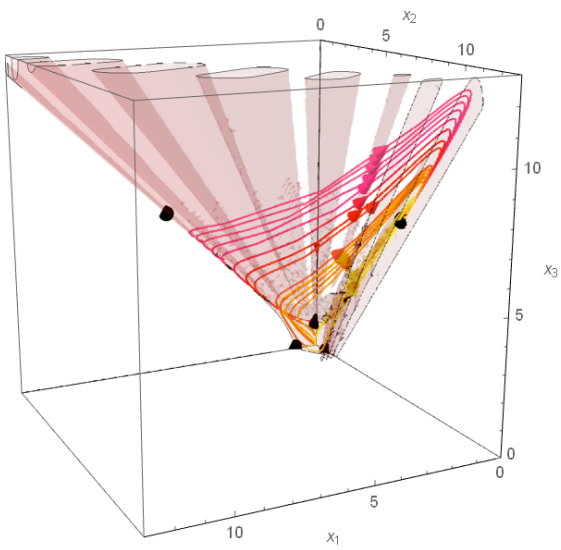

(d) $\phi^{-1}(0)$ with some orbits

Figure 6.8: The dynamics of a system with parameters given by matrix A (6.22). Figure (d) uses the same surface $\phi^{-1}(0)$ as (c) but has been made lighter for better visibility. There is an attracting interior steady state at $(0.25, 7.625, 8.0625)$ (near the top right) which is near one of the 2-species interior steady states.

6.6 Taking the cofactor m to be degree 2

For a different approach to the system (6.1) with A as in (6.22), we consider taking the cofactor m with a higher degree. If m is of degree 2 in x_1, x_2, x_3, then $\phi_1 = 0$ meaning there are no degree 1 terms in ϕ. This may be beneficial in this case as two of the 2-species carrying simplices are not close to the unit simplex on the corresponding planes. If $m = -x_1 - x_2 - x_3$, the zero set $\phi^{-1}(0)$ of the first two terms is the unit simplex ($1 - x_1 - x_2 - x_3 = 0$), whereas if $m = -x_1^2 - x_2^2 - x_3^2$, the zero set of the first two terms is $2 - x_1^2 - x_2^2 - x_3^2 = 0$ which will be part of the sphere centred at the origin with radius $\sqrt{2}$. This lies above the unit simplex. Recall equation (6.13) where we now take m to be of degree 2 and label ϕ as Φ in this case:

$$\sum_{n=0}^{\infty} \nabla\Phi_n \cdot (x - \text{diag}[x]Ax) = m \sum_{n=0}^{\infty} \Phi_n. \tag{6.23}$$

Comparing coefficients gives:

$$\begin{aligned}
\Phi_1 &= 0 \\
\Phi_2 &= \frac{1}{2} m\Phi_0 \\
\Phi_3 &= \frac{1}{3} \nabla\Phi_2 \cdot \text{diag}[x]Ax \\
\Phi_n &= \frac{1}{n} \left(m\Phi_{n-2} - \nabla\Phi_{n-1} \cdot \text{diag}[x]Ax\right); \quad n \geq 4.
\end{aligned} \tag{6.24}$$

We can set $\Phi_0 = 1$, and have chosen $m = -x_1^2 - x_2^2 - x_3^2$ for the plot in Figure 6.9a. The plot for this surface also used terms up to Φ_{26} ($K = 26$) however it took 13 times longer to produce (70 minutes) than Figure 6.8c, this may be due to numerical instabilities in the regions we have cut out of the plot, after it was computed. For this system, it is not clear whether $\phi^{-1}(0)$ or $\Phi^{-1}(0)$ is more accurate to the balance simplex (or to what we would expect it to appear like based on the orbits of $\mathcal{R}(0)$).

Figure 6.9b shows $\Phi^{-1}(0)$ for the system from Figure 6.4. There is only one

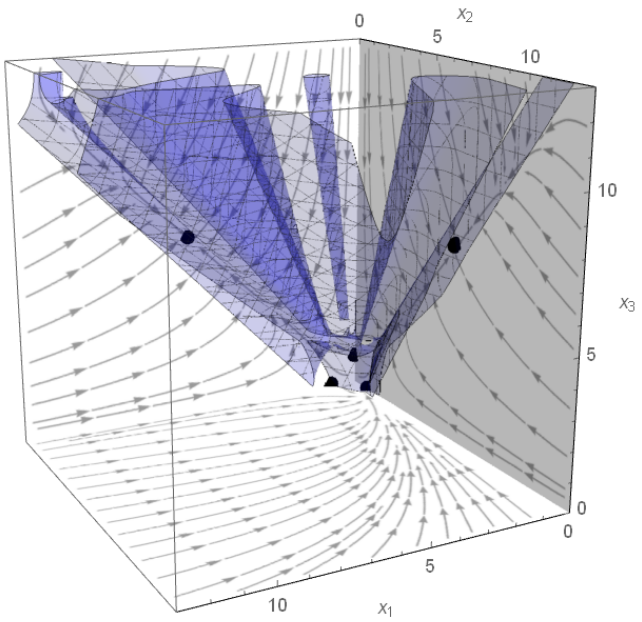

(a) $\Phi^{-1}(0)$ for the system from Figure 6.8 with $K = 26$

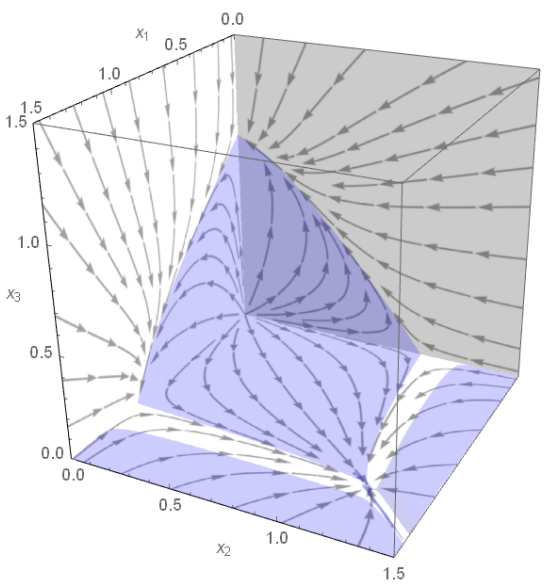

(b) $\Phi^{-1}(0)$ for the system from Figure 6.4 with $K = 81$

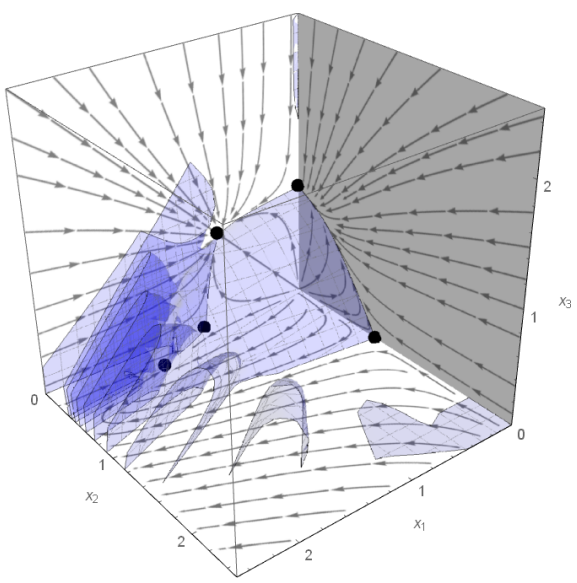

(c) $\Phi^{-1}(0)$ for the system from Figure 6.7b with $K = 25$

Figure 6.9: The surface $\Phi^{-1}(0)$ with $m = -x_1^2 - x_2^2 - x_3^3$ is shown in blue.

surface in most of $\mathbb{R}^3_{>0}$, however two still appear near the bottom co-operative plane. This surface is not as accurate on the boundaries as it intersects a few of the plotted orbits, even for $K = 81$. This plot took 11 hours to produce, compared to Figure 6.4 which took 13 hours, we suspect this is due to the latter having two surfaces.

In Figure 6.9c, we plot $\Phi^{-1}(0)$ for the system from Figure 6.7b. In this case, we only have one surface appearing but the numerical problems with the folds are still present and do not improve with larger K. The execution time for this plot is similar to that for $\phi^{-1}(0)$ (3 minutes). Typically when K is small, we do not see a significant difference in the execution times of $\phi^{-1}(0)$ and $\Phi^{-1}(0)$.

We now consider an example where we can compare these surfaces to the carrying simplex when it is explicitly defined. From Chapter 4, an example is the system with parameters $\alpha_{ij} = \frac{1}{2}$ for $i \neq j$ (Figure 4.5). We will refer to its carrying simplex as Σ, part of which is shown as the solid green surface in Figure 6.10. In this case, $\Phi^{-1}(0)$ (Figure 6.10b) only has one surface whereas $\phi^{-1}(0)$ has two (Figure 6.10a). For small K (< 20), the lower surface of $\phi^{-1}(0)$ is closer to Σ than $\Phi^{-1}(0)$ is. The lower surface of $\phi^{-1}(0)$ rises as K increases, with the upper limit appearing to be Σ. For $\Phi^{-1}(0)$ the opposite is true, it lies above Σ and converges downwards as K increases. In Figure 6.10 ($K = 30$), $\Phi^{-1}(0)$ took 40 minutes to plot whereas $\phi^{-1}(0)$ took 61 minutes, this may be due to it having two surfaces. Ignoring the upper surface herein, both $\phi^{-1}(0)$ and $\Phi^{-1}(0)$ converge quickly to Σ around the axial steady states as K increases, however the convergence near the interior steady state and 2-species interior steady states is slower. In Figure 6.10c, we see that near the region of the species 1 and 3 interior steady state, $\Phi^{-1}(0)$ is closer to Σ than $\phi^{-1}(0)$ is. Figure 6.10d shows the region near the interior steady state, this is where convergence is slowest. Both of these surfaces are within a distance of 0.02 from Σ, showing that the lower surface of $\phi^{-1}(0)$ and $\Phi^{-1}(0)$ are good approximations of the carrying simplex in this case.

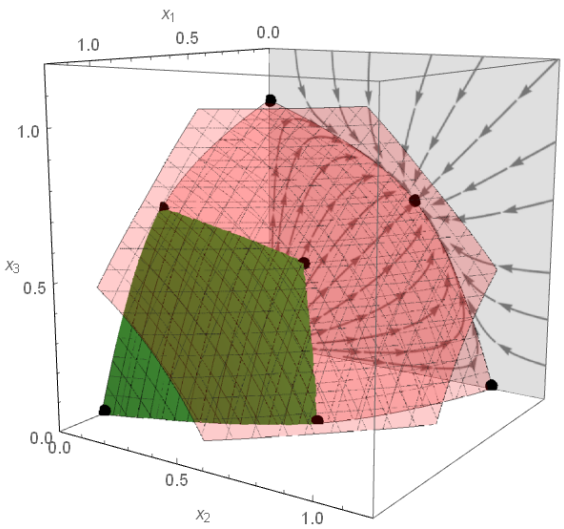

(a) $\phi^{-1}(0)$ $(K = 30)$

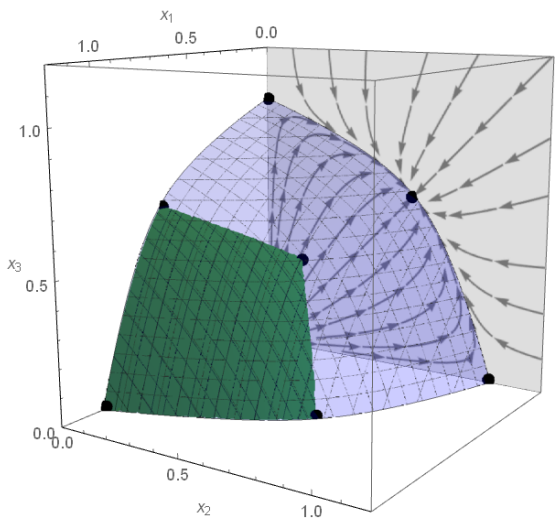

(b) $\Phi^{-1}(0)$ $(K = 30)$

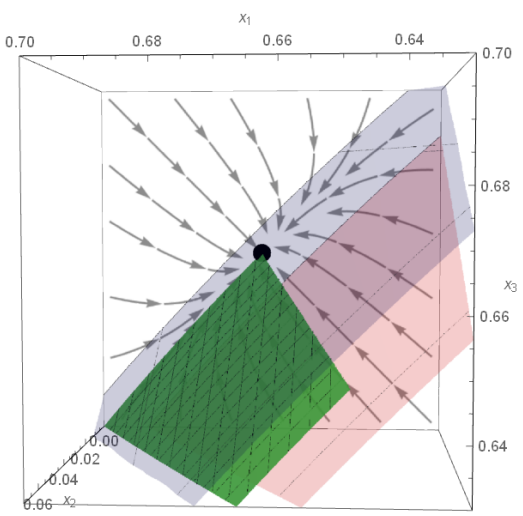

(c) Comparison near the interior boundary steady state

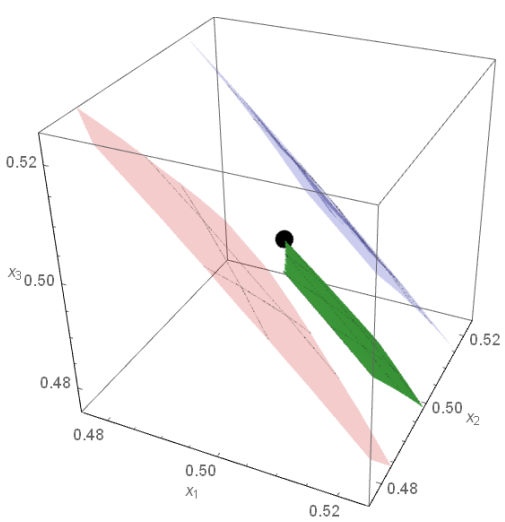

(d) Comparison near the interior steady state

Figure 6.10: A competitive system where $\alpha_{ij} = \frac{1}{2}$ for $i \neq j$. The carrying simplex is explicitly known as discussed in Chapter 4, Section 4.3 (a portion is shown as the solid green surface).

6.7 Conclusions

We have shown plots of the surface $\phi^{-1}(0)$ for finite K (i.e. the zero set of (6.19)) which generally matches well with the balance simplex in the 2-species subsystems. Since we can only plot $\phi^{-1}(0)$ with finite K, we think of the set $\phi^{-1}(0)$ as a good approximation for the balance simplex, rather than the balance simplex itself. They give us an idea of the shape of the balance simplex, but perhaps not its smoothness in the interior $\mathbb{R}^3_{>0}$, particularly near any cusps from co-operating species (e.g. Figure 6.4). By using the function ϕ, this improves on the plots from Chapter 4 with the parametric series solution which did not always converge on the interior and was only applicable to the parameter case where $A \in \mathcal{A}$ (6.20). The methods in this chapter work outside of this parameter space, however it does not work as well if the 2-species subsystems have regions of strong curvature (e.g. 6.7b) or are co-operative with the interior steady state is relatively far from the origin (e.g. Figure 6.8).

We have not yet considered the convergence of the series for ϕ; during its derivation, we took the gradient operator inside the infinite sum to obtain equation (6.13). The potential lack of convergence may have caused issues with numerical instabilities greatly increasing the execution time and quality of plots with a large K (e.g. the system with matrix A as (6.22)). In the cases where two surfaces appear, the upper surface moves closer to the lower surface as K increases, however, it is not obvious what happens in the limit as $K \to \infty$. In some cases, using the cofactor $m = -x_1^2 - x_2^2 - x_3^2$ instead of $-x_1 - x_2 - x_3$ removes this upper surface (Figures 6.9b and 6.10b), however this is not true for all cases, we have tested it with the system from Figure 6.7a and the upper surface on the boundaries still appear. This choice of m also makes the zero set less accurate on the boundaries (in general) for small values of K (< 20). For plots to give a quick and decent approximation for the balance simplex, we would recommend using $m = -x_1 - x_2 - x_3$ and trying $m = -x_1^2 - x_2^2 - x_3^2$ if two surfaces appear.

Chapter 7

The Balance Manifold of Planar Kolmogorov Systems

In this chapter, we discuss the results from our most recent paper [19] where we focus on general 2-dimensional Kolmogorov systems rather than scaled Lotka–Volterra systems. Many biological systems have opposing processes that lead eventually to a state where the processes are in a state of balance [86] (e.g. the concept of homeostasis). In physical systems, a classic example is a balance of forces which may result in an equilibrium, e.g. a pendulum at rest at its lowest point.

In ecology, population density changes are due to a multitude of processes that contribute to population growth and decline [46]. These processes are in turn controlled by factors such as fecundity, competition, co-operation, predation, environmental factors and so on. As we have mentioned in Chapter 1, the scaled Lotka–Volterra systems are limited in how realistic they are to modelling animal populations. By considering general Kolmogorov models, this will include population models with different and less basic functions for per-capita growth rates. This chapter will give some sufficient conditions in these models for a balance manifold to exist, based on stability analysis and index theory [69]. The balance manifold that we introduce is similar to the balance simplex we have been discussing thus far, except it may not project radially 1-to-1 to the unit probability simplex.

7.1 Background

For deterministic continuous-time single-species population models, the conditions sufficient for the existence of a unique positive environmental carrying capacity K, at which the population eventually settles, are well-understood [37, 47]: the per-capita growth rate is a continuous function $f : \mathbb{R}_{\geq 0} \to \mathbb{R}$ with $f(0) > 0$, $f(x) < 0$ for $x > K$ and $f^{-1}(0) = \{K\}$. The key features behind a unique, attracting carrying capacity are: (i) the origin is repelling, (ii) infinity is repelling, and (iii) the positive equilibrium K is unique. At the carrying capacity, there is a balance between the

growth and decline of the population, meaning all non-zero population densities are attracted to this state.

An analogous concept of balance exists in higher dimensions. For competitive systems, Hirsch [35, 36] introduced carrying simplices which are hypersurfaces that asymptotically attract all non-zero initial population densities and contains all non-zero steady states. One interesting property of a carrying simplex is that all non-trivial dynamics, such as periodic orbits, occur on it.

In Chapter 3, we have developed an analytic formula for an analogue of the carrying simplex which can also be applied to some non-competitive systems, namely the scaled Lotka–Volterra systems. In this context it is referred to as a balance simplex, which can still be projected 1-to-1 and onto the unit simplex by radial projection. However many other properties no longer hold from carrying simplices. For example, the balance simplex is no longer C^1-continuous on the interior, nor is it the graph of a decreasing function (which both hold for the planar carrying simplex [4, 36, 63, 85]).

7.2 General Kolmogorov population models

We examine a general planar Kolmogorov-type system

$$\begin{aligned} \frac{dx_1}{dt} &= F_1(x_1, x_2) = x_1 f_1(x_1, x_2), \\ \frac{dx_2}{dt} &= F_2(x_1, x_2) = x_2 f_2(x_1, x_2), \end{aligned} \tag{7.1}$$

where we only consider (7.1) on the phase space $\mathbb{R}^2_{\geq 0}$ and the functions $f_1, f_2 : \mathbb{R}^2_{\geq 0} \to \mathbb{R}^2_{\geq 0}$ are C^1-continuous on an open set containing $\mathbb{R}^2_{\geq 0}$. Such a system is often used to model the ecological dynamics of a closed habitat in which two species interact [47].

Our standing assumptions for (7.1) are:

A1 The origin 0 and infinity are repellers;

A2 There are unique axial steady states $q_1 = (\bar{x}_1, 0)$ and $q_2 = (0, \bar{x}_2)$, $\bar{x}_1 > 0, \bar{x}_2 > 0$;

A3 All steady states of (7.1) are hyperbolic, i.e. the eigenvalues of the Jacobian (see equation (7.10)) at all steady states have non-zero real parts;

A4 Intraspecific competition exists for each species:

$$\frac{\partial f_1}{\partial x_1}(x) < 0, \ \frac{\partial f_2}{\partial x_2}(x) < 0, \ x = (x_1, x_2) \in \mathbb{R}^2_{\geq 0}. \tag{7.2}$$

As usual, we denote the flow of the system by $\varphi(\cdot, t) : \mathbb{R}^2_{\geq 0} \to \mathbb{R}^2_{\geq 0}$ or $\varphi_t(x)$ when x is fixed. One important property of this system is that the axes are invariant (forwards and backwards in time). The interior $\mathbb{R}^2_{>0}$ also remains invariant.

To elucidate what its means to say that infinity is a repeller for (7.1) we make a co-ordinate change to bring infinity into view. We define the inversion map $X = (X_1, X_2) : \mathbb{R}^2_{\geq 0} \setminus (0,0) \to \mathbb{R}^2_{\geq 0}$ via

$$X_1(x) = \frac{x_1}{x_1^2 + x_2^2}, \tag{7.3}$$

$$X_2(x) = \frac{x_2}{x_1^2 + x_2^2}. \tag{7.4}$$

Then X maps infinity in (x_1, x_2) co-ordinates to the origin in (X_1, X_2) co-ordinates. Infinity is repelling in (7.1) when the origin of the transformed system

$$\frac{dX_1}{dt} = (X_2^2 - X_1^2)\widetilde{F}_1(X_1, X_2) - 2X_1X_2\widetilde{F}_2(X_1, X_2), \tag{7.5}$$

$$\frac{dX_2}{dt} = (X_1^2 - X_2^2)\widetilde{F}_2(X_1, X_2) - 2X_1X_2\widetilde{F}_1(X_1, X_2), \tag{7.6}$$

is unstable, where $\widetilde{F}_i(X_1, X_2) = F_i(x_1(X), x_2(X))$ for $i = 1, 2$. To obtain the basin of repulsion of infinity in (7.1) we can alternatively find the basin of repulsion of the origin in (7.6) and map back to x_1, x_2 co-ordinates.

Definition 7.2.1 A balance manifold Σ for (7.1) is a globally attracting (on $\mathbb{R}^2_{\geq 0}\backslash\{0\}$), compact, connected set that is equal to the union of the boundaries of the basins of repulsion of the origin and of infinity, i.e. $\Sigma = \partial\mathcal{R}(0) \cup \partial\mathcal{R}(\infty)$.

Remark 7.2.1 *Again, we use the term manifold here to keep the terminology consistent with the carrying simplex. However, the balance manifold is generally not smooth everywhere, but it is composed piecewise of analytic manifolds.*

Remark 7.2.2 *Note that since the balance manifold is globally attracting on $\mathbb{R}^2_{\geq 0}\backslash\{0\}$, it is invariant for the flow of (7.1) and necessarily contains all non-zero steady states.*

Recall that the balance manifold Σ is analogous to the carrying simplex which exists in the competitive case where $\frac{\partial f_1}{\partial x_2} < 0$ and $\frac{\partial f_2}{\partial x_1} < 0$ in $\mathbb{R}^2_{\geq 0}$ [36]. Similar to the Lotka–Volterra systems, we want the balance manifold to separate the basins of repulsion of the origin and of infinity.

A simple, but important, consequence of assumption A4 is:

Lemma 7.2.3 *Under the assumption (7.2) there can be no non-trivial interior closed orbits for (7.1).*

Proof: Let $\mathcal{C}$ be a closed orbit lying completely in $\mathbb{R}^2_{>0}$. By the Divergence Theorem [81] with $B(x) = \frac{1}{x_1 x_2}$

$$\int_{\partial\mathcal{C}} BF \cdot n \, dS = \int_{\mathcal{C}} \operatorname{div}(BF) \, dV \tag{7.7}$$

where n denotes the outward pointing unit normal vector of $\partial\mathcal{C}$ (taken anticlockwise),

dS is a line element and dV is a volume element. Note that for $x \in \mathbb{R}^2_{>0}$:

$$\operatorname{div}(B(F_1, F_2)) = \frac{1}{x_2}\frac{\partial f_1}{\partial x_1} + \frac{1}{x_1}\frac{\partial f_2}{\partial x_2} < 0$$

meaning the right hand side of (7.7) is negative. If $\mathcal{C}$ is a non-trivial periodic orbit, then $F \cdot n = 0$ on $\mathcal{C}$, meaning the left hand side of (7.7) is 0, which is a contradiction.

If $\mathcal{C}$ is not a non-trivial interior periodic orbit, then it must be a homoclinic orbit of the interior steady state x^*. We find that $F \cdot n = 0$ on $\mathcal{C} \setminus \{x^*\}$. At x^*, the unit normal is well defined,

$$n = \frac{\nabla F}{|\nabla F|}, \tag{7.8}$$

$$\nabla F(x^*) = \left(x_1^* \frac{\partial f_1}{\partial x_1}(x^*),\, x_2^* \frac{\partial f_2}{\partial x_2}(x^*) \right)^T \neq 0. \tag{7.9}$$

Since x^* is only one point, the left hand side of (7.7) is still 0, giving another contradiction. □

While this rules out interior homoclinic orbits, it does not rule out homoclinic orbits from a boundary steady state. For this possibility we have

Lemma 7.2.4 *Under the assumptions A1-A4 it is not possible for the unstable orbit of an axial saddle steady state of (7.1) to be a homoclinic orbit.*

Proof: Without loss of generality assume the axial saddle steady state with a homoclinic orbit is $q_1 = (\bar{x}_1, 0)$. By assumption A3 and the Stable Manifold Theorem [69], the saddle q_1 has a 1-dimensional unstable manifold $W^u(q_1)$ and a 1-dimensional stable manifold $W^s(q_1)$. Since the dynamics on the axes are bounded, and there is a unique steady state on each axis, $W^s(q_1)$ is the x_1-axis.

Let $x^0 = (x_1^0, x_2^0) \in W^u(q_1)$ with $x^0 > 0$. Then if the unstable orbit of q_1 is a

homoclinic orbit, $\varphi_t(x^0) \to q_1$ as $t \to \infty$, so that $x^0 \in W^s(q_1) = \{(x,0) : x \in \mathbb{R}_{>0}\}$, a contradiction to $x_2^0 > 0$. □

It will be useful to note the Jacobian of the system (7.1):

$$\mathcal{J}(x_1,x_2) = \begin{pmatrix} f_1(x_1,x_2) + x_1\frac{\partial f_1}{\partial x_1}(x_1,x_2) & x_1\frac{\partial f_1}{\partial x_2}(x_1,x_2) \\ x_2\frac{\partial f_2}{\partial x_1}(x_1,x_2) & f_2(x_1,x_2) + x_2\frac{\partial f_2}{\partial x_2}(x_1,x_2) \end{pmatrix}. \tag{7.10}$$

At the origin,

$$\mathcal{J}(0,0) = \begin{pmatrix} f_1(0,0) & 0 \\ 0 & f_2(0,0) \end{pmatrix}, \tag{7.11}$$

so to satisfy assumption A1 we require $f_1(0,0) > 0$ and $f_2(0,0) > 0$ for the origin to be repelling.

Assumption A2 requires that (7.1) has a unique positive steady state on each axis, which will be the carrying capacity of each individual species. Consider the axial state $q_2 = (0, \bar{x}_2)$ where $\bar{x}_2 > 0$ and $f_2(q_2) = 0$. The Jacobian here is

$$\mathcal{J}(q_2) = \begin{pmatrix} f_1(q_2) & 0 \\ \bar{x}_2\frac{\partial f_2}{\partial x_1}(q_2) & \bar{x}_2\frac{\partial f_2}{\partial x_2}(q_2) \end{pmatrix}. \tag{7.12}$$

Assumption A1 ensures that q_2 is asymptotically stable on the x_1-axis. The invariant x_2-axis has the associated eigenvalue $\bar{x}_2\frac{\partial f_2}{\partial x_2}(q_2)$, and so we require $\frac{\partial f_2}{\partial x_2}(q_2) < 0$. We also assume $f_1(q_2) \neq 0$ to avoid a non-hyperbolic steady state. The sign of $f_1(q_2)$ determines whether this axial steady state is a saddle point (positive) or a stable node (negative).

Similarly, at the other axial steady state, $q_1 = (\bar{x}_1, 0)$, we require $\frac{\partial f_1}{\partial x_1}(q_1) < 0$, and the sign of $f_2(q_1)$ determines whether q_1 is a saddle point or a stable node.

By considering the Poincaré index of steady states (see, for example, [69]), we

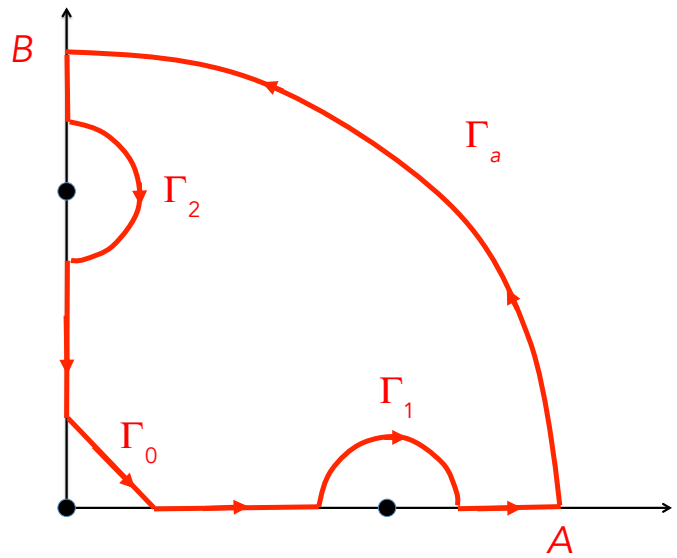

Figure 7.1: $\Gamma = \Gamma_0 \cup \Gamma_1 \cup \Gamma_a \cup \Gamma_2$ is the closed curve in red traversed anticlockwise, looping around each axial steady state. Γ_0 is sufficiently close to the origin such that the vector field is pointing away from the origin, and Γ_a is arbitrarily far from the origin such that Γ contains all possible interior steady states. Note that the red arrows are not the flow of the vector field on Γ, but the orientation of Γ.

can determine the possible stability types of the steady state of (7.1).

Definition 7.2.2 ([31]) Let Γ be a piecewise smooth, closed curve traversed anti-clockwise and consisting of only ordinary points of the vector field (i.e. no steady states). Let θ be the angle between the flow of the vector field at a point on Γ and the positive horizontal axis. Consider a point $x^0 \in \Gamma$. Since the flow is continuous, as we traverse around Γ, back to x^0, the variation of θ will be a multiple of 2π, say $2k\pi$; $k \in \mathbb{Z}$. The index of Γ, denoted I_Γ, is k.

We let $[\theta]_\gamma$ denote the change in the angle θ as we traverse a curve γ, so that $I_\Gamma = \frac{[\theta]_\Gamma}{2\pi}$. Let Γ be the closed curve orientated anticlockwise as shown in Figure 7.1. There are different components to $\Gamma = \Gamma_0 \cup \Gamma_1 \cup \Gamma_a \cup \Gamma_2$. As the origin is an unstable node, $[\theta]_{\Gamma_0} = -\frac{\pi}{2}$.

To calculate the change in angle along the component Γ_a, we bring infinity into view via the inversion map (7.4). Then infinity is repelling in (7.1) when the origin of the system in X_1, X_2 co-ordinates is unstable. Thus using continuity, and the fact

that the dynamics on the axes remain unchanged with this transformation, we find that $[\theta]_{\Gamma_a} = \frac{\pi}{2}$.

We first discuss the case where there are no interior steady states, thus $I_\Gamma = 0$ since it encloses no steady states [31]. If q_1 (the axial steady state on the positive x_1-axis) is a saddle, then $[\theta]_{\Gamma_1} = +\pi$, whereas if q_1 is a stable node, $[\theta]_{\Gamma_1} = -\pi$. The same holds with the other axial steady state q_2 and the component Γ_2. Suppose that both q_1 and q_2 are saddles, then $[\theta]_\Gamma = -\frac{\pi}{2} + \pi + \frac{\pi}{2} + \pi = 2\pi$. Hence it is not possible that both of q_1, q_2 are saddles in this case. Similarly q_1, q_2 cannot both be stable nodes, since then we would have $[\theta]_\Gamma = -2\pi$. Thus the only possible case is when one axial steady state is a saddle and the other is a stable node.

On the other hand, if there are interior steady states, then with Γ_a chosen so that all interior steady states lie inside Γ, we find that the sum of the indices of the interior steady states is the index of Γ [31].

We now discuss the case where there is a unique interior steady state x^*. The index of Γ is equal to the index of x^*. If both q_1, q_2 are saddles, then the index of x^* is equal to $+1$. With the assumption of x^* being hyperbolic and intraspecific competition (preventing interior closed orbits) it follows that x^* must be stable and a node or spiral. If both q_1, q_2 are stable nodes, then the index of x^* is equal to -1, so that x^* must be a saddle. Lastly, the case where one axial steady state is a saddle and the other is a stable node is not possible; x^* would have an index of zero, contradicting its hyperbolicity.

To summarise

Lemma 7.2.5 *For the system (7.1) under the assumptions A1-A4:*

1. *If there is no interior steady state, one axial steady state must be a saddle and the other a stable node.*

2. *If there is a unique interior steady state, then*

(a) If both axial fixed points are saddles, the interior fixed point must be a stable node or a stable spiral.

(b) If both axial fixed points are stable nodes, the interior fixed point is a saddle.

(c) It is not possible that one axial fixed point is a saddle if the other is a stable node.

7.3 Case 1: no interior fixed point

Without loss of generality, let us suppose that q_1 is a saddle and q_2 a stable node.

Lemma 7.3.1 *Consider the system (7.1), under the assumptions A1-A4. Assume there is no interior steady state. Suppose one of these axial steady states is a saddle point, and the other is a stable node. Then the balance manifold is formed of the unique heteroclinic orbit connecting the axial steady states (along with these steady states).*

Proof: Since we are only considering hyperbolic steady states, the saddle q_1 has a 1-dimensional unstable manifold $W^u(q_1)$. Let $x^0 \in W^u(q_1)$ in $\mathbb{R}^2_{>0}$ and $O^+(x^0)$ be the forward orbit through x^0. By assumption A1, $O^+(x^0)$ is bounded and so by the Poincaré–Bendixson Theorem [84] $\omega(x^0)$ contains a steady state, say p. By Lemmas 7.2.3 and 7.2.4, there are no homoclinic orbits, so $p \neq q_1$. Moreover, the origin (which we will denote by 0 here) is repelling so $p \neq 0$. This leaves $p = q_2$, and since q_2 is asymptotically stable, we find that $\omega(x^0) = \{q_2\}$. Explicitly, since $q_2 \in \omega(x^0)$ there exists, by definition, a $t_k \to \infty$ (with $k \to \infty$) such that $\varphi_{t_k}(x^0) \to q_2$. Hence there also exists a K' such that $\varphi_{t_{K'}}(x^0) \in \mathcal{B}(q_2)$ and $\varphi_t(x^0) \in \mathcal{B}(q_2)$ for all $t > t_{K'}$, and so $\omega(x^0) = \{q_2\}$. This means $\overline{O^+(x^0)}$ (the closure of $O^+(x^0)$) is a curve that connects $x^0 \in W^u(q_1)$ to q_2 and we obtain the existence of a heteroclinic orbit

$\mathcal{H} = W^u(q_1) \setminus \{q_1\}$.

Next we show that $\overline{\mathcal{H}} = \partial\mathcal{R}(0) = \partial\mathcal{R}(\infty)$. $\overline{\mathcal{H}}$ divides $\mathbb{R}^2_{\geq 0}$ into two disjoint connected and invariant components, say $\mathcal{H}^-$ containing the origin and $\mathcal{H}^+ = \mathbb{R}^2_{\geq 0} \setminus (\overline{\mathcal{H}} \cup \mathcal{H}^-)$. Let $x^0 \in \mathcal{H}^-$ and consider $O^-(x^0)$. Since $x^0 \notin \overline{\mathcal{H}} = W^u(q_1) \cup \{q_2\}$, there is no subsequence $t_k \to -\infty$ with $\varphi_{t_k}(x^0) \to q_1$ and hence $q_1 \notin \alpha(x^0)$. By the Poincaré–Bendixson Theorem we must have $0 \in \alpha(x^0)$. Since the origin is an asymptotically stable node backwards in time (and q_2 is an unstable node in backwards time), we see that $\alpha(x^0) = \{0\}$. Hence $\mathcal{H}^- = \mathcal{R}(0)$.

Next we map $\mathcal{H}^+$ to $X(\mathcal{H}^+)$ using the inversion (7.4) and consider the transformed dynamics (7.6). Examining these dynamics near the transformed steady states shows that their stability types remain the same. This gives the same phase portrait topology as the previous paragraph, and we conclude that $\mathcal{H}^+ = \mathcal{R}(\infty)$.

Hence for the case where q_1 is a saddle and q_2 a stable node, we have the balance manifold

$$\overline{\mathcal{H}} = \partial\mathcal{R}(0) = \partial\mathcal{R}(\infty) = W^u(q_1) \cup \{q_2\}.$$

□

To summarise, we have shown:

Theorem 7.3.2 *For a balance manifold to exist in the case where (7.1) has no interior steady state, the following conditions are sufficient:*

1. *$f_1(0,0) > 0$, $f_2(0,0) > 0$; the origin is repelling.*
2. *Infinity is repelling.*
3. *There exists a unique axial steady state $q_2 = (0, \bar{x}_2)$ on the positive x_2-axis satisfying $f_2(q_2) = 0$, $\frac{\partial f_2}{\partial x_2}(q_2) < 0$ and $f_1(q_2) \neq 0$.*

4. *There exists a unique axial steady state* $q_1 = (\bar{x}_1, 0)$ *on the positive* x_1*-axis satisfying* $f_1(q_1) = 0, \frac{\partial f_1}{\partial x_1}(q_1) < 0$ *and* $f_2(q_1) \neq 0$.

5. $f_1(q_2)f_2(q_1) < 0$*; the axial steady states are of different stability types and are hyperbolic.*

7.4 Case 2: a unique interior fixed point

We now consider the case where there is a unique interior steady state $x^* = (x_1^*, x_2^*)$. The first four conditions from Theorem 7.3.2 are still required. The Jacobian at the interior steady state is:

$$\mathcal{J}(x^*) = \begin{pmatrix} x_1^* \dfrac{\partial f_1}{\partial x_1}(x^*) & x_1^* \dfrac{\partial f_1}{\partial x_2}(x^*) \\ x_2^* \dfrac{\partial f_2}{\partial x_1}(x^*) & x_2^* \dfrac{\partial f_2}{\partial x_2}(x^*) \end{pmatrix}. \tag{7.13}$$

By assumption x^* is hyperbolic and it may be (asymptotically) stable or a saddle.

Lemma 7.4.1 *Suppose the system (7.1) under the assumptions A1-A4 has a unique interior fixed point* x^**. Suppose additionally that both axial steady states are saddle points. Then* x^* *is stable and the balance manifold is formed of the two heteroclinic orbits connecting the axial steady states to* x^* *(along with these steady states).*

Proof: That x^* is stable follows from 2(a) in Lemma 7.2.5. Each axial steady state is a hyperbolic saddle with 1-dimensional stable and unstable manifolds, recall that its stable manifold is the axis it lies on. Let $W^u(q_1)$ be the unstable manifold of q_1 and choose $x^0 \in W^u(q_1)$ in $\mathbb{R}^2_{>0}$. By the Poincaré–Bendixson Theorem, $\omega(x^0)$ must contain a steady state p, and $p \neq 0$ since the origin is repelling and $p \neq q_1$ by Lemma 7.2.4. Moreover $p \neq q_2$.

To see this, note that if $q_2 \in \omega(x^0)$ there exists $t_k \to \infty$ (with $k \to \infty$) such that $\varphi_{t_k}(x^0) \to q_2$. Recall that $W^s(q_2)$ is precisely the invariant x_2-axis. Noting the

Hartman–Grobman [69] theorem, the local dynamics around q_2 are known and it follows that $\varphi_{t_k}(x^0) \not\to q_2$, a contradiction. Hence we are left with $p = x^*$, which is asymptotically stable thus there is a heteroclinic orbit $\mathcal{H}_2 = W^u(q_1) \setminus \{q_1\}$ between q_1 and x^*. Similarly there is a heteroclinic orbit $\mathcal{H}_3 = W^u(q_2) \setminus \{q_2\}$ linking q_2 and x^*.

Let $\mathcal{H} = \mathcal{H}_2 \cup \mathcal{H}_3$. Next we show that $\partial\mathcal{R}(0) = \overline{\mathcal{H}} = \overline{W^u(q_1) \cup W^u(q_2)}$. We know that $\overline{\mathcal{H}}$ divides $\mathbb{R}^2_{\geq 0}$ into two disjoint connected and invariant components, say $\mathcal{H}^-$ containing the origin and $\mathcal{H}^+ = \mathbb{R}^2_{\geq 0} \setminus (\overline{\mathcal{H}} \cup \mathcal{H}^-)$. Let $x^0 \in \mathcal{H}^-$. We will show that $\alpha(x^0) = \{0\}$. By the Poincaré–Bendixson Theorem, $\alpha(x^0)$ contains a steady state p and as x^* is attracting, $p \neq x^*$. Moreover, $p \notin \{q_1, q_2\}$ since $x^0 \notin W^u(q_1) \cup W^u(q_2)$. Hence $p = 0$ and since the origin is an unstable node, $\alpha(x) = \{0\}$ and $\mathcal{H}^- = \mathcal{R}(0)$, $\overline{\mathcal{H}} = \partial\mathcal{R}(0)$. As in Lemma 7.3.1, we may use the inversion map (7.4) to establish that $\mathcal{H}^+ = \mathcal{R}(\infty)$ and $\overline{\mathcal{H}} = \partial\mathcal{R}(\infty)$.

We conclude that in this case the balance manifold

$$\overline{\mathcal{H}} = \partial\mathcal{R}(0) = \partial\mathcal{R}(\infty) = \overline{W^u(q_1) \cup W^u(q_2)}.$$

□

Lemma 7.4.2 *Suppose the system (7.1), under assumptions A1-A4 has a unique interior fixed point x^*. Suppose additionally that both axial steady states are stable nodes. Then x^* is a saddle point and the two unstable orbits of x^* have different ω-limits, each equal to exactly one of the axial steady states.*

Proof: That x^* is a saddle follows from 2(b) in Lemma 7.2.5. By the Poincaré-Bendixson Theorem each unstable orbit of x^* has a ω-limit set that contains a steady state, which in neither case can be the origin, since the origin is an unstable node, nor x^*, since there are no interior homoclinic orbits by Lemma 7.2.3.

Consider one of the unstable orbits of x^*, denoted by γ_1. Since q_1 and q_2 are

asymptotically stable, γ_1 has its ω-limit in $\{q_1, q_2\}$, i.e. γ_1 is a heteroclinic orbit connecting x^* to either q_1 or q_2. The same is true other unstable orbit of x^*, γ_2.

Suppose that γ_1 and γ_2 connect to the same ω-limit, say q_1. These two heteroclinic orbits γ_1, γ_2 enclose a bounded and invariant region R^* and $x^* \in \overline{R^*}$. Since x^* is a hyperbolic saddle, $W^s(x^*) \cap R^* \neq \emptyset$. Choose $x^0 \in W^s(x^*) \cap R^*$. By the Poincaré–Bendixson Theorem, $\alpha(x^0)$ contains a steady state, say p. We know that $p \neq x^*$ since there are no interior closed orbits, and $p \neq q_2$ because $\overline{R^*}$ is invariant and disjoint from the x_2-axis. Hence we must have $p = q_1$. But this is not possible because q_1 is a stable node. Thus γ_1 and γ_2 are heteroclinic orbits which do not share the same ω-limit.

Let $\mathcal{H} = \gamma_1 \cup \gamma_2$. Next we show that $\partial\mathcal{R}(0) = \overline{\mathcal{H}} = \overline{W^u(x^*)}$. We know that $\overline{\mathcal{H}}$ divides $\mathbb{R}^2_{\geq 0}$ into two disjoint connected and invariant components, say $\mathcal{H}^-$ containing the origin and $\mathcal{H}^+ = \mathbb{R}^2_{\geq 0} \setminus (\overline{\mathcal{H}} \cup \mathcal{H}^-)$. Let $x^0 \in \mathcal{H}^-$. We will show that $\alpha(x^0) = \{0\}$. By the Poincaré-Bendixson Theorem, $\alpha(x^0)$ contains a steady state p and as q_1, q_2 are stable nodes $p \notin \{q_1, q_2\}$. Moreover, $p \neq x^*$ since $x^0 \notin W^u(x^*)$. Hence $p = 0$. The remainder of the proof is similar to that of Lemma 7.4.1.

In this case the balance manifold

$$\overline{\mathcal{H}} = \partial\mathcal{R}(0) = \partial\mathcal{R}(\infty) = \overline{W^u(x^*)}.$$

□

To summarise, we have shown:

Theorem 7.4.3 *For a balance manifold (connecting all non-zero steady states) to exist for the system (7.1) in the case where there is a unique interior steady state x^*, the following conditions are sufficient:*

1. *$f_1(0,0) > 0$, $f_2(0,0) > 0$; the origin is repelling.*

2. *Infinity is repelling.*

3. *There exists a unique axial steady state* q_2 *on the* x_2*-axis satisfying* $f_2(q_2) = 0, \frac{\partial f_2}{\partial x_2}(q_2) < 0$ *and* $f_1(q_2) \neq 0$.

4. *There exists a unique axial steady state* q_1 *on the* x_1*-axis satisfying* $f_1(q_1) = 0, \frac{\partial f_1}{\partial x_1}(q_1) < 0$ *and* $f_2(q_1) \neq 0$.

5. $f_1(q_2)f_2(q_1) > 0$*; both axial steady states are of the same stability-type and are hyperbolic.*

6. *There is intraspecific competition for each species;* $\frac{\partial f_1}{\partial x_1} < 0,\ \frac{\partial f_2}{\partial x_2} < 0$ *in* $\mathbb{R}^2_{>0}$.

7.5 Structural stability

For dynamical systems, it is important to ask whether they are structurally stable [75], especially those which are used to model real systems [94]. A system is structurally stable if it remains topologically unchanged when the system (i.e. its vector field) is affected by a small perturbation. Consider two systems for $x \in \mathbb{R}^2$ in some compact region $\Omega \subset \mathbb{R}^2$

$$\frac{dx}{dt} = F(x), \tag{7.14}$$

$$\frac{dx}{dt} = G(x). \tag{7.15}$$

The 'distance' between these two systems can be measured by the following metric [50, 76]:

Definition 7.5.1 The distance between systems (7.14) and (7.15) in a compact region $\Omega \subset \mathbb{R}^2$ is given by:

$$d_1 = \sup_{x \in \Omega} \{\|F(x) - G(x)\| + \|\mathcal{J}(F) - \mathcal{J}(G)\|\} \tag{7.16}$$

where $\mathcal{J}$ is the Jacobian matrix and the norm is the Frobenius norm in the relevant dimension. The systems are ε-close in Ω if $d_1 \leq \varepsilon$; in which case (7.15) is considered a small perturbation of (7.14).

Theorem 7.5.1 (Andronov and Pontryagin [50, 76]) *A smooth dynamical system (7.14) is structurally stable in a compact region $\Omega \subset \mathbb{R}^2$ if and only if:*

1. *it has a finite number of equilibria and limit cycles in Ω, all of which are hyperbolic,*
2. *there are no saddle points with a homoclinic orbit and there are no heteroclinic orbits connecting two saddle points in Ω.*

The system (7.1) we consider with conditions from Theorems 7.3.2 or 7.4.3 is therefore structurally stable as it satisfies the conditions of Theorem 7.5.1. In the case where two steady states are saddle points, we know there must be three non-zero steady states total. In Theorem 7.4.3 we imposed conditions to ensure both axial steady states will be the saddle points in this scenario. In the proof of Lemma 7.4.1, we showed there is no heteroclinic orbit between these saddle points. Lemmas 7.2.3 and 7.2.4 show there are no saddle points with homoclinic orbits.

Therefore the balance manifold we have found (composed of heteroclinic orbits) is also structurally stable in the sense that it still exists when the system is affected by a small perturbation. This means the balance manifold is not a rare or atypical structure, but occurs in a range of systems, some of which are characterised by the conditions in Theorems 7.3.2 and 7.4.3.

7.6 Example models

In Chapter 3 we found an explicit, analytic solution for the balance manifold in scaled Lotka–Volterra systems (the intrinsic growth rates and intraspecfic interaction

coefficients are all equal to 1 for both species). Now we show some (numerical) plots of the balance manifold for different Kolomogorov-type systems.

7.6.1 Higher order polynomial per-capita growth rates

We can consider higher order polynomial functions for the per-capita growth rates f and g. This enables the nullclines $f = 0$ and $g = 0$ to be slightly more complex, affecting the shape of the orbits in the phase plane. In Figure 7.2, we have the system:

$$\begin{aligned}
\frac{dx_1}{dt} &= x_1 f_1(x_1, x_2) \\
&= x_1 \left[-x_1^2 + x_1 - 10(x_2 - 1)(2x_2 - 6)(2x_2 - 1) \right], \\
\frac{dx_2}{dt} &= x_2 f_2(x_1, x_2) \\
&= x_2 \left[14 - 0.2x_1^2 - 3x_2^2 \right]. \qquad (7.17)
\end{aligned}$$

This system satisfies the conditions of Theorem 7.4.3 apart from the final one requiring intraspecific competition. In this model, $\frac{\partial f_1}{\partial x_1} = 1 - 2x_1$ which is not always negative in $\mathbb{R}^2_{>0}$. From Figure 7.2, we can see that there are no periodic orbits and x^* is a stable node. This demonstrates that our requirement of intraspecific competition (assumption A4 and condition 7 of Theorem 7.4.3) is not necessary for the existence of a balance manifold.

7.6.2 Facultative mutualism

In co-operative Lotka–Volterra models, if the interspecific interaction rates are too large, population densities can become unbounded which goes against our assumption that infinity is repelling. Wolin [95] introduced facultative mutualism models for

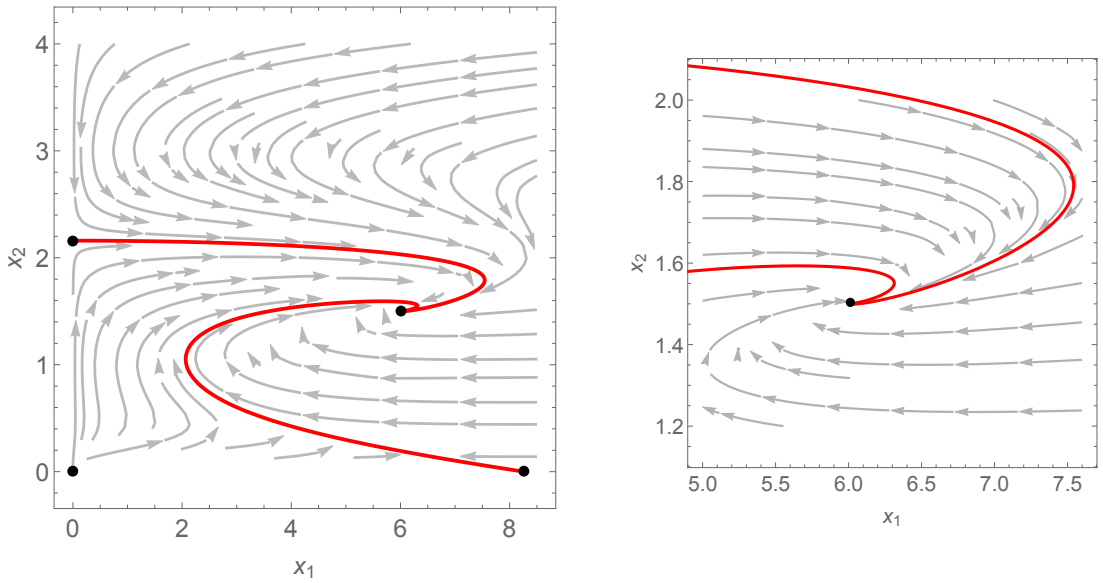

Figure 7.2: The phase plane of the system (7.17) with a close-up of the interior steady state in the right figure. The balance manifold is the solid red curve and the black points are steady states. In this system, there is a unique interior steady state and species 1 does not experience intraspecific competition in $\mathbb{R}^2_{>0}$.

which the orbits are always bounded. A facultative mutualist is a species which can exist without the presence of its mutualistic partner species. We consider a model where both species have a per-capita birth rate which is increased by high recipient densities through a hyperbolic functional response:

$$\begin{aligned}\frac{dx_1}{dt} &= x_1\left(r_1 - \frac{b_1 x_1}{1+\alpha_{12}x_2} - d_1 x_1\right),\\ \frac{dx_2}{dt} &= x_1\left(r_2 - \frac{b_2 x_2}{1+\alpha_{21}x_1} - d_2 x_2\right),\end{aligned} \tag{7.18}$$

where all the parameters are positive. There is a unique interior steady state x^* which always exists and is stable. This model satisfies our assumptions for the case with one interior steady state. An example of this system, along with its balance manifold, is shown in Figure 7.3.

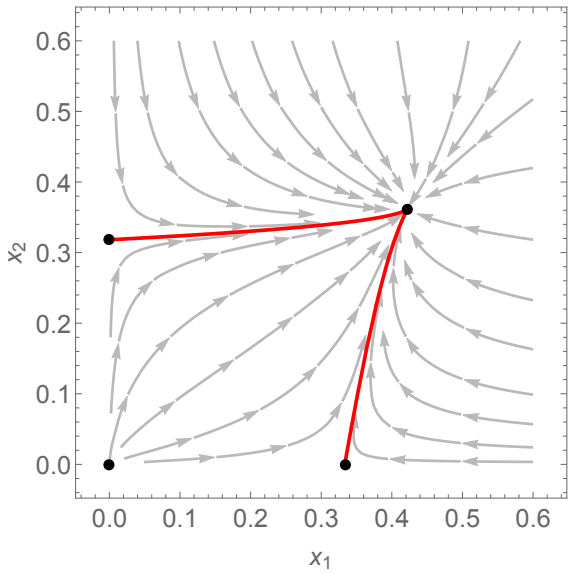

Figure 7.3: The phase plane of the co-operative system (7.18), with the balance manifold shown in red.

7.6.3 Holling type-II predator-prey interaction

Consider the system

$$\begin{aligned} \frac{dx_1}{dt} &= x_1\left[\rho\left(1-\frac{x_1}{K}\right)-\frac{\gamma x_2}{A+x_1}\right], \\ \frac{dx_2}{dt} &= x_2\left[\frac{\sigma x_1}{A+x_1}+\mu-\alpha x_2\right]. \end{aligned} \tag{7.19}$$

Here, x_1 is the prey and x_2 is the predator density, and all parameters are positive. The equation for the prey shows a type-II Holling functional response [38], where there is a maximal feeding rate γ for the predator. The model has been modified from the classic predator-prey model as the predator has an alternative food source that supports logistic growth to carrying capacity $\frac{\mu}{\alpha}$ in the absence of prey. An example of this is if the predator is omnivorous [48].

There is a unique axial steady state on each axis; $(K,0)$ and $\left(0,\frac{\mu}{\alpha}\right)$. There is also intraspecific competition for both species and at most one interior steady state x^*. In this model, infinity is repelling. Note that $\frac{dx_1}{dt}<0$ for any $x_1>K$ and $x_2\geq 0$. This means there exists some time $T\geq 0$ such that $x_1(t)\in[0,K]$ for all $t>T$. In

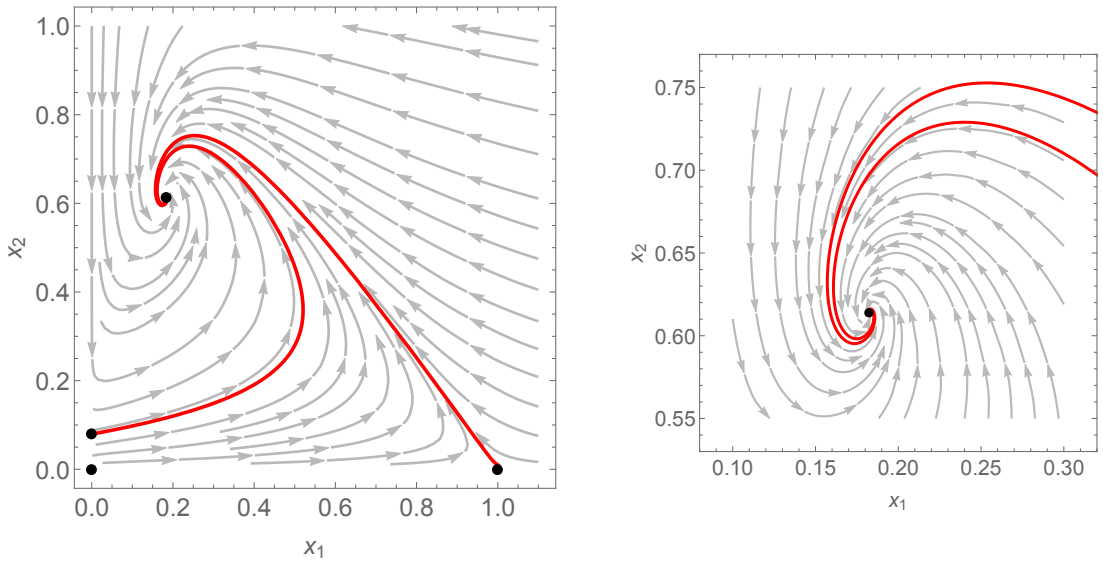

Figure 7.4: The phase plane and balance manifold of the system (7.19) with a close-up of the interior steady state in the right figure. In this model of predator-prey dynamics, there is no possibility of periodic orbits since both species always experience intraspecific competition.

this case, note that

$$\frac{dx_2}{dt} \leq x_2\left(\frac{\sigma K}{A+K} + \mu - \alpha x_2\right) \qquad \text{for all } t > T. \tag{7.20}$$

The expression on the right hand side is negative when

$$x_2 > \frac{1}{\alpha}\left(\frac{\sigma K}{A+K} + \mu\right). \tag{7.21}$$

This means that for any initial condition, there is some time T_B such that for all $t > T_B$ the solution $(x_1(t), x_2(t))$ lies in the compact box $B = [0, K] \times \left[0, \frac{1}{\alpha}\left(\frac{\sigma K}{A+K} + \mu\right)\right]$. Thus infinity is indeed repelling in this model.

When the parameters of (7.19) are all positive, the model satisfies our conditions of the existence of a balance manifold in both of the cases where x^* does and does not exist. An example of the former case, with the balance manifold depicted, is shown in Figure 7.4.

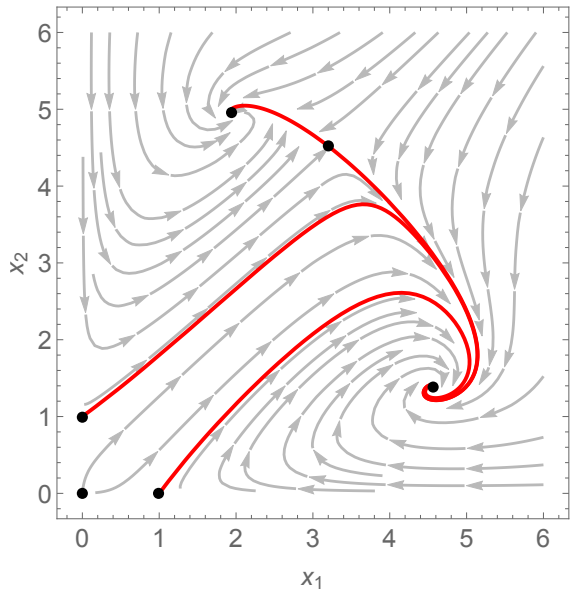

Figure 7.5: The phase plane and balance manifold of a system from [103] with varying interspecific interactions. In this case the boundary of the basin of repulsion of the origin and of infinity are not equal.

7.7 Conclusions

We have provided several computable conditions in Theorems 7.3.2 and 7.4.3 which lead to the existence of what we have called the balance manifold in planar Kolmogorov systems, where solutions that are growing from the origin, with those declining from infinity are balanced. We have discussed the cases where there is at most one interior steady state x^*. The next logical step would be to consider systems where there is more than one interior steady state. For example, Zhang et al. [103] considered a two-species model with transitions between types of population interactions; the interspecific interactions can change sign with species density. In their model they found up to three interior steady states, an example of which is shown in Figure 7.5. Unlike our previous examples, in this case the boundary of the basin of repulsion of the origin and of infinity are not equal, but $\partial\mathcal{R}(0) \subset \partial\mathcal{R}(\infty)$ and the balance manifold is equal to $\partial\mathcal{R}(\infty)$. This is why we use the union of these boundaries in Definition 7.2.1 instead of being equal to both of these boundaries.

Some of the conditions we have provided are necessary for a balance manifold

to exist. For example, the requirement that there is exactly one axial steady state on each axis. This condition is equivalent to requiring the existence of the balance manifold in all the 1-dimensional subcases of the system. Some of our conditions are sufficient but not necessary for the existence of a balance manifold, such as intraspecific competition in $\mathbb{R}^2_{>0}$ (see system (7.17)).

The balance manifold differs from the competitive carrying simplex as some properties of the carrying simplex no longer hold. For example, in non-competitive cases where there is an interior steady state, the balance manifold may no longer be C^1 at this point. The balance manifold can also have a curvature which changes sign, and may not project radially 1-to-1 on the line joining both axial steady states. An example of these can be found in Figure 7.4 where we consider a predator-prey type model.

The planar balance manifold is an important part of understanding similar manifolds in higher-dimensional Kolmogorov models. For example, where there are 3 species, in seeking to define a balance manifold we need a balance manifold to exist when one of the species is absent, i.e. in a planar model of the kind studied here.

Chapter 8

Concluding Remarks

In this thesis, we have extended the concept of a carrying simplex to non-competitive systems, with the focus being on scaled Lotka–Volterra systems. We have not seen this extension being explored in the literature before, and we refer to the manifold as the balance simplex Σ, or balance manifold when it is does not radially project 1-to-1 to the unit simplex.

In Chapter 2, we proved the existence of Σ in some non-competitive 2-species scaled Lotka–Volterra systems, namely those where the interspecific interaction coefficients satisfy $\alpha_{12}, \alpha_{21} < 2$, $\alpha_{12}, \alpha_{21} \neq 1$ (ensuring the steady states are hyperbolic) and the system is not co-operative. This parameter space includes cases where species are weakly competitive, or where there is a predator-prey type relationship between the species and predation is not very strong. The work in this chapter was based on the Hadamard graph transform method [29] used by Baigent in [4, 5], showing that Σ attracted all non-zero solution orbits and was invariant to the flow of the system. Our calculations involved transforming the system into (u, N)-co-ordinates, where u is the proportion of species 1, and N is the total number of individuals in the system. Despite not being to extend these methods for any α_{12} or $\alpha_{21} \geq 2$, in Chapter 3 we found explicit expressions for the balance simplex in any parameter case (where the system is bounded), proving its existence as the manifold formed of heteroclinic orbits, separating solutions which grow from the origin and those which decline from infinity.

By transforming the 2-species system into polar co-ordinates in Chapter 3, we were able to solve the equations using an integrating factor. This gave the general solution to the system, for which we were able to identify the balance simplex by setting the constant of integration to 0. The solution contained an integral which we could write in the form of a Gaussian hypergeometric function, greatly simplifying the parametric form of the solution (Section 3.7). We also had a second solution based on an equivalent system which was used to avoid complex terms in the integrand of

the first solution. If the interior steady state exists, both solutions are needed and each defines the unique heteroclinic orbit from one of the axial steady states to the interior steady state, thus in this case Σ is defined piecewise. If the interior steady state does not exist, only one of the solutions is needed. We also gave the explicit solutions for Σ in some special cases (Section 3.9), for example if α_{12} or $\alpha_{21} = 1$. Thus the explicit form of Σ is now known in any parameter case of the 2-species scale Lotka–Volterra system as long as the dynamics remain bounded.

With the explicit expression of Σ now known for the 2-species system, the curvature of Σ can now be explicitly analysed. We know that the curvature of the carrying simplex has been an area of interest (e.g. [4, 5, 99, 100]) thus this can be a topic for future research. We were not able to simplify the expression for the curvature of Σ algebraically but there may be particular parameter cases which can be analysed. We have already seen that if $\alpha_{12} + \alpha_{21} = 2$, even in non-competitive systems, the balance simplex is the line $x_2 = 1 - x_1$.

In Chapters 4, 5 and 6 we explored the balance simplex in 3-species scaled Lotka–Volterra systems. There are analogous, higher dimensional versions of the Gaussian hypergeometric function, called Appell hypergeometric functions [2, 6], however we were not able to find an exact solution for the 3-species system. In Chapter 4, we found a series solution in the form $\{x_1, x_2, x_3\} = \{G, T_1G, T_2G\}$, where $T_1 = \frac{x_2}{x_1}$ and $T_2 = \frac{x_3}{x_1}$ are the variables of the infinite series G. We can plot this solution as a surface. By only using the condition that $G(0, 0) = 1$, i.e. the point $(1, 0, 0)$ lies on this surface, the solution matches exactly on the boundary with one of our 2-species solution, in the hypergeometric series form. However, our 3-species series solution was only valid for the parameter case $\mathcal{A}$ where the dynamics of the system are bounded and all $\alpha_{ij} < 1$ and $\alpha_{ij}\alpha_{ji} < 1$ for $i \neq j$, $i, j \in \{1, 2, 3\}$. Biologically, this excludes the case where species are strongly competitive or strongly co-operative. It also excludes the case where one species is heavily predated on by another. The

solution is defined piecewise, with each part associated to one of the three axial steady states. We saw that this solution was not an effective way to plot the balance simplex in general since the series is not guaranteed to converge in the whole of $\mathbb{R}^3_{>0}$ (e.g. Figure 4.1a), however, by taking the solution in a neighbourhood of each axial steady state, we were able to use it to prove the existence of the balance simplex in this parameter case. Additionally, in the special case where every $\alpha_{ij} = \frac{n}{n+1};\ n \in \mathbb{N}$, the series G is finite and our solution gives the exact form of the balance simplex, still defined piecewise (Section 4.3). A topic for future research is finding a similar series solution in the remaining parameter cases. This will likely involve a different relationship between the variables (i.e. a different T_1 and T_2).

In Chapter 5, we prove the existence of the balance simplex for 3-species scaled Lotka–Volterra systems where the interaction matrix A is strictly copositive, meaning the average fitness of the population is always positive. Since the diagonal entries of A are always 1 and we only consider systems with bounded dynamics, we believe the parameter space where A is strictly copositive covers many different types of systems. In the future, it would be interesting to explore the size of this parameter space, and compare it to $\mathcal{A}$. We have seen that these parameter spaces are not subsets of each other and their intersection is non-empty.

In Chapter 6, we find a more accurate and reliable way of plotting Σ in the 3-species case, compared to the parametric series solution in Chapter 4. The method resembles finding a Darboux polynomial [22] for the system, except we look for an infinite series ϕ. Using the cofactor $m = -x_1 - x_2 - x_3$, we solve for ϕ and plot its zero set (for the finite version, up to degree K) to get an approximation of Σ, denoted $\phi^{-1}(0)$. Even with $K = 25$, in most cases $\phi^{-1}(0)$ matches well to the boundary dynamics and 2-species balance simplex and typically takes 3 minutes to produce. The plots typically improve with increasing K, however for some cases numerical instabilities occur. In the future, it is worth exploring these issues and perhaps

considering an alternate method of plotting an approximation of Σ in these cases (e.g. Figure 6.8). Our research does not focus directly on numerical methods, but a numerical solution to Σ should be possible. The advantage of the methods conducted in this thesis, however, is the insight gained.

Some of the $\phi^{-1}(0)$ plots showed two surfaces, of which the lower surface matches what we expect of Σ. By using the cofactor $m = -x_1^2 - x_2^2 - x_3^2$ instead, the upper surface no longer appeared in most of these examples (e.g. Figure 6.10), however this does not help with numerical instabilities (see Figure 6.9b). It would be interesting to explore the effects of different cofactors m, in particular we have not yet explored cofactors which are not homogeneous in degree.

In Chapter 7, we discussed the balance manifold (which may not radially project 1-to-1 to the unit simplex) for planar Kolmogorov models where the per-capita growth rates are C^1-continuous. This covers a wide range of ecological systems, some examples of which are shown in Section 7.6. We found sufficient conditions for the existence of a balance manifold when there is at most one interior steady state for the system (Theorems 7.3.2 and 7.4.3). These conditions were derived by considering the stability and Poincaré index [69] of all the steady states.

The next stage would be to consider systems with more than one interior steady state. We saw in Figure 7.5 that $\partial\mathcal{R}(0) \neq \partial\mathcal{R}(\infty)$ which is why in this chapter we defined the balance manifold to be $\Sigma = \partial\mathcal{R}(0) \cup \partial\mathcal{R}(\infty)$. If applying the Hadamard graph transform method we discussed in Chapter 2, we would find that the limit of the sequence of functions from above and below would not be the equal. It would be interesting to explore if one limit set will always be contained in the other or if this requires additional conditions on the parameters.

A vital part of the scaled Lotka–Volterra model is that the intrinsic growth rates for all species are equal. This feature means the dynamics of the species proportions u can be decoupled from the dynamics of the total population size N. The qualitative

behaviour of the u-dynamics can be determined through Jacobian analysis or Bomze's classification [10,11] (in the 3-species case), meaning we can solve for $N(u(t), t)$. This was particularly important in Chapters 2 and 5. Finding an explicit solution for Σ in Chapter 3 was made easier due to the intrinsic growth rates and intraspecific interaction coefficients being equal to 1 for all species. If these values were different for all species, we expect this to be more challenging. We believe the methods discussed for plotting Σ in Chapter 6 will work in higher dimensions, or more general Kolmogorov models.

Our work in this thesis has extended the study of the carrying simplex to non-competitive systems. Despite some properties of carrying simplices no longer holding, we believe the balance simplex and balance manifold are worth studying. In particular, we have shown for the 2- and 3-species scaled Lotka–Volterra system, Σ is asymptotically complete meaning the dynamics of the system can still be reduced to a hypersurface. We hope the results and methods we have discussed will be useful to other researchers in the near future.

Bibliography

[1] V. Antonov, W. Fernandes, V. G. Romanovski, and N. L. Shcheglova. First integrals of the May–Leonard asymmetric system. *Mathematics*, 7(3):292, 2019.

[2] P. Appell. Sur les séries hypergéometriques de deux variables et sur des équations différentielles linéaires aux dérivées partielles. *Comptes Rendus*, 90:296–298, 1880.

[3] O. Babelon, D. Bernard, and M. Talon. *Introduction to classical integrable systems*. Cambridge University Press, 2003.

[4] S. Baigent. Convexity-preserving flows of totally competitive planar Lotka–Volterra equations and the geometry of the carrying simplex. *Proceedings of the Edinburgh Mathematical Society*, 55(1):53–63, 2012.

[5] S. Baigent. Geometry of carrying simplices of 3-species competitive Lotka–Volterra systems. *Nonlinearity*, 26(4):1001, 2013.

[6] W. Bailey. *Generalized Hypergeometric Series*. Cambridge tracts in mathematics and mathematical physics. Stechert-Hafner service agency, 1964.

[7] H. Bateman. *Higher Transcendental Functions [Volumes I-III]*. McGraw-Hill Book Company, 1953.

[8] G. Birkhoff and G. Rota. *Ordinary Differential Equations*. Wiley, fourth edition, 1989.

[9] G. Blé, V. Castellanos, J. Llibre, and I. Quilantán. Integrability and global dynamics of the May–Leonard model. *Nonlinear Analysis: Real World Applications*, 14(1):280–293, Feb. 2013.

[10] I. M. Bomze. Lotka-Volterra equation and replicator dynamics: a two-dimensional classification. *Biological Cybernetics*, 48(3):201–211, 1983.

[11] I. M. Bomze. Lotka-Volterra equation and replicator dynamics: new issues in classification. *Biological Cybernetics*, 72(5):447–453, 1995.

[12] P. Brunovský. Controlling nonuniqueness of local invariant manifolds. *J. Reine Angew. Math*, 446:115–135, 1994.

[13] L. Cairó. Darboux first integral conditions and integrability of the 3D Lotka-Volterra system. *Journal of Nonlinear Mathematical Physics*, 7(4):511–531, 2000.

[14] L. Cairó and J. Llibre. Darboux integrability for 3D Lotka-Volterra systems. *Journal of Physics A: Mathematical and General*, 33(12):2395, 2000.

[15] X. Chen, J. Jiang, and L. Niu. On Lotka–Volterra equations with identical minimal intrinsic growth rate. *SIAM Journal on Applied Dynamical Systems*, 14(3):1558–1599, 2015.

[16] Y. Chen and F. Zhang. Dynamics of a delayed predator–prey model with predator migration. *Applied Mathematical Modelling*, 37(3):1400–1412, 2013.

[17] S.-Y. Chiang. An application of Lotka–Volterra model to Taiwan's transition from 200 mm to 300 mm silicon wafers. *Technological Forecasting and Social Change*, 79(2):383–392, 2012.

[18] A. Ching and S. Baigent. The balance simplex in non-competitive 2-species

scaled Lotka–Volterra systems. *Journal of Biological Dynamics*, 13(1):128–147, 2019.

[19] A. Ching and S. Baigent. Manifolds of balance in planar ecological systems. *Applied Mathematics and Computation*, 358:204–215, 2019.

[20] C.-A. Comes. Banking system: three level Lotka-Volterra model. *Procedia Economics and Finance*, 3:251–255, 2012.

[21] F. Courchamp, T. Clutton-Brock, and B. Grenfell. Inverse density dependence and the Allee effect. *Trends in ecology & evolution*, 14(10):405–410, 1999.

[22] G. Darboux. Mémoire sur les équations différentielles algébriques du premier ordre et du premier degré. *Bulletin des sciences mathématiques et astronomiques*, 2(1):151–200, 1878.

[23] E. DiBenedetto. *Partial Differential Equations*. Birkhäuser Boston, 2013.

[24] O. Diekmann, Y. Wang, and P. Yan. Carrying simplices in discrete competitive systems and age-structured semelparous populations. *Discrete and Continuous Dynamical Systems*, 20(1):37–52, 2008.

[25] S. R. Dunbar. Travelling wave solutions of diffusive Lotka-Volterra equations. *Journal of Mathematical Biology*, 17(1):11–32, 1983.

[26] H. Freedman and J. Wu. Periodic solutions of single-species models with periodic delay. *SIAM Journal on Mathematical Analysis*, 23(3):689–701, 1992.

[27] I. Gladwell, L. Shampine, and S. Thompson. *Solving ODEs with MATLAB*. Cambridge University Press, 2003.

[28] B. Grammaticos, J. Moulin-Ollagnier, A. Ramani, J.-M. Strelcyn, and S. Wojciechowski. Integrals of quadratic ordinary differential equations in R3: the

Lotka-Volterra system. *Physica A: Statistical Mechanics and its Applications*, 163(2):683–722, 1990.

[29] J. Hadamard. Sur litération et les solutions asymptotiques des équations différentielles. *Bull. Soc. Math. France*, 29:224–228, 1901.

[30] K.-P. Hadeler. On copositive matrices. *Linear Algebra and its Applications*, 49:79–89, 1983.

[31] P. Hartman. *Ordinary Differential Equations*. Classics in Applied Mathematics. Society for Industrial and Applied Mathematics, 2002.

[32] A. Hastings. Global stability in Lotka-Volterra systems with diffusion. *Journal of Mathematical Biology*, 6(2):163–168, 1978.

[33] M. W. Hirsch. Systems of differential equations which are competitive or cooperative: I. limit sets. *SIAM Journal on Mathematical Analysis*, 13(2):167–179, 1982.

[34] M. W. Hirsch. Systems of differential equations that are competitive or cooperative II: Convergence almost everywhere. *SIAM Journal on Mathematical Analysis*, 16(3):423–439, 1985.

[35] M. W. Hirsch. Systems of differential equations which are competitive or cooperative: III. competing species. *Nonlinearity*, 1(1):51, 1988.

[36] M. W. Hirsch. On existence and uniqueness of the carrying simplex for competitive dynamical systems. *Journal of Biological Dynamics*, 2(2):169–179, 2008.

[37] J. Hofbauer and K. Sigmund. *Evolutionary Games and Population Dynamics*. Cambridge University Press, 1998.

[38] C. S. Holling. Some characteristics of simple types of predation and parasitism. *The Canadian Entomologist*, 91(7):385–398, 1959.

[39] H.-C. Hung, Y.-C. Chiu, H.-C. Huang, and M.-C. Wu. An enhanced application of Lotka–Volterra model to forecast the sales of two competing retail formats. *Computers & Industrial Engineering*, 109:325–334, 2017.

[40] J. Jiang, J. Mierczyński, and Y. Wang. Smoothness of the carrying simplex for discrete-time competitive dynamical systems: a characterization of neat embedding. *Journal of Differential Equations*, 246(4):1623–1672, 2009.

[41] J. Jiang and L. Niu. On the equivalent classification of three-dimensional competitive Leslie-Gower models via the boundary dynamics on the carrying simplex. *Journal of Mathematical Biology*, 74(5):1–39, sep 2016.

[42] W. Kaczor and M. Nowak. *Problems in Mathematical Analysis: Integration*. Problems in Mathematical Analysis. American Mathematical Soc.

[43] D. W. Kahn. *Introduction to global analysis*. Courier Corporation, 2007.

[44] E. Kamke et al. Zur Theorie der Systeme gewöhnlicher Differentialgleichungen. II. *Acta Mathematica*, 58:57–85, 1932.

[45] J.-H. Kim, G.-L. Lippi, and H. Maurer. Minimizing the transition time in lasers by optimal control methods: Single-mode semiconductor laser with homogeneous transverse profile. *Physica D: Nonlinear Phenomena*, 191(3-4):238–260, 2004.

[46] S. Kingsland and S. Kingsland. *Modeling Nature*. Science and Its Conceptual Foundations series. University of Chicago Press, 1995.

[47] M. Kot. *Elements of Mathematical Ecology*. Cambridge University Press, 2001.

[48] P. Kratina, R. M. LeCraw, T. Ingram, and B. R. Anholt. Stability and persistence of food webs with omnivory: is there a general pattern? *Ecosphere*, 3(6):1–18, 2012.

[49] Y. Kuang. *Delay differential equations: with applications in population dynamics*, volume 191. Academic Press, 1993.

[50] Y. A. Kuznetsov. *Elements of applied bifurcation theory*, volume 112. Springer Science & Business Media, 2013.

[51] M. LaMar and M. Zeeman. CSimplex, a Geomview module for visualizing the carrying simplex of a competitive Lotka–Volterra system.

[52] S.-J. Lee, D.-J. Lee, and H.-S. Oh. Technological forecasting at the Korean stock market: A dynamic competition analysis using Lotka–Volterra model. *Technological Forecasting and Social Change*, 72(8):1044–1057, 2005.

[53] X. Liang and J. Jiang. The classification of the dynamical behavior of 3-dimensional type K monotone Lotka-Volterra systems. *Nonlinear Analysis: Theory, Methods & Applications*, 51(5):749–763, 2002.

[54] X. Liang and J. Jiang. The dynamical behaviour of type-K competitive Kolmogorov systems and its application to three-dimensional type-K competitive Lotka–Volterra systems. *Nonlinearity*, 16(3):785–801, 2003.

[55] A. J. Lotka. Contribution to the theory of periodic reactions. *The Journal of Physical Chemistry*, 14(3):271–274, 1910.

[56] A. J. Lotka. Analytical note on certain rhythmic relations in organic systems. *Proceedings of the National Academy of Sciences*, 6(7):410–415, 1920.

[57] J. Luukkainen and J. Väisälä. Elements of Lipschitz topology. In *Annales Academiae Scientiarum Fennicae. Mathematica*, volume 3, pages 85–122, 1977.

[58] R. S. Maier. The integration of three-dimensional Lotka-Volterra systems. *Proceedings of the Royal Society A: Mathematical, Physical and Engineering Sciences*, 469(2158):20120693–20120693, July 2013.

[59] R. M. May and W. J. Leonard. Nonlinear aspects of competition between three species. *SIAM Journal on Applied Mathematics*, 29(2):243–253, 1975.

[60] R. Mchich, P. Auger, and J.-C. Poggiale. Effect of predator density dependent dispersal of prey on stability of a predator–prey system. *Mathematical Biosciences*, 206(2):343–356, 2007.

[61] J. Mierczyński. The C^1 property of carrying simplices for a class of competitive systems of ODEs. *Journal of Differential Equations*, 111(2):385–409, 1994.

[62] J. Mierczyński. On peaks in carrying simplices. In *Colloq. Math*, volume 81, pages 285–292, 1999.

[63] J. Mierczyński. Smoothness of unordered curves in two-dimensional strongly competitive systems. *Applicationes Mathematicae*, 25(4):449–455, 1999.

[64] T. Modis. Technological forecasting at the stock market. *Technological Forecasting and Social Change*, 62(3):173–202, 1999.

[65] T. Namba. Competitive co-existence in a seasonally fluctuating environment. *Journal of Theoretical Biology*, 111(2):369–386, 1984.

[66] M. Ò Searcòid. *Metric spaces*. Springer Science & Business Media, 2006.

[67] K. M. Page and M. A. Nowak. Unifying evolutionary dynamics. *Journal of Theoretical Biology*, 219(1):93–98, 2002.

[68] J. Perez, A. Füzfa, T. Carletti, L. Mélot, and L. Guedezounme. The Jungle Universe: coupled cosmological models in a Lotka–Volterra framework. *General Relativity and Gravitation*, 46(6):1753, 2014.

[69] L. Perko. *Differential equations and dynamical systems*, volume 7. Springer Science & Business Media, 2013.

[70] J. Rosenberg et al. Applications of analysis on Lipschitz manifolds. In *Miniconference on Harmonic Analysis and Operator Algebras*, pages 269–283. Centre for Mathematics and its Applications, Mathematical Sciences Institute, 1987.

[71] W. Rudin. *Principles of Mathematical Analysis*. International series in pure and applied mathematics. McGraw-Hill, third edition, 1976.

[72] A. Ruiz-Herrera. Exclusion and dominance in discrete population models via the carrying simplex. *Journal of Difference Equations and Applications*, 19(1):96–113, 2013.

[73] S. Shahin, F. Vallini, F. Monifi, M. Rabinovich, and Y. Fainman. Heteroclinic dynamics of coupled semiconductor lasers with optoelectronic feedback. *Optics letters*, 41(22):5238–5241, 2016.

[74] W. Shen and Y. Wang. Carrying simplices in nonautonomous and random competitive Kolmogorov systems. *Journal of Differential Equations*, 245(1):1–29, 2008.

[75] L. Shilnikov, A. Shilnikov, D. Turaev, and L. Chua. *Methods of Qualitative Theory in Nonlinear Dynamics. Part I* . World Scientific, 12 1998.

[76] L. Shilnikov, A. Shilnikov, D. Turaev, and L. Chua. *Methods of Qualitative Theory in Nonlinear Dynamics. Part II.* World Scientific, 09 2001.

[77] S. Smale. On the differential equations of species in competition. *Journal of Mathematical Biology*, 3(1):5–7, 1976.

[78] H. L. Smith. Periodic competitive differential equations and the discrete dynamics of competitive maps. *Journal of Differential Equations*, 64(2):165–194, 1986.

[79] H. L. Smith. *Monotone dynamical systems: an introduction to the theory of competitive and cooperative systems*. Number 41. American Mathematical Soc., 2008.

[80] J. M. Smith and G. R. Price. The logic of animal conflict. *Nature*, 246(5427):15, 1973.

[81] M. Spivak. *Calculus on manifolds: a modern approach to classical theorems of advanced calculus*. CRC Press, 2018.

[82] P. A. Stephens, W. J. Sutherland, and R. P. Freckleton. What is the Allee effect? *Oikos*, pages 185–190, 1999.

[83] W. Terrell. *Stability and Stabilization: An Introduction*. Princeton University Press, 2009.

[84] G. Teschl. *Ordinary differential equations and dynamical systems*. American Mathematical Soc., 2012.

[85] A. Tineo. On the convexity of the carrying simplex of planar Lotka–Volterra competitive systems. *Applied Mathematics and Computation*, 123(1):93–108, 2001.

[86] G. J. Tortora and B. Derrickson. *Principles of anatomy & physiology*. John Wiley & Sons, Incorporated, 2017.

[87] M. van Baalen, V. Krivan, P. C. van Rijn, and M. W. Sabelis. Alternative food, switching predators, and the persistence of predator-prey systems. *The American Naturalist*, 157(5):512–524, May 2001.

[88] V. S. Varma. Exact solutions for a special prey-predator or competing species system. *Journal of Mathematical Biology*, 39:619–622, July 1977.

[89] E. Venturino. The influence of diseases on Lotka-Volterra systems. *Rocky Mountain J. Math.*, 24(1):381–402, 03 1993.

[90] N. J. Vilenkin and A. U. Klimyk. *Representation of Lie Groups and Special Functions: Volume 1.* Mathematics and its Applications. Kluwer Academic Publishers, 1991.

[91] V. Volterra. Variazioni e fluttuazioni del numero d'individui in specie animali conviventi. *Memoria della Regia Accademia Nazionale dei Lincei, Series 6*, 2:31–113, 01 1926.

[92] Y. Wang and J. Jiang. Uniqueness and attractivity of the carrying simplex for discrete-time competitive dynamical systems. *Journal of Differential Equations*, 186(2):611–632, 2002.

[93] G. Wanner and E. Hairer. *Solving ordinary differential equations II.* Springer Berlin Heidelberg, 1996.

[94] S. Wiggins. *Introduction to applied nonlinear dynamical systems and chaos*, volume 2. Springer Science & Business Media, 2003.

[95] C. L. Wolin and L. R. Lawlor. Models of facultative mutualism: density effects. *The American Naturalist*, 124(6):843–862, 1984.

[96] R. Xu, M. A. Chaplain, and F. A. Davidson. Periodic solution for a three-species Lotka-Volterra food-chain model with time delays. *Mathematical and Computer Modelling*, 40(7-8):823–837, 2004.

[97] T. Yasuhiro. *Global dynamical properties of Lotka-Volterra systems.* World Scientific, 1996.

[98] E. C. Zeeman. Classification of quadratic carrying simplices in two-dimensional competitive Lotka-Volterra systems. *Nonlinearity*, 15(6):1993–2018, Oct. 2002.

[99] E. C. Zeeman and M. L. Zeeman. On the convexity of carrying simplices in competitive Lotka-Volterra systems. Routledge, 1994.

[100] E. C. Zeeman and M. L. Zeeman. An n-dimensional competitive Lotka–Volterra system is generically determined by the edges of its carrying simplex. *Nonlinearity*, 15(6):2019, 2002.

[101] E. C. Zeeman and M. L. Zeeman. From local to global behavior in competitive Lotka-Volterra systems. *Trans Amer Math Soc*, 355(2):713–734, 2003.

[102] M. L. Zeeman. Hopf bifurcations in competitive three-dimensional Lotka–Volterra systems. *Dynamics and Stability of Systems*, 8(3):189–216, 1993.

[103] B. Zhang, Z. Zhang, Z. Li, and Y. Tao. Stability analysis of a two-species model with transitions between population interactions. *Journal of Theoretical Biology*, 248(1):145–153, 2007.

[104] X. A. Zhang, Z. J. Liang, and L. S. Chen. The global dynamics of a class of vector fields in $\mathbb{R}^3$. *Acta Mathematica Sinica, English Series*, 27(12):2469–2480, 2011.

[105] J. Zu. Global qualitative analysis of a predator–prey system with Allee effect on the prey species. *Mathematics and Computers in Simulation*, 94:33–54, 2013.